



International Agreement Report

In-Tube Steam Condensation in the Presence of Air Under Transient Conditions

Prepared by:
A. Tanrikut

Turkish Atomic Energy Authority
Eskisehir Yolu 06530 Ankara Turkey

O. Yesin
Mechanical Engineering Department
Middle East Technical University
06531 Ankara Turkey

M.B. Rubin, NRC Project Manager

**Office of Nuclear Regulatory Research
U.S. Nuclear Regulatory Commission
Washington, DC 20555-0001**

May 2007

Prepared as part of
The Agreement on Research Participation and Technical Exchange
Under the International Code Assessment and Maintenance Program (CAMP)

**Published by
U.S. Nuclear Regulatory Commission**

ABSTRACT

The experimental investigation of condensation of pure vapor and air/vapor mixture in case of loss of coolant (feed-water) to the secondary side of a condenser imposes a special case since boil-off rate at the secondary side directly affects condensation process inside a condenser tube. The motivation for this special case comes from the experiment performed at the UMCP 2X4 integral test loop at the University of Maryland, which is a 1/500 scaled test facility of a PWR with once-through type steam generators, concerning loss of residual heat removal system during operation with reduced coolant inventory. The first phase of this type the experiment performed at the UMCP 2X4 test facility comprises the boiler-condenser mode (BCM) of operation during which one steam generator is active. However when the steam generator becomes inactive due to loss of feed-water (LOFW) to the secondary side (second phase), heat transfer from primary to secondary side that is mainly by condensation degrades and system pressure escalates. To address the issue outlined here, two experiments were performed at the METU-CTF, including the first phase (BCM) and second phase (LOFW) of the scenario: pure steam and air/steam mixture. These transients showed that the system pressurization is almost linear by time at constant vaporization rate inside the boiler. Similar observation was made for the results of UMCP 2X4 experiment. Besides this, the METU-CTF results show that vapor suction rate, effective condensation length and overall heat transfer rate are the function of boil-off rate of coolant and air mass fraction, as expected.

In this report, the results of experiments performed at the METU-CTF concerning in-tube steam condensation at BCM steady state condition and transient (LOFW) are presented, for both pure steam and air/steam mixture cases. The results of RELAP5 simulation are also discussed. Although given in NUREG/IA-0184, the report on in-tube steam condensation in the presence of air at steady-state condition, a brief description of the METU-CTF test facility is also given in this report. Then the experimental results of the UMCP 2X4 test facility are presented with emphasize given to RELAP5 simulations. The recent version of the RELAP5 code (RELAP5/mod3.3 (beta)) was used in calculations performed for this technical report.

PAPERWORK REDUCTION ACT STATEMENTS

This NUREG does not contain information collection requirements and, therefore, is not subject to the requirements of the Paperwork Reduction Act of 1995 (44 U.S.C. 3501 et seq.).

Public Protection Notification

The NRC may not conduct or sponsor, and a person is not required to respond to, a request for information or an information collection requirement unless the requesting document displays a currently valid OMB control number.

FOREWORD

This work was generated by international partners under the Code Assessment and Maintenance Program (CAMP) and constitutes the contributing organization's contribution to international thermal hydraulic code development. The contents of this report should not be viewed as an official NRC endorsement of the products or services of other persons or entities that may be referred to herein. Nor should this report be viewed as binding the NRC in its rulemaking, licensing or adjudicatory process.

CONTENTS

	Page No.
Abstract	iii
Foreword.....	v
Contents.....	vii
List of Figures.....	ix
Executive Summary	xi
Acknowledgments.....	xiii
Acronyms and Abbreviations	xv
Nomenclature.....	xvii
1 INTRODUCTION.....	1
2 EXPERIMENTS PERFORMED AT THE METU-CTF SEPARATE EFFECT TEST FACILITY AND RELAP5 SIMULATION	3
2.1 GENERAL.....	3
2.2 DESCRIPTION OF THE METU-CTF TEST FACILITY	3
2.2.1 <i>Steam/gas Supply</i>	<i>3</i>
2.2.2 <i>Connecting Piping and Pipe Fittings.....</i>	<i>4</i>
2.2.3 <i>Test Section.....</i>	<i>4</i>
2.2.4 <i>Instrumentation</i>	<i>5</i>
2.2.5 <i>Data Acquisition System</i>	<i>11</i>
2.3 OPERATING PROCEDURES OF THE TEST FACILITY AND SPECIFICATIONS OF EXPERIMENTS UNDER TRANSIENT CONDITIONS.....	12
2.3.1 <i>System Check.....</i>	<i>12</i>
2.3.2 <i>Experiments.....</i>	<i>14</i>
2.3.3 <i>Specifications of Experiments Under Transient Conditions.....</i>	<i>15</i>
2.4 DATA REDUCTION PROCEDURE	16
2.5 RESULTS AND DISCUSSION OF METU-CTF EXPERIMENTS	19
2.6 RESULTS OF RELAP5 SIMULATIONS	28
2.6.1 <i>Pure Steam Runs.....</i>	<i>28</i>
2.6.2 <i>Air/steam Mixture Runs</i>	<i>38</i>
3 EXPERIMENTAL INVESTIGATION OF COOLING EFFECTIVENESS UNDER COLD SHUTDOWN CONDITION AND RELAP5 SIMULATION	49
3.1 GENERAL.....	49
3.2 DESCRIPTION OF THE UMCP 2X4 TEST FACILITY	49
3.3 DESCRIPTION OF THE EXPERIMENT AND RELAP5 ANALYSIS	50
3.4 RESULTS AND DISCUSSION.....	52
3.4.1 <i>Effect of SG-A Fine Node Modelling.....</i>	<i>63</i>
3.4.2 <i>Computational Aspect of the Analysis.....</i>	<i>65</i>
3.4.3 <i>Comparison of METU-CTF and UMCP Data with respect to Geometry and Hydrodynamics</i>	<i>67</i>
3.4.4 <i>Comparison of RELAP5/mod3.2 and RELAP5/mod3.3 versions</i>	<i>68</i>
CONCLUSION	73
LIST OF REFERENCES.....	77

A. RELAP5 INPUT OF THE METU-CTF	A-1
B. RELAP5 INPUT OF THE UMCP 2X4 TEST FACILITY	B-1
C. SPECIFICATIONS OF INSTRUMENTATION AND DATA ACQUISITION SYSTEMS OF METU-CTF.....	C-1
D. ERROR ANALYSIS FOR METU-CTF MEASUREMENTS.....	D-1

LIST OF FIGURES

Figure 2.2-1 Flow Diagram of the METU-CTF	4
Figure 2.2-2 Inner Wall Measurement Technique	6
Figure 2.2-3 Installation Locations of the Thermocouples	7
Figure 2.2-4 Comparison of Thermocouple and Reference Temperature Measurements at $T_n=50\text{ }^\circ\text{C}$ (Water).....	8
Figure 2.2-5 Comparison of Thermocouple and Reference Temperature Measurements at $T_n=97\text{ }^\circ\text{C}$ (Water).....	8
Figure 2.2-6 Comparison of Thermocouple and Reference Temperature Measurements at $T_n=150\text{ }^\circ\text{C}$ (Air).....	9
Figure 2.2-7 Comparison of Thermocouple and Reference Temperature Measurements at $T_n=180\text{ }^\circ\text{C}$ (Air).....	9
Figure 2.2-8 Calibration Relation of the Pressure Transducer	10
Figure 2.2-9 Characteristics of the Orifice with the Diameter of 12.5 mm	11
Figure 2.3-1 Comparison of Predicted (RELAP5) and Measured Inner Wall Temperature	14
Figure 2.4-1 Energy Balance on a Control Volume of the Jacket Pipe	17
Figure 2.5-1 System Pressure for Loss of Coolant Transient.....	20
Figure 2.5-2 Cummulative Heat Transfer Rate Along the Condenser Tube	21
Figure 2.5-3 Coolant Temperature Profile for Loss of Coolant Transient (Pure Vapor)	22
Figure 2.5-4 Inner Wall Temperature Profile for Loss of Coolant Transient.....	22
Figure 2.5-5 Temperature Difference Across Inner Wall And Coolant.....	23
Figure 2.5-6 Coolant Temperature Profile for Loss of Coolant Transient (Air/Vapor Mixture)	24
Figure 2.5-7 Inner Wall Temperature for Loss of Coolant Transient (Air/Vapor Mixture)	25
Figure 2.5-8 Comparison of Coolant Temperature Profiles for Steady-state	26
Figure 2.5-9 Comparison of Inner Wall Temperature Profiles for Steady-state	26
Figure 2.5-10 Comparison of Coolant Temperature Profiles for Transient	27
Figure 2.5-11 Comparison of Inner Wall Temperature Profiles for Transient	27
Figure 2.6-1 Nodalization Scheme of the METU-CTF for RELAP5 Computer Code.....	30
Figure 2.6-2 Experimental and RELAP5 Results for Coolant Temperature.....	31
Figure 2.6-3 Experimental and RELAP5 Results for Local Heat Flux Distributions	31
Figure 2.6-4 Experimental and RELAP5 Results for Cummulative Heat Transfer Rate	32
Figure 2.6-5 Experimental and RELAP5 Results for Coolant Temperature (0.4 m, 1.2 m and 2 m from bottom)	33
Figure 2.6-6 Experimental and RELAP5 Results for Local Heat Flux Distributions	34
Figure 2.6-7 Experimental and RELAP5 Results for Cummulative Heat Transfer Rate	35
Figure 2.6-8 Experimental and RELAP5 Results for Coolant Temperature.....	35
Figure 2.6-9 RELAP5 Results for Local Flux at Different Times.....	36
Figure 2.6-10 Liquid Collapsed Level in Primary and Secondary Sides.....	37
Figure 2.6-11 RELAP5 Result for Total Power of the Condenser	38
Figure 2.6-12 RELAP5 Results for Air and Static Qualities obtained by Measured T_{wi} .	40
Figure 2.6-13 Experimental and RELAP5 Results for Coolant Temperature.....	40
Figure 2.6-14 Experimental and RELAP5 Results for Local Heat Flux Distributions	41
Figure 2.6-15 Experimental and RELAP5 Results for Cummulative Heat Transfer Rate	42
Figure 2.6-16 Experimental and RELAP5 Results for Coolant Temperature (0.4 m, 1.6 m and 2 m from bottom)	43
Figure 2.6-17 Experimental and RELAP5 Results for Coolant Temperature (R5-base: standard input, R5-Tw: T_{wi} given as boundary condition)	44
Figure 2.6-18 RELAP5 Results for Air Quality and Heat Flux ($t=20\text{ s}$)	45
Figure 2.6-19 RELAP5 Results for Air Quality and Heat Flux ($t=120\text{ s}$)	46

Figure 2.6-20 RELAP5 Results for Air Quality and Heat Flux (t=1020 s)	47
Figure 2.6-21 Liquid Collapsed Level in Primary and Secondary Sides.....	48
Figure 2.6-22 RELAP5 Result for Total Power of the Condenser	48
Figure 3.2-1 UMCP Test Facility	50
Figure 3.3-1 RELAP5 Model of UMCP Test Facility	52
Figure 3.4-1 Upper Plenum Pressure	54
Figure 3.4-2 Liquid Temperature at the Upper Plenum of Vessel.....	54
Figure 3.4-3 Void Fractions in Core	55
Figure 3.4-4 Heat Flux in Tubes of SG-A	55
Figure 3.4-5 Heat Transfer Modes in Tubes of SG-A	56
Figure 3.4-6 Secondary Side Level of SG-A	56
Figure 3.4-7 RELAP5 Results for Air Quality and Heat Flux (t=9000 s)	58
Figure 3.4-8 RELAP5 Results for Air Quality and Heat Flux (t=10,500 s)	58
Figure 3.4-9 RELAP5 Results for Air Quality and Heat Flux (t=15,000 s)	59
Figure 3.4-10 RELAP5 Results for Air Quality and Heat Flux (t=18,000 s)	59
Figure 3.4-11 RELAP5 Results for Core and SG-A Power.....	60
Figure 3.4-12 RELAP5 Results for Collapsed Level in SG-A	60
Figure 3.4-13 RELAP5 Results for Collapsed Level in Vessel and Pressurizer	61
Figure 3.4-14 RELAP5 Result for Flow at the inlet of SG-A Primary Side	62
Figure 3.4-15 RELAP5 Result for Core Flow	62
Figure 3.4-16 Comparison of System Pressure for Coarse and Fine Node Modeling...	63
Figure 3.4-17 Comparison of SG-A Level for Coarse and Fine Node Modeling.....	64
Figure 3.4-18 Heat Flux in SG-A Tubes for Fine Node Modeling.....	64
Figure 3.4-19 Time Step and Courant Time Step of the RELAP5 Calculation	65
Figure 3.4-20 CPU Time of the RELAP5 Calculation	66
Figure 3.4-21 Mass Error of RELAP5 Calculation	66
Figure 3.4-22 Upper Plenum Pressure (R5/m32 and R5/m33).....	69
Figure 3.4-23 Secondary Side Level of SG-A (R5/m32 and R5/m33).....	69
Figure 3.4-24 Heat Transfer Modes in Tubes of SG-A (R5/m32 and R5/m33).....	70
Figure 3.4-25 Heat Flux in Tubes of SG-A (R5/m32 and R5/m33).....	70
Figure 3.4-26 Mass Error of RELAP5 Calculation (R5/m32 and R5/m33).....	71
Figure 3.4-27 CPU Time of the RELAP5 Calculation (R5/m32 and R5/m33)	71

EXECUTIVE SUMMARY

The experimental investigation of condensation of pure steam and air/steam mixture in case of loss of coolant (feed-water) to the secondary side of a condenser imposes a special case since boil-off rate at the secondary side directly affects condensation process inside a condenser tube. The motivation for the experimental investigations undertaken at the Middle East Technical University Condenser Test Facility (METU-CTF) comes from the experiment performed at the test loop in the University of Maryland, College Park (UMCP 2X4), which is a 1/500 scaled test facility of a PWR with the once-through type steam generators. The experimental data of the UMCP 2X4 test facility addresses the safety problem of loss of residual heat removal system during operation with reduced coolant inventory. The first phase of this type of experiment performed at the UMCP 2X4 test facility comprises the Boiler-Condenser Mode (BCM) of operation during which one steam generator is active. However when the steam generator becomes inactive due to Loss Of Feed-Water (LOFW) to the secondary side (second phase), heat transfer from primary to secondary side that is mainly by condensation degrades and system pressure escalates.

To address the issue outlined above, two experiments were performed at the METU-CTF, including the first phase (BCM) and second phase (LOFW) of the scenario, for pure steam and air/steam mixture. The experiments were performed under BCM of operation for 100 s and then the coolant (feed-water) were cut off and LOFW transient was initiated. The total period of both tests is 1100 s. These transients showed that the system pressurization is almost linear by time at constant vaporization rate inside the boiler, i.e. the rate of increase is about 0.6 mbar/s, for both pure steam and air/steam mixture cases. Similar observation was made for the results of the UMCP 2X4 experiment. The METU-CTF results show that the vapor suction rate during BCM decreases considerably when some amount of air is trapped in the condenser tube prior to the start of the experiment. The effective condensation length is the function of boil-off rate of coolant and air mass fraction in condenser tube. It is evident from the coolant temperature profiles at the secondary side that the overall heat transfer rate is suppressed in transient with air/vapor mixture, which results in less boil-off rate compared to the corresponding pure steam transient. There is a general agreement between the RELAP5 results and data for coolant temperature trends for pure steam case at the METU-CTF, both qualitatively and quantitatively. The comparison of RELAP5 results with the experimental data shows that the coolant temperatures for steady state (BCM) are in agreement with the data while it yields an overestimation of about 8–10°C for the thermocouple above mid-plane of the jacket pipe during transient. The comparison of RELAP5 results with the experimental data for air/steam mixture case shows that the coolant temperatures for steady state (BCM) are in agreement with the data, with a maximum deviation of 3°C, while it yields an overestimation of about 20°C, for the thermocouple above mid plane of the jacket pipe during transient. The total heat load (8.3 kW) of METU-CTF condenser in air/steam case, for BCM, is predicted well by the code with a deviation of +4.6%. As in the case of pure steam, the flow and heat transfer regimes in the secondary side play an important role for the simulation of this kind of transients. The RELAP5 analyses show that the simulations for pure steam and air/steam mixture cases are not sensitive to the number of volumes of the input model.

The RELAP5 results are in agreement with the data of the UMCP test facility concerning the simulation of loss of residual heat removal system, which results in BCM operation, and LOFW transients. The code underpredicts the system pressure during BCM steady

state by 6% compared to the experimental data. In transient phase of the simulation (LOFW), the code follows the trend of the data, however, it then yields an overprediction after 15,000 s. During BCM steady state period, condensation of steam in the uppermost steam generator tube volume of the RELAP5 model always dominates the total heat transfer while the active volume shifts downwards during LOFW transient due to boil-off of feed-water at the secondary side. The air inside the tubes was also forced to accumulate in lower volumes in the progress of time. Since the transient is not so fast, the fine node model of UMCP steam generator tubes with 22 volumes yielded similar results to those of the base model with coarse node model with 11 volumes. It is important to note that the effective condensation length remains invariant with respect to the volume number. The mass error is improved in RELAP5/mod3.3 (beta version) compared to the earliest version available (RELAP5/mod3.2); the mass error in RELAP5/mod3.2 calculation escalates to about +2.6 kg at 9,000 s (end of the BCM period) while it is -0.03 kg in RELAP5/mod3.3. The mass error calculated by mod3.2 increases almost linearly to a value of +2.7 kg during transient whereas it remains almost stable (-0.005 kg) in mod3.3 calculation.

ACKNOWLEDGEMENTS

The authors would like to acknowledge the generous sponsorship of the Turkish Atomic Energy Authority, the International Atomic Energy Agency and the Middle East Technical University for the experiments performed at the METU-CTF.

ACRONYMS AND ABBREVIATIONS

BCM	Boiler-condenser mode
ID	Inner diameter
LOFW	Loss of feed water
METU-CTF	Middle East Technical University Condensation Test Facility
OD	Outer diameter
OTSG	Once through type of steam generator
SG	Steam generator
TAEA	Turkish Atomic Energy Authority
UMCP	University of Maryland, College Park

KEYWORDS: Condensation heat transfer, condenser performance, noncondensable gas, boiler-condenser mode of operation, loss of feed water transient.

NOMENCLATURE

Latin Symbols:

A	Coefficient of exponential fitting expression, °C
B	Coefficient of exponential fitting expression, m ⁻¹
BCM	Boiler-Condenser Mode
c _p	Specific heat at constant pressure, J/kg·°C
d, D	Diameter, m
dT	Temperature difference, °C
h	Convective heat transfer coefficient, W/m ² ·°C
h	Enthalpy, J/kg
LOFW	Loss of Feed Water
\dot{m}	Mass flow rate, kg/s
P	Pressure, bar
q	Heat transfer rate, W
q''	Heat flux, W/m ²
r	Correlation coefficient
Re	Reynolds number
S	Deviation from fitting curve
t	Time (s)
T	Temperature, °C
x	Axial distance, m
X	quality

Greek Symbols:

α	Flow coefficient
μ	Dynamic viscosity, kg/m·s
ρ	Density, kg/m ³
σ	Standard deviation

Subscripts:

C	Central
cw	Cooling water
D	Based on diameter
h	Hydraulic
i	Inner, inlet
l	Liquid
n	Nominal
s	Saturation, static
v	Vapor phase
w	Wall
wc	between inner wall and coolant
wi	inner wall

1 INTRODUCTION

The Turkish Atomic Energy Authority (TAEA) is willing to follow the technological development trends in advanced and innovative nuclear reactor systems. A part of our long-term research and development efforts is planned to concentrate on passive cooling systems. The primary objectives of the passive design features are to simplify the design, which assures the minimized demand on operator, and to improve plant safety. The research on passive systems mainly comprises the computer code assessment studies and includes the applications for both old and new generation reactor systems. To accomplish these features the operating principles of passive safety systems should be well understood by an experimental validation program. Such a validation program is also important for the assessment of advanced computer codes, which are currently used for design and licensing procedures. The condensation mode of heat transfer plays an important role for the passive heat removal applications in the current nuclear power plants (e.g. decay heat removal via steam generators in case of loss of heat removal system) and advanced water-cooled reactor systems. But it is well established that the presence of noncondensable gases can greatly inhibit the condensation process due to the build-up of noncondensable gas concentration at the liquid/gas interface. The isolation condenser of passive containment cooling system of the simplified boiling water reactors is a typical application area of in-tube condensation in the presence of noncondensable. The research work at the TAEA concerning the application of condensation in the presence of air, as a noncondensable gas, was first undertaken for a PWR with Once Through Steam Generator (OTSG) for which experimental data were available. These experimental data were obtained from the integral test loop of the University of Maryland at College Park (UMCP), addressing a very important safety issue called the loss of residual heat removal system after reactor shutdown. The experimental data were used for the assessment of RELAP5 thermal-hydraulic computer code and both the effect of Nusselt model, incorporated in the code as the condensation model, and the effect of nodalization model were investigated [1]. But the lack of measurements for the inside of the steam generator has led us to the conclusion that the separate effect test is strongly needed for the investigation of in-tube condensation and the effect of noncondensables on the condensation mode of heat transfer. Thus, an experimental study which could enable us for the fundamental investigation of condensation in the presence of air was planned in cooperation with the Mechanical Engineering Department of the Middle East Technical University (METU), Ankara, in the frame of a project (Project No: 94403507) between the TAEA and METU. The project is partially sponsored by the International Atomic Energy Authority (IAEA) under the Coordinated Research Program (Contract No: 8905/R0) which is entitled "Thermohydraulic Relationships for Advanced Water Cooled Reactors".

The experimental program undertaken at the METU covers a wide range of steam and air/steam mixture flow rates under forced convection, steady-state conditions and has the purpose to investigate the inhibiting effect of air on steam condensation process [2]. The results of this experimental study performed at steady-state condition were planned to be supplementary in nature for other experimental investigations such as those performed at the Massachusetts Institute of Technology (MIT), Cambridge, and University of California, Berkeley, (UCB). The data bases of MIT and UCB were used for RELAP5 assessments [3,4]. These investigations undertaken at MIT and UCB aim to support Passive Containment Cooling System (PCCS) and Isolation Condenser (IC) designs of the Simplified Boiling Water Reactor design, with relatively lower Reynolds number compared to the METU-CTF. Per commitment stated in the CAMP (Thermalhydraulic Code Applications and Maintenance Program) agreement between the TAEA and the United States Nuclear Regulatory Commission (USNRC), signed on February 1998, the

experimental data on in-tube steam condensation in the presence of air for steady-state case were opened to the USNRC in 2000 and its report was published (NUREG/IA-0184) by the USNRC.

As part of the commitment made to the USNRC in 2001, the experimental data under transient condition were also opened to the USNRC. The experiments performed at the METU-CTF under transient conditions cover two main cases: pure steam and air/steam mixture. The experiments were performed such that the test facility were run under Boiler-Condenser Mode (BCM) of operation for 100 s and then the coolant (feed-water) were cut off and Loss of Feed Water (LOFW) transient was initiated. The total period of both tests is 1100 s. The simulation of the UMCP test facility for the case of loss of residual heat removal system after reactor shutdown was also repeated by using RELAP5/mod3.3 (beta test version) and the results are discussed in detail in this report.

2 EXPERIMENTS PERFORMED AT THE METU-CTF SEPARATE EFFECT TEST FACILITY AND RELAP5 SIMULATION

2.1 GENERAL

In this part of the report, the Middle East Technical University-Condensation Test Facility (METU-CTF) [5] is described and experimental results are presented. A detailed discussion for RELAP5 results by comparing some of the parameters by experimental results is also given. The information pertaining to the description of the METU-CTF including the measurement system and operating procedures was also given in NUREG/IA-0184 (In-tube Steam Condensation in the Presence of Air) [6], however some of this information is repeated in following sections.

2.2 DESCRIPTION OF THE METU-CTF TEST FACILITY

The test facility (METU-CTF) was installed at the Mechanical Engineering Department of the Middle East Technical University (METU) in the frame of a project between the Turkish Atomic Energy Authority (TAEA) and the METU. The project is partially sponsored by the International Atomic Energy Authority (IAEA) under the Coordinated Research Program (Contract No: 8905/R0) which is entitled "Thermohydraulic Relationships for Advanced Water Cooled Reactors". The experimental apparatus consisting of an open steam or steam/gas system and an open cooling water system is depicted in the flow diagram given in Figure .

2.2.1 Steam/gas Supply

Steam is generated in a boiler (1.6 m high, 0.45 m ID) by using four immersion type sheathed electrical heaters. Three of these heaters have a nominal power of 10 kW each and the fourth one has a power of 7.5 kW, at 380 V. All the heaters can be individually controlled by switching on or off. One of these heaters, i.e. the one with 7.5 kW power, is connected to a variac for continuous control of power.

The boiler tank was designed to withstand an internal pressure of 15 bars (at $T=20\text{ }^{\circ}\text{C}$) and was tested at this pressure. The maximum operating pressure of the tank is 10 bars. To ensure dry steam at the exit of the boiler, a mechanical separator directly connected to the exit nozzle was installed. However, electrical pre-heating with three heaters (0.5 kW per heater) is also available at the entrance of the test section to increase the temperature of steam, so that steam is guaranteed to be 100% dry. The boiler tank was thermally insulated to reduce environmental heat loss.

Compressed air can be supplied either to the boiler tank (directly to the water) or to the steam line via a nozzle (after the orifice meter) on the horizontal part of the pipe, which connects the boiler and the test section. Preference was given to the first method; i.e. injection to the boiler, during most of the experiments since system behavior is more stable compared to the second method, when air mass flow rate is increased. When air injection was performed by the second method (to the horizontal piping), air injected passes through the preheating section so that local steam condensation was avoided at the entrance of the test section due to thermal inequilibrium of steam and air. The air supply system consists of an air compressor and three compressed air tanks with a total capacity of 600 liters. The maximum pressure of the compressed air system is 10 bars.

The boiler tank is equipped with the measuring instruments given below:

- level gauge with an operating pressure of 16 bars and a test pressure of 32 bars,
- safety vent valve of spring lift type with an operating pressure of 12 bars,
- pressure controller for cutting the power off at a predetermined maximum pressure setting,
- pressure gauge (1–16 bars),
- relief valve (19.05 mm ID).

2.2.2 Connecting Piping and Pipe Fittings

The pipe connecting the boiler tank and the test section has a length of approximately 2 m and an ID of 38.1 mm. The pipe was connected to the boiler tank via an isolation valve. This isolation valve (38.1 mm ID) is used to isolate the boiler until inside pressure of the tank is increased to a pre-determined level. The measurements performed on this part of the experimental facility are mass flow rate via a differential pressure transmitter and temperature. There are three electric heaters (0.5 kW each at 220 V) installed to the horizontal part of the piping between the orifice meter and the test section. The pipe connecting the boiler and the test section was thermally insulated.

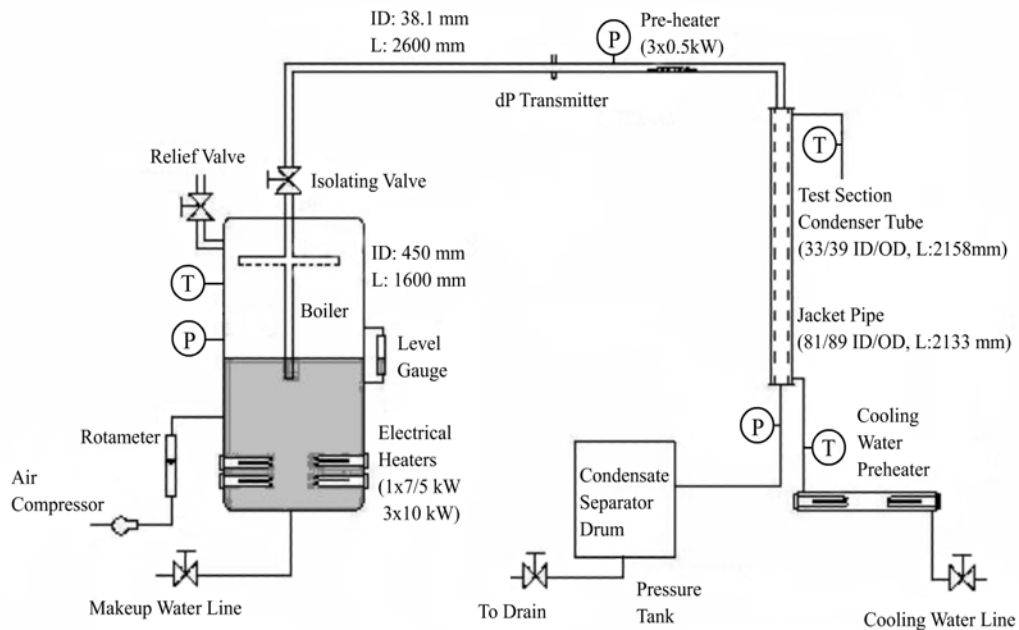


Figure 2.2-1 Flow Diagram of the METU-CTF

2.2.3 Test Section

The test section is a heat exchanger of countercurrent type that is steam or steam/gas mixture flows downward inside the condenser tube (inner tube) and cooling water flows upward inside the jacket pipe (outer pipe).

2.2.3.1 Condenser Tube

The condenser tube consists of a 2.15 m long seamless stainless steel tube with 33/39 mm ID/OD and is flanged at both ends with sealing materials. The condenser tube was flanged to the inlet (33.5/42.6 mm ID/OD) and exit (33.5/42.6 mm ID/OD) pipes of the test section. The total length of the inlet pipe from the horizontal part of the pipe section down to the condenser tube is approximately 33 cm ($10 \times d_i$, where d_i is the inner diameter of the tube) and this length is long enough for the mixture flow to become fully developed before entering the condenser. It should also be noted that some uncertainties (such as irregular film development or dropwise condensation) associated with the liquid film development at the entrance of the condenser tube are expected to occur in this development region since the entrance region was not thermally insulated. A pressure measurement port was located at the vertical part of the inlet pipe flanged to the condenser tube.

A total of 13 holes (1.5 mm diameter) were drilled with an angle of 30° at different elevations along the condenser tube length to fix the thermocouples for inner wall temperature measurements. The condenser tube was tested at 10 bars pressure to check that inner wall of the tube was not pierced during the drilling process.

The outlet of the condenser tube is connected to a tank via exit part of the test section. This tank is used to keep the system pressure at a constant level by controlling the flow rate of steam or air/steam mixture through a valve connected to the tank. The measured parameters at the exit of the test section are pressure and temperature.

2.2.3.2 Jacket Pipe

The jacket pipe surrounding the condenser tube is made of sheet iron and has a length of 2.133 m and 81.2/89 mm ID/OD. The cooling water is supplied via a nozzle, which has been welded on the jacket pipe. Similarly, cooling water outlet consists of a nozzle that is connected to the building water discharge system. Inner diameter of all these nozzles is 12.7 mm. A total of 15 holes (1.5 mm diameter) were drilled radially at different elevations for installation of the thermocouples to be used for cooling water temperature measurements. The measured cooling water temperature is used to determine heat flux profile along the annulus region. The jacket pipe was thermally insulated to reduce environmental heat losses.

2.2.4 Instrumentation

The details of the technical features of the equipment are given in Appendix C.

2.2.4.1 Thermocouples

Thirteen thermocouples were inserted into the holes that have been drilled on the outer surface of the stainless steel condenser tube with an angle of 30° and soldered by silver. These thermocouples are used for inner wall temperature measurement. The distance between the inner wall and the tips of thermocouples is approximately 0.5 mm (Figure).

Fifteen thermocouples, to be used for cooling water temperature measurement, were inserted into the holes, drilled on the outer surface of the jacket pipe, and fixed by compression fittings sealed by Teflon material. Thirteen of these thermocouples are at the same elevation as the thermocouples to be used for inner wall temperature

measurements. Besides this, two additional thermocouples were inserted at the same elevation but at a 180° offset orientation. The purpose of these two additional temperature measurements is to observe the angular variation of the cooling water temperature.

Ten thermocouples were fixed to a 2 mm diameter Inconel guide wire and installed at the central position of the condenser tube for the central temperature measurements. The guide wire was fixed at both ends of the test section.

The installation locations of all thermocouples are given in Figure .

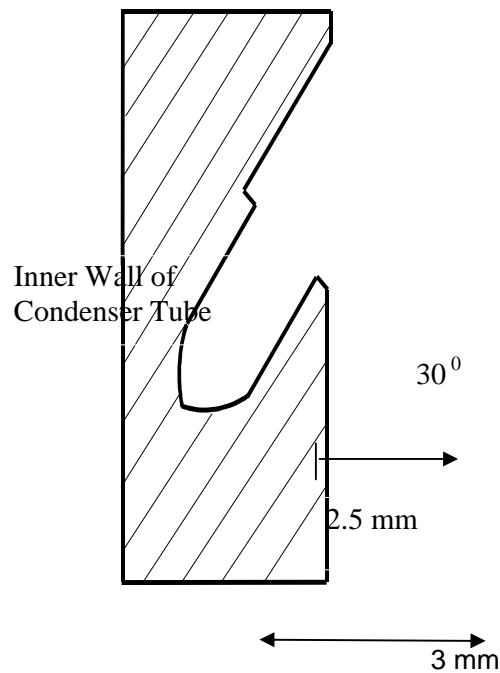


Figure 2.2-2 Inner Wall Measurement Technique

All thermocouples for inner wall and cooling water temperature measurements are of L-type (Fe-Const type designed according to the DIN Standard) and sheathed by Inconel material. The thermocouples used for condenser tube central temperature measurements are of J-type (Fe-Const type designed according to the USA standards) and these thermocouples have a temperature-voltage relation very similar to those of L-type thermocouples. The nominal outside diameter and wire diameter of all sheathed thermocouples is approximately 1.5 mm and 0.3 mm, respectively. The precision of this type of thermocouples, which belong to second tolerance class according to the standard IEC 584-2, is $\pm 2.5^\circ\text{C}$ between -40°C and 333°C .

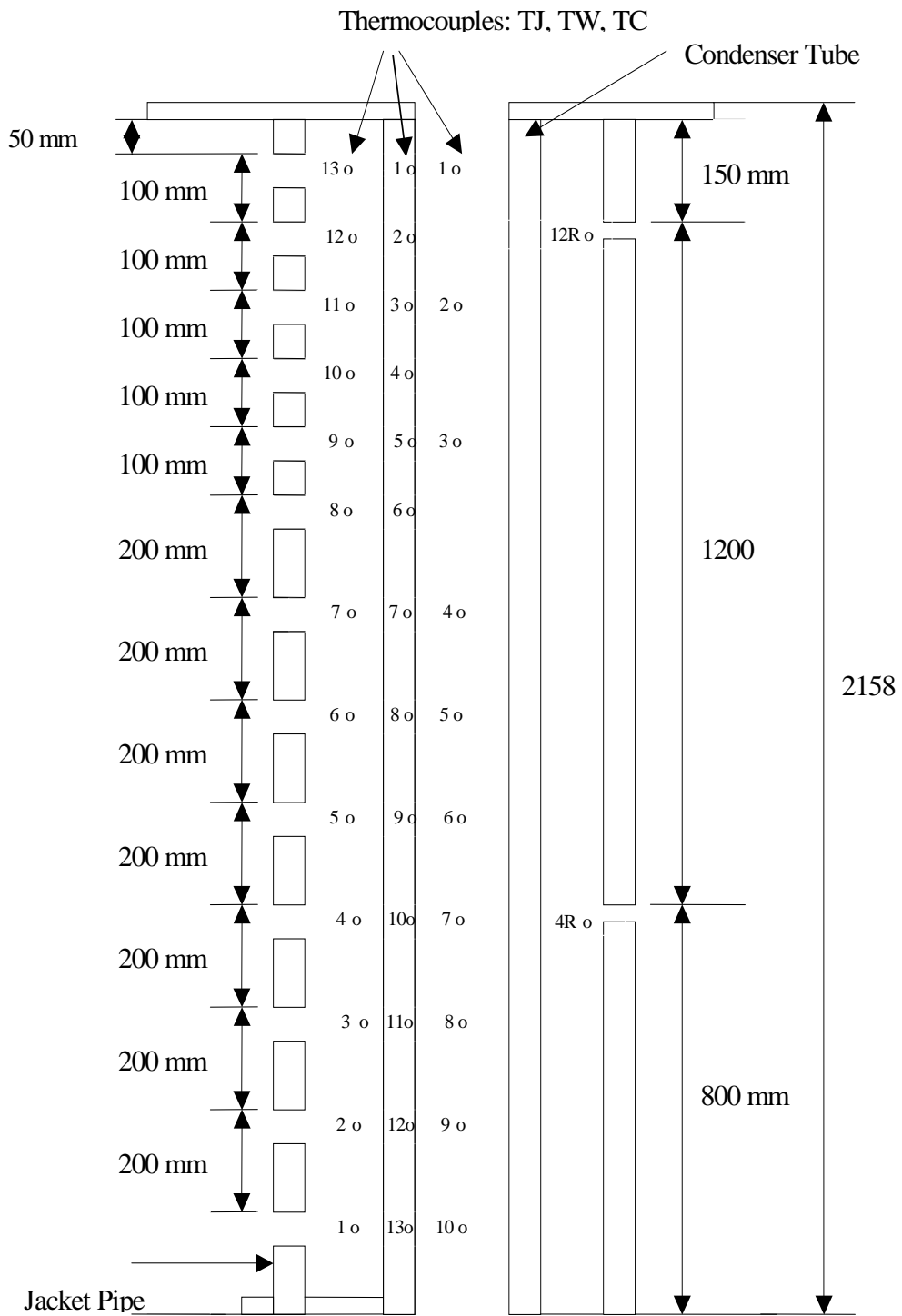


Figure 2.2-3 Installation Locations of the Thermocouples

The deviation of each thermocouple measurement as compared with the mercury thermometer and T-type thermocouple (manufactured by OMEGA) measurements is given in Figure , Figure , Figure and Figure for $T_n=50^\circ\text{C}$, 97°C , 150°C and 180°C , respectively. As a result of these comparisons, maximum deviations from reference measurement (shown by REF. T in figures) are found to be -0.82% , -1.16% , -1.13% and $+0.83\%$ for nominal temperature settings of 50°C , 97°C , 150°C and 180°C , respectively.

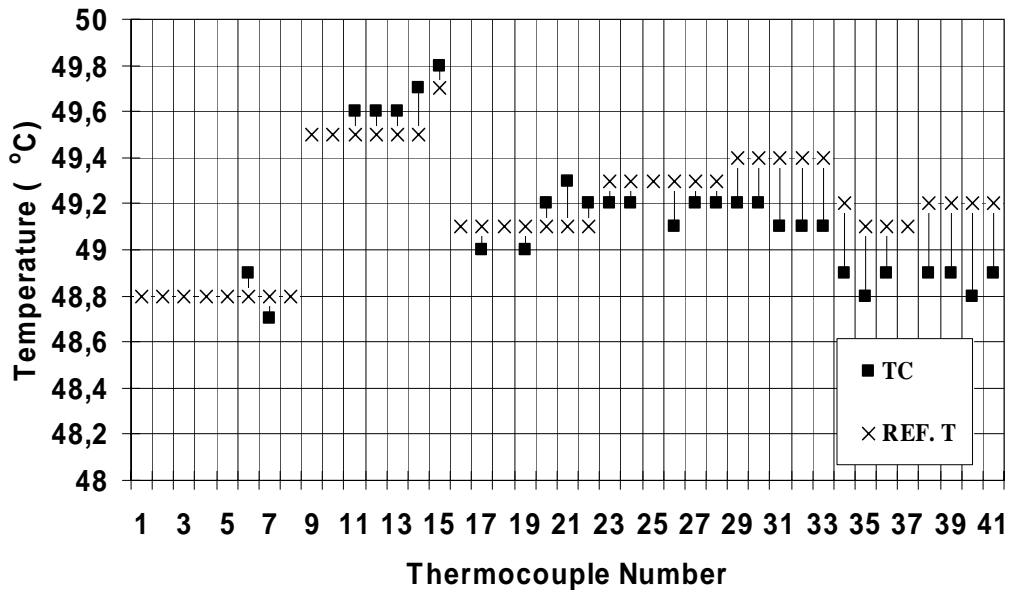


Figure 2.2-4 Comparison of Thermocouple and Reference Temperature Measurements at $T_n=50^\circ\text{C}$ (Water)

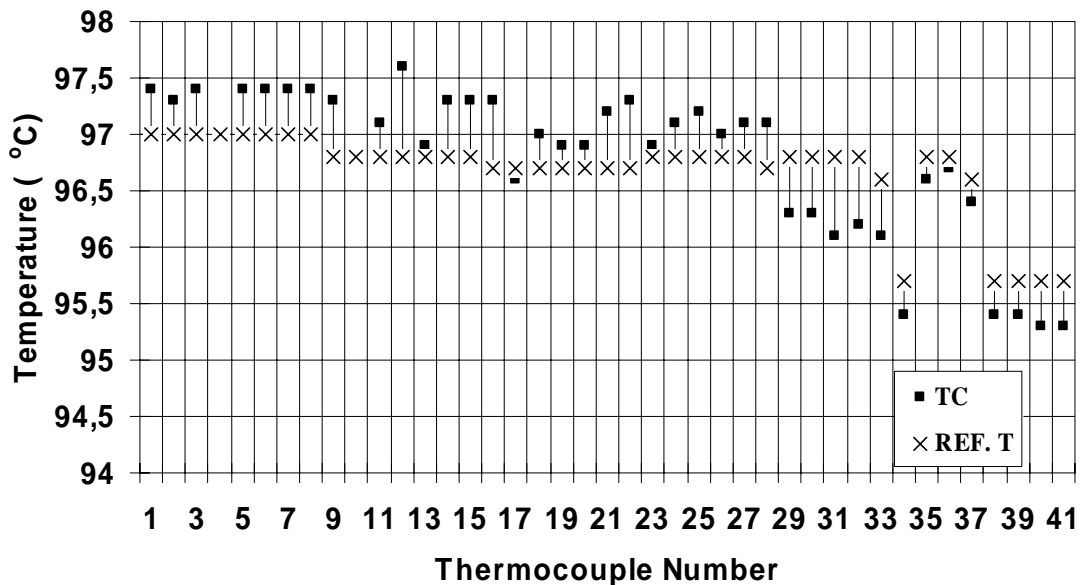


Figure 2.2-5 Comparison of Thermocouple and Reference Temperature Measurements at $T_n=97^\circ\text{C}$ (Water)

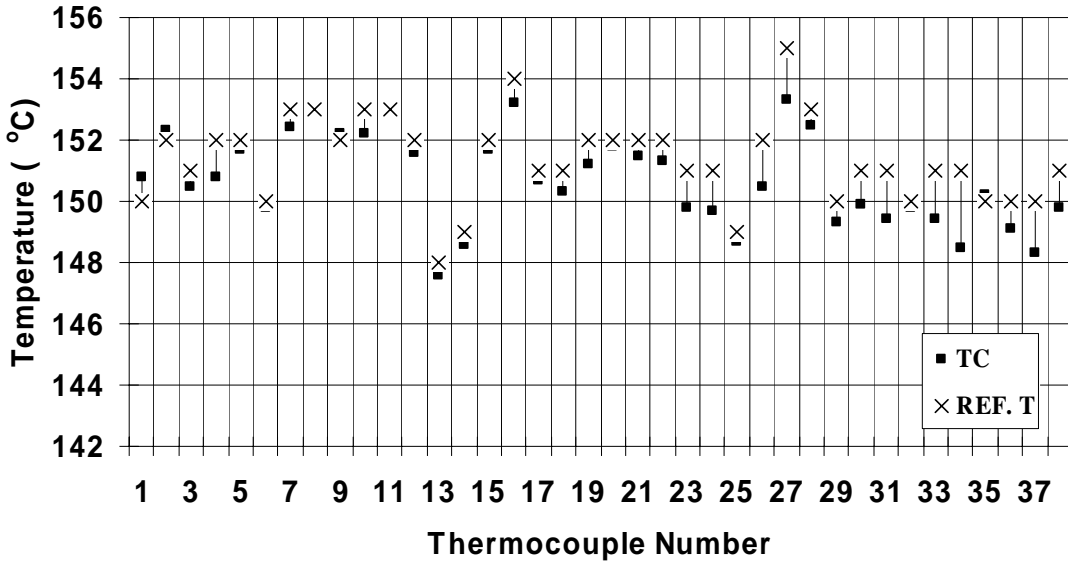


Figure 2.2-6 Comparison of Thermocouple and Reference Temperature Measurements at $T_n=150\text{ }^\circ\text{C}$ (Air)

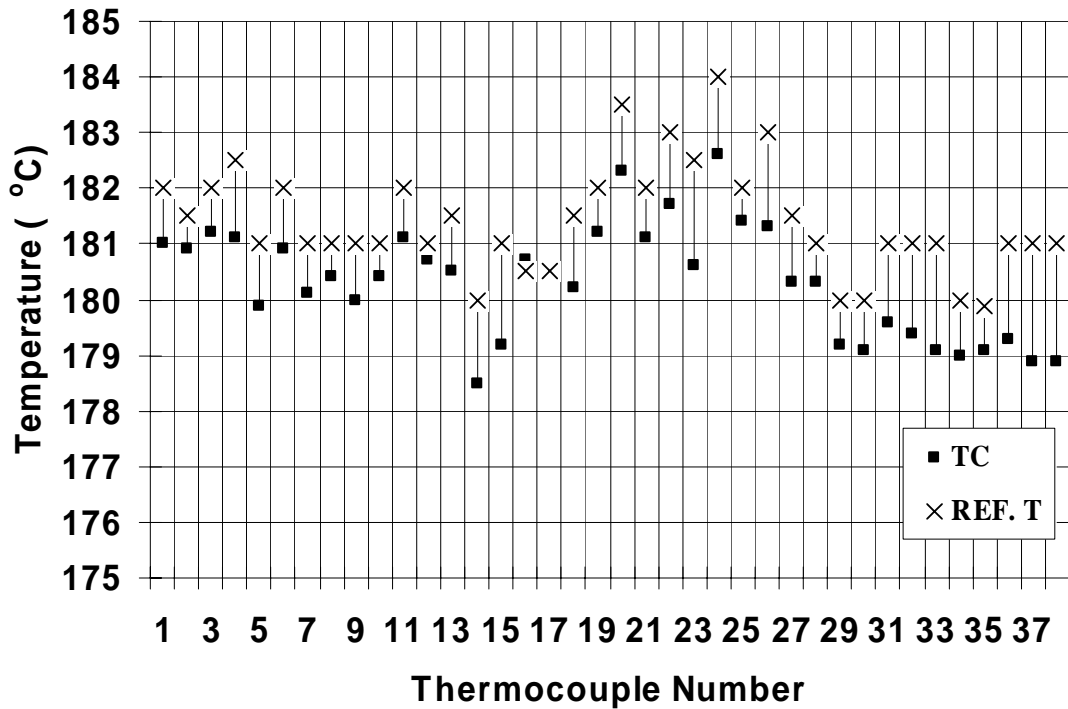


Figure 2.2-7 Comparison of Thermocouple and Reference Temperature Measurements at $T_n=180\text{ }^\circ\text{C}$ (Air)

2.2.4.2 Pressure Transducer

A strain gauge type pressure transducer, installed at the entrance of the test section, can be used for pressure measurement in the interval of 0–6 bars (g) and has an output of 4–20 mA. The power supply of the transmitter is 24V DC. The calibration of this transmitter was made by using air as the operating medium and the result of this calibration is shown in Figure .

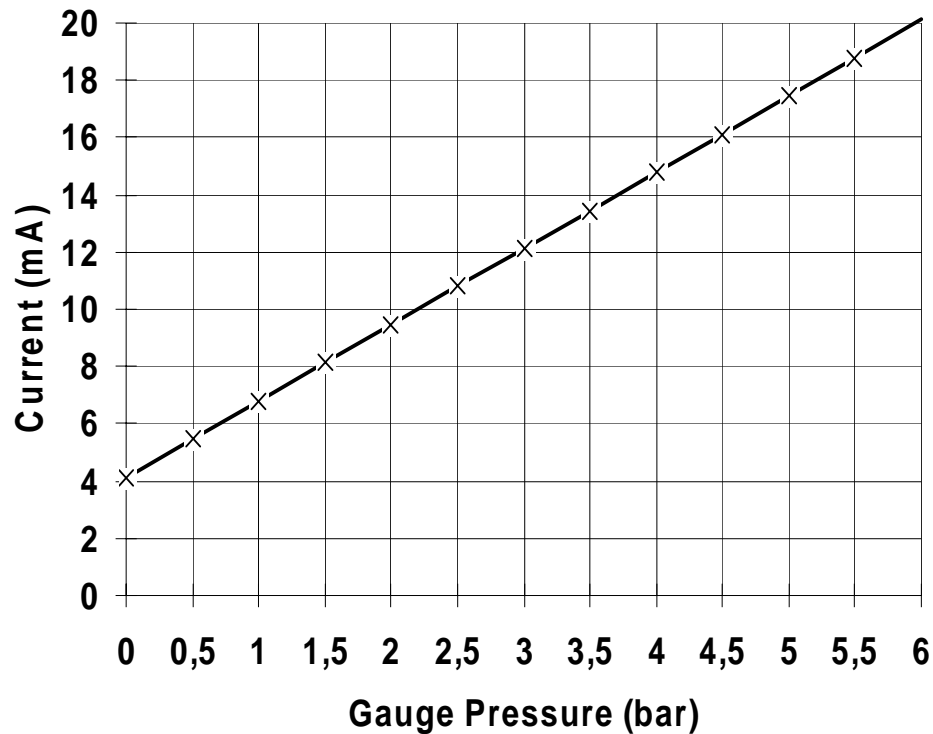


Figure 2.2-8 Calibration Relation of the Pressure Transducer

2.2.4.3 Flowmeter

The flow rate measurement of steam is performed by the differential pressure transmitter. The device produces current in the range of 4–20 mA corresponding to the differential pressure range of the transmitter which is 11.7–70 kPa. The current output of the device is linear with respect to differential pressure.

Three types of orifices with flow diameters of 6, 10 and 12.5 mm were calibrated by using water as operating medium and flow coefficients, as a function of Reynolds number, were obtained. The characteristic of the orifice (flow diameter: 12.5 mm) used in the experiments is shown in Figure . The data obtained during calibration was fitted using the following relation:

$$\alpha = 0.2 * \ln(\text{Re}) - 1.458 \quad (2.1)$$

where α is the flow coefficient and Re is Reynolds number.

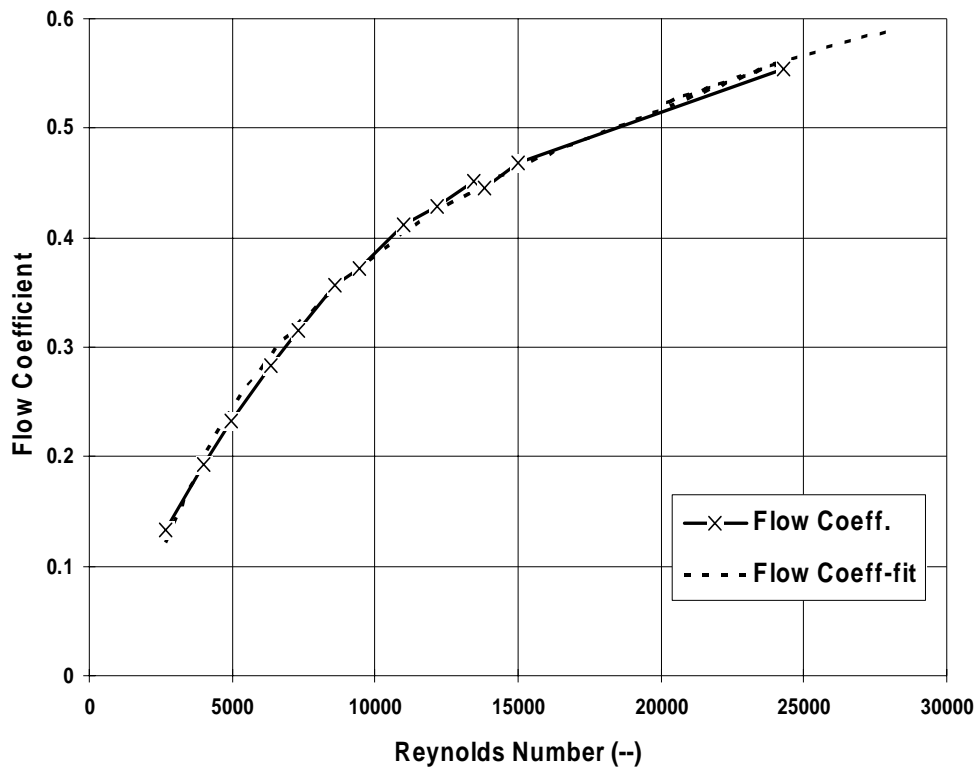


Figure 2.2-9 Characteristics of the Orifice with the Diameter of 12.5 mm

2.2.5 Data Acquisition System

The data acquisition system consists of one multifunctional analog and digital I/O card (data acquisition card, PCL-812PG), three programmable amplifier and channel multiplexing daughter board (PCLD-889) for the analog input channels of the data acquisition card which have a total of 48 channels, and an IBM-486 computer system. The data acquisition card and multiplexers are the products of Advantech Co., Ltd, and technical details are given in Appendix C.

Total of 40 thermocouple wires was mounted on the multiplexing daughter cards. The temperatures were continuously monitored on the colour monitor during experiments. The GENIE software was installed to read, display, and log data to disk. The GENIE software, which is the product of Advantech Co., Ltd., is designed to run in the Microsoft Windows 95 environment. GENIE provides an intuitive object oriented graphical user interface that simplifies control strategy and display setups. The user can design his own strategy for controlling signals during experiments or any kind of industrial process.

2.3 OPERATING PROCEDURES OF THE TEST FACILITY AND SPECIFICATIONS OF EXPERIMENTS UNDER TRANSIENT CONDITIONS

The operating procedure of the METU-CTF consists of two main stages: system check and experiments. The former stage is important to understand the response of thermocouples at certain operating conditions and to estimate the rate of environmental heat losses. The second stage includes system start-up, data logging and system shutdown.

2.3.1 System Check

2.3.1.1 Isothermal Check of Thermocouples

The isothermal check of the thermocouples was done at various temperature levels. The results of these two tests are given in Table 2.3.1. The first test ($T \sim 20 \text{ }^\circ\text{C}$) was performed with stagnant water while the second one ($T \sim 110 \text{ }^\circ\text{C}$) was under high flow rate ($1.72 \times 10^{-2} \text{ kg/s}$) and high pressure ($P \sim 1.4 \text{ bars}$) conditions. In the second test, steam and two-phase flow was established in the condenser tube and jacket pipe, respectively. Apart from the isothermal check of the thermocouples, the second test has also shown that the centrally located thermocouples were operating properly, at least in the range of thermocouple tolerances, when the saturation temperature ($T \sim 110 \text{ }^\circ\text{C}$) was concerned.

Table 2.3.1. Data Collected in the Isothermal Check of Thermocouples (TC)

TC No	TC Code	Temperature ($^\circ\text{C}$)	
1	TC-1	19.4	
2	TC-2	19.8	111.5
3	TC-3	19.5	110.7
4	TC-4	19.9	110.3
5	TC-5	19.9	109.7
6	TC-6	19.9	111.6
7	TC-7	19.5	112.4
8	TC-8	19.9	110.3
9	TC-9	19.5	110.7
10	TC-10	19.5	109.8
11	TC-11	19.9	109.4
12	TW-1	17.6	106.7
13	TW-2	17.9	107.9
14	TW-3	18.0	105.3
15	TW-4	18.0	109.3
16	TW-5	18.5	108.5
17	TW-6	18.5	109.8
18	TW-7	18.5	107.0
19	TW-8	18.5	108.9
20	TW-9	18.0	109.8
21	TW-10	18.5	109.3
22	TW-11	18.5	109.7
23	TW-12	18.0	110.3

24	TW-13	18.5	109.8
25	TJ-1	16.6	104.0
26	TJ-2	16.5	104.4
27	TJ-3	16.1	105.8
28	TJ-4	16.1	104.9
29	TJ-5	17.1	105.3
30	TJ-6	17.1	104.0
31	TJ-7		104.3
32	TJ-8	15.1	103.5
33	TJ-9		106.1
34	TJ-10	16.6	103.4
35	TJ-11	15.6	103.5
36	TJ-12	16.1	
37	TJ-13		104.3
38	TJ-4R	15.7	104.8
39	TJ-12R		104.0

Notes: TC: central thermocouple

TW: wall thermocouples

TJ: jacket thermocouples

R extension stands for thermocouple at the reverse side of the one with the same number

2.3.1.2 Prediction of Environmental Heat Loss

The effect of environmental heat loss on measurements was tested by water under stagnant conditions. Both sides of the test section were filled with hot water fed directly from the boiler. The data collection duration was 422 s. The insulation of the test section is effective so that rate of temperature decrease was measured to be ~ 0.007 °C/s which yields a maximum heat loss of about 0.1 kW at this operating condition.

2.3.1.3 Prediction of Fin Effect for Inner Wall Temperature Measurements

As described in Section 0, inner wall temperature measurements were performed by thirteen thermocouples inserted into the holes, which have been drilled on the outer surface of the condenser tube with an angle of 30° and soldered by silver. The sheathed thermocouple wires are passing through the jacket pipe so that the inner wall temperature measurements could be affected by local cooling water temperature by a possible fin effect.

A test was performed by filling the condenser tube with stagnant water ($T \sim 80$ °C) and by keeping the cooling water ($T_i \sim 17$ °C) flowing through the jacket pipe at a rate of about 0.25 kg/s. The reason for keeping the hot water stagnant inside the condenser tube was to check the difference between the bulk and inner wall temperatures. It was expected that the difference would be small if fin effect was not dominant. It is seen that the temperature difference is about 8 °C and 4 °C at 20 s and 160 s, respectively. It is clear that the difference is more at the beginning of the transient process during which the system temperature is high. It should also be noted that a temperature profile could develop in radial direction due to local natural convection currents so that the measured temperature difference between centerline and inner wall seems reasonable. To support this, the wall temperature at exactly the same radial distance from the inner surface (0.5 mm) is also predicted by the RELAP5/mod3 thermal-hydraulic system analysis computer code [7] by imposing the same test boundary conditions, and as illustrated in Figure , the

discrepancy was small (± 2 °C). Because of this reason, no correction was made for the inner wall measurements.

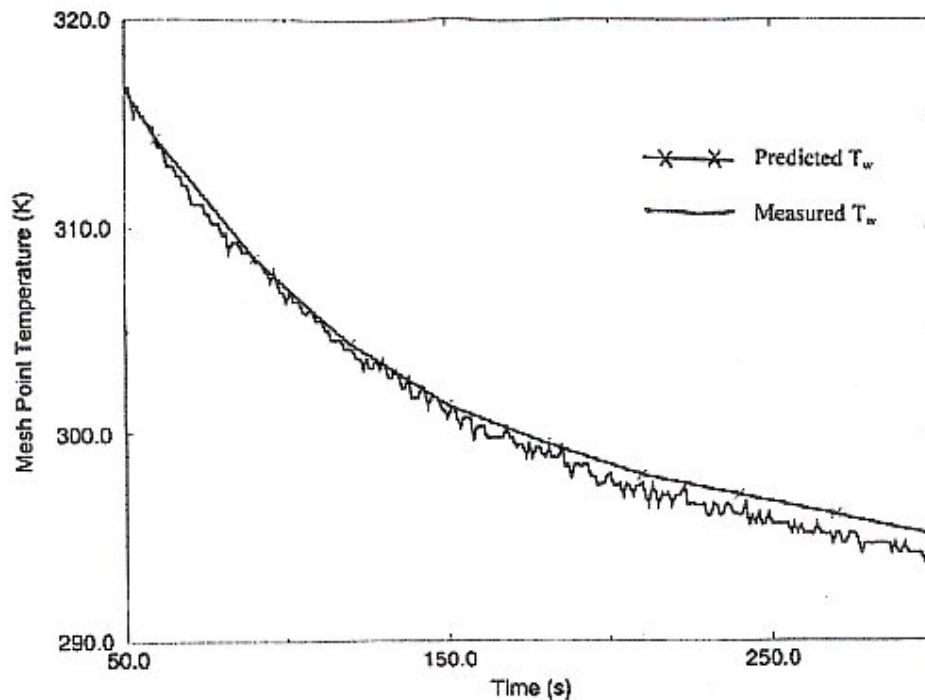


Figure 2.3-1 Comparison of Predicted (RELAP5) and Measured Inner Wall Temperature

2.3.1.4 Reproducibility of Data

It is important to demonstrate the reproducibility of the data and some experiments were repeated at nearly the same operating conditions to see whether the data can be reproduced reasonably close. The inlet air mass fraction of these experiments is about 10%. Maximum deviation found from these two sets of experiments are; 6% and 10%, for $P_n=2$ bars and $P_n=3$ bars, respectively. Primary reasons of deviation are the system pressure, vapor flow rate, and cooling water flow rate. However, the percent deviations may be considered as reasonable when the uncertainty band of heat flux is considered. The uncertainty band of heat flux was calculated to be 11% (Appendix D).

2.3.2 Experiments

The experimental procedure comprises the stages of system start-up, transient process to steady-state condition, data logging, and system shutdown.

2.3.2.1 System Start-up

First step for the system start-up is the preparation of the boiler by checking water inventory. Then system check is made through the control of the following equipment:

1. Valve position of fresh water inlet of the boiler: closed
2. Valve position of compressed air inlet to the boiler: closed
3. Isolation valve of the boiler: closed
4. Control of boiler pressure controller: set to the predetermined

- pressure level
5. Control of electrical heaters
 6. Drainage of condensate accumulated inside of the rotameters at the exit of the compressor tanks
 7. Control of pressure inside of compressor tanks
 8. Start of cooling water flow through the jacket pipe
 9. Adjust the flow rate to a predetermined value
 10. Open the valve at the exit of the discharge tank
 11. Open the boiler isolation valve slowly when pressurization is completed
 12. Dump vapor to atmosphere for at least 15 minutes
 13. Check for temperature reading at upstream of the test section whether air was swept out by vapor flow.
 14. Adjust system pressure and vapor flow rate by controlling the valve at the exit of the discharge tank
 15. Turn on the electrical pre-heaters
 16. Open valve for air injection
 17. Adjust air flow rate via rotameter

2.3.2.2 Operating at Steady-state, Transient Conditions and Data Logging

Monitoring the system parameters, i.e. temperature, pressure, and flow rate, on computer via data acquisition system, performed the control of the steady-state conditions. Data recording was not started before desired steady-state operating condition was reached. After steady-state condition was sustained, the data logging was started. Data were recorded with one-second intervals approximately for a two minutes period. During data logging, special care was given to the control of compressed air flow rate, vapor or mixture flow rate, and system pressure. The transient case was performed with 10 kW constant power and the exit part of the condenser tube was closed to trap pure vapor or air /vapor mixture inside the tube. The cooling water was turned off after the steady state period (100 s). The data recording for transient case lasted 1100 s, including steady-state period, with intervals of one second. The system pressure was recorded for 10 s intervals in transient runs.

2.3.2.3 System Shutdown

System shutdown was started by putting off the electrical heaters in the boiler and at the pre-heating section. Then, compressed air injection was terminated along with fully opening of the valve at the exit of the discharge tank. Vapor inside the dome of the boiler was discharged till the system pressure was about 1 bar. Finally, the cooling water flow was terminated.

2.3.3 Specifications of Experiments Under Transient Conditions

The experiments performed at the METU-CTF under transient condition (loss of coolant flow) cover the following parametric ranges:

- Pure Steam Run: $P = 2.12$ bars for BCM period
 Pressure increases to 2.7 bars at the end of transient period
 $\dot{m}_{cw} = 0.18$ kg/s for BCM period
 $\dot{m}_v = 0.017$ kg/s (for BCM) and below the measurable limit for transient part
- Air/steam Run: $P = 2.25$ bars for BCM period
 Pressure increases to 2.8 bars in the end of transient period

$\dot{m}_{cw} = 0.18$ kg/s for BCM period

$\dot{m}_v =$ Below the measurable limit for both BCM and transient periods,

It is important to note that the local air mass fraction inside the condenser tube was not measured and/or calculated.

2.4 DATA REDUCTION PROCEDURE

The data reduction process outlined below was applied to the transient data depending on the parameters measured, i.e. some parameters could not be calculated due to lack of data.

A. Averages of all the measured parameters were taken for 10 s and recorded on the computer during experiments. The total data logging period of experiments under steady-state condition were about 1.5–2 minutes. The period of data logging was 1100 s for BCM and transient runs. The oscillatory behavior was observed only for cooling water temperature with a period of 3–4 s, however, the amplitude of the oscillations was small (± 1 °C). The source of such oscillations observed for the jacket cooling water measurements was turbulence inside the annular region of the jacket pipe, as expected.

B. The following exponential curve was used to fit the cooling water temperature data measured inside the jacket pipe,

$$T(x) = Ae^{-Bx} \quad (2.2)$$

Before a decision was given for the type of fitting, different forms were tested, such as polynomials, power law, quadratic, and exponential. In general, all these types of fitting models yield close results with respect to the correlation coefficient which is defined as

$$r = \sqrt{\frac{\sigma^2 - S^2}{\sigma^2}} \quad (2.3)$$

where σ and S are standard deviation and deviation from the fitting curve. However, exponential form is more realistic when the behavior of the heat flux, as the function of the axial distance, is concerned. The correlation coefficient was calculated to be between 0.98 and 1.0, which is quite acceptable.

C. Spatial derivative of cooling water temperature $T(x)$ found in step (B) was used to predict the heat flux profile in the annulus of jacket pipe. Since the environmental heat loss from the jacket pipe is very low no correction was applied to the heat flux profile prediction. The local heat flux at the inner tube wall, based on inner diameter (d_i) of the condenser tube, was calculated from

$$q''(x) = -\frac{\dot{m}_{cw} c_p}{\pi d_i} \frac{dT_{cw}(x)}{dx} \quad (2.4)$$

The derivation of Equation (2.4) was based on the energy balance given in Figure , for steady state and steady flow conditions.

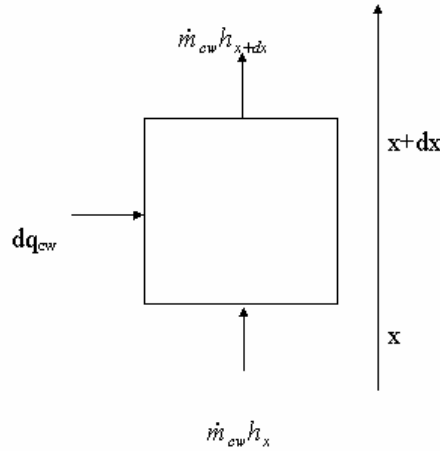


Figure 2.4-1 Energy Balance on a Control Volume of the Jacket Pipe

The energy balance then yields

$$dq_{cw} = \dot{m}_{cw} (h_{x+dx} - h_x) \quad (2.5)$$

or

$$dq_{cw} = \dot{m}_{cw} dh \quad (2.6)$$

and by inserting $dh=c_p dT$, we get

$$dq_{cw} = \dot{m}_c c_p dT \quad (2.7)$$

D. The experimental heat transfer coefficient was then calculated from

$$h(x) = \frac{q''(x)}{T_c(x) - T_w(x)} \quad (2.8)$$

E. The absolute system pressure was calculated from the measured gauge pressure at the inlet of the test section by considering the measured local absolute pressure in Ankara. This modification for the measured absolute system pressure was needed to calculate the correct saturation temperature of vapor at the inlet of the test section, and partial pressure and saturation temperature of vapor along the tube.

F. The mass flow rate of vapor or air/vapor mixture and associated Reynolds number were calculated. For this step, the calibration data of the orifice, i.e. flow coefficient and Reynolds number relation given in Section 0, were used.

Mass flow rate computation is purely a mathematical process once a calibration curve of the orifice has been generated. Since flow coefficient is dependent on Reynolds number, which is dependent on mass flow rate, final value of the flow coefficient, and hence of mass flow rate, can be obtained iteratively using an initial chosen value of Reynolds number.

For the computation of mass flow rate, the method given in BSI-1042 [8] was used. Initial guess for the Reynolds number was 10^6 and the iterative procedure included the calculation of flow coefficient from Equation 2.1, and mass flow rate from the relation of Reynolds number based on internal pipe diameter (D) at the upstream of the orifice:

$$\text{Re}_D = \frac{\dot{m}D}{A_D\mu} \quad (2.9)$$

Here \dot{m} and μ are given for vapor or air/vapor mixture, depending on the method of air injection, i.e. if air is injected to water inside the boiler then mixture properties should be used.

Then, differential pressure over the orifice as calculated from

$$\Delta P = \frac{1}{2\rho} \left(\frac{\dot{m}}{\alpha \frac{\pi}{4} d^2} \right)^2 \quad (2.10)$$

was compared to the one measured and the iteration, by changing the Reynolds number guess, continued till the calculated differential pressure was equal to the measured one. The density (ρ) in Equation (2.10) is calculated by considering upstream condition of the orifice (vapor or air/vapor mixture depending on the method of air injection).

2.5 RESULTS AND DISCUSSION OF METU-CTF EXPERIMENTS

The experimental investigation of condensation of pure vapor and air/vapor mixture in case of loss of coolant (or feed-water) in secondary side of condenser imposes a special case since boil-off rate directly affects condensation process inside a condenser tube. The motivation for this special case comes from the analysis [1] of the experiment concerning loss of residual heat removal system during reduced coolant inventory operation with inactive steam generators, performed at the UMCP 2X4 integral test loop [9,10,11]. The first phase of this type of analysis comprises the boiler-condenser mode (BCM) of operation during which steam generator is active. However when the steam generator becomes inactive due to loss of feed-water to the secondary side (second phase), heat transfer from primary to secondary side that is mainly by condensation degrades and system pressure escalates. To address the issue outlined here, two experiments were performed at the METU-CTF, including the first phase (BCM) and second phase (loss of coolant) of the scenario.

As given in Section 0, the power of the heaters in boiler tank was set to 10 kW throughout the whole test period and the exit part of the condenser tube (primary side) was closed. A steady-state condition could be reached for BCM in pure vapor case, however the BCM represents a quasi-steady condition for air/vapor mixture case. The time dependent pressure trends are presented in

Figure . The pressure increase upon loss of coolant is almost linear by time and the rate of increase is about 0.6 mbar/s, for both cases. The Re_v was predicted to be between 50,000 (top position) and 25,000 (bottom position) for pure vapor case during BCM whereas the mass flow rate was far below the measuring limit ($Re_v < 40,000$) of the orifice meter for air/vapor mixture case. This shows that the vapor was sucked into the condenser tube due to condensation in BCM and the rate of suction drops considerably when some amount of air is trapped in the condenser tube prior to the start of experiment. However, the vapor flow rate rapidly decreases during transient as the result of diminishing heat transfer rate and falls below the measuring limit of the orifice meter even for pure vapor case. It is clear that the rate of vapor suction is the function of condensation rate and hence a comparison of total heat transfer rates in cases with and without air could be good evidence (Figure); during BCM mode of operation in pure vapor case the total heat transfer rate is 19 kW which is as twice as that of air/vapor mixture case, i.e. 8 kW. This implies that the vapor suction rate was greater than the boil-off rate of water in the boiler during BCM in pure vapor run, since the heater power was set to 10 kW during whole period.

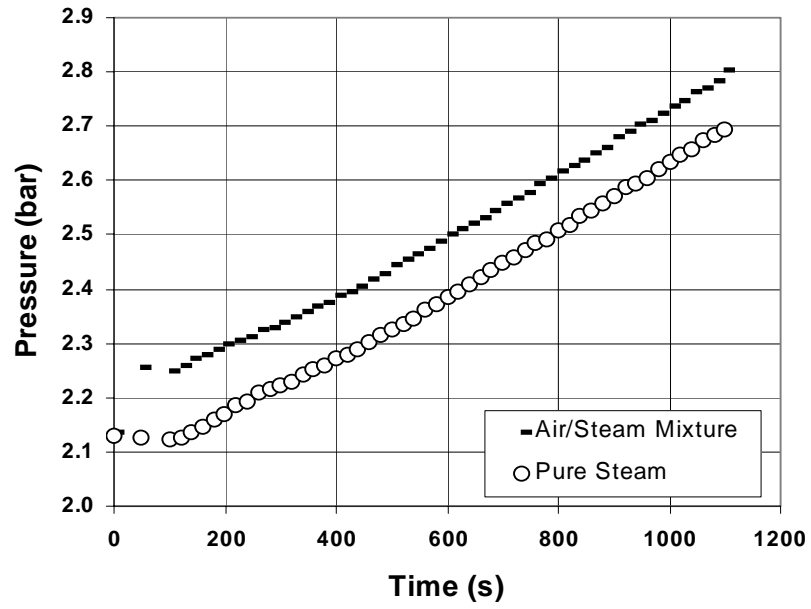


Figure 2.5-1 System Pressure for Loss of Coolant Transient

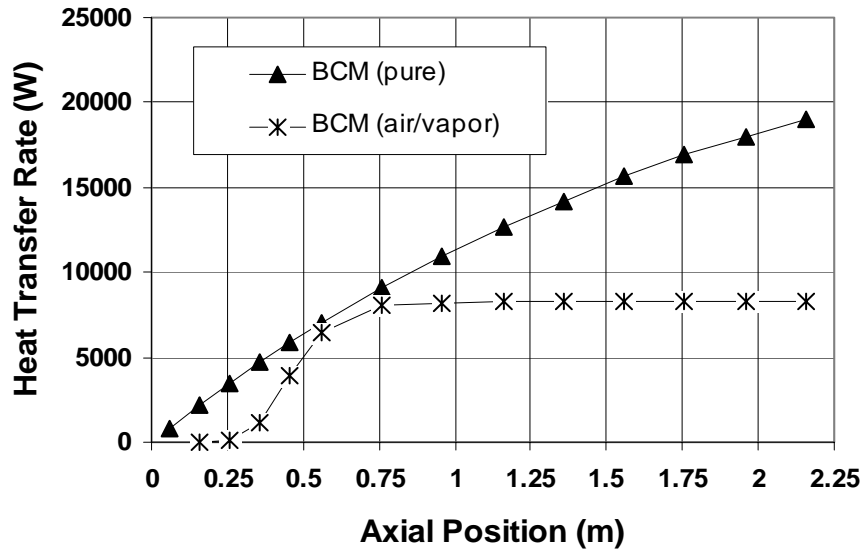


Figure 2.5-2 Cumulative Heat Transfer Rate Along the Condenser Tube

The temperature of coolant in jacket pipe is presented in Figure , for pure vapor case. It is clearly seen that at 200 s the bulk temperature of coolant reaches to 96°C at the exit. When time progresses to 600 s, about 25% of the coolant channel becomes full of saturated vapor and this remains almost unchanged till 1100 s. The similarity of coolant temperature profiles at 600 s and 1100 s implies that the heat transfer rate in radial direction and its axial dependency does not change considerably due to diminishing condensation heat transfer from the primary side. The governing parameter for this occurrence is the effective condensation length that gets smaller as coolant mixture level drops in secondary side. Since vapor in primary side was trapped inside the tube, it is likely to have a liquid accumulation at the bottom of the tube from the beginning of the experiment, which then further decreases the effective condensation length. This is evidenced from the measured inner wall temperature as presented in Figure ; in this figure shortening of effective condensation length for steady-state and transient measurements is clearly seen by observing a sharp decrease in temperature towards the bottom of tube.

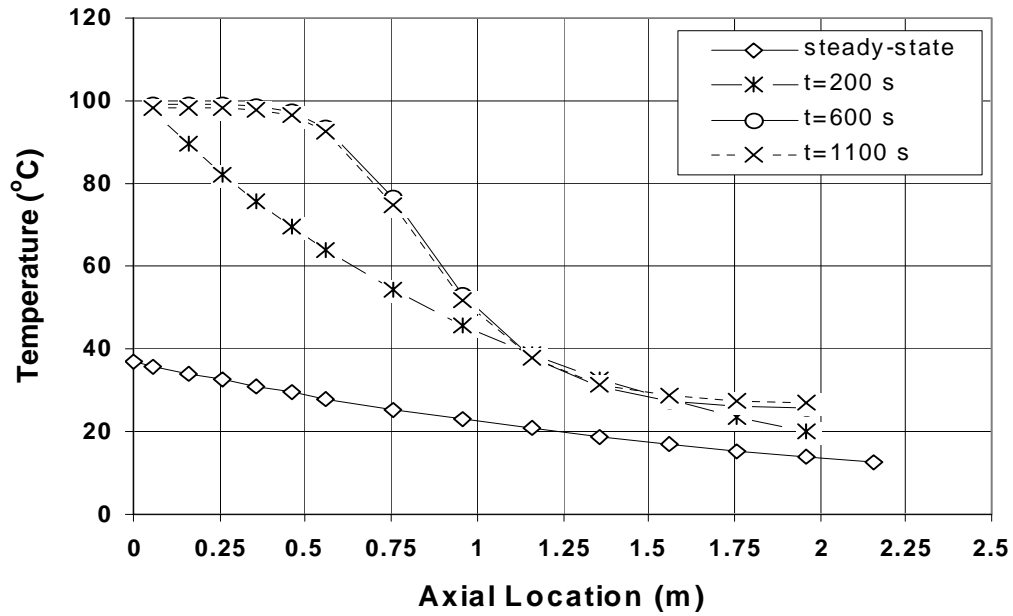


Figure 2.5-3 Coolant Temperature Profile for Loss of Coolant Transient (Pure Vapor)

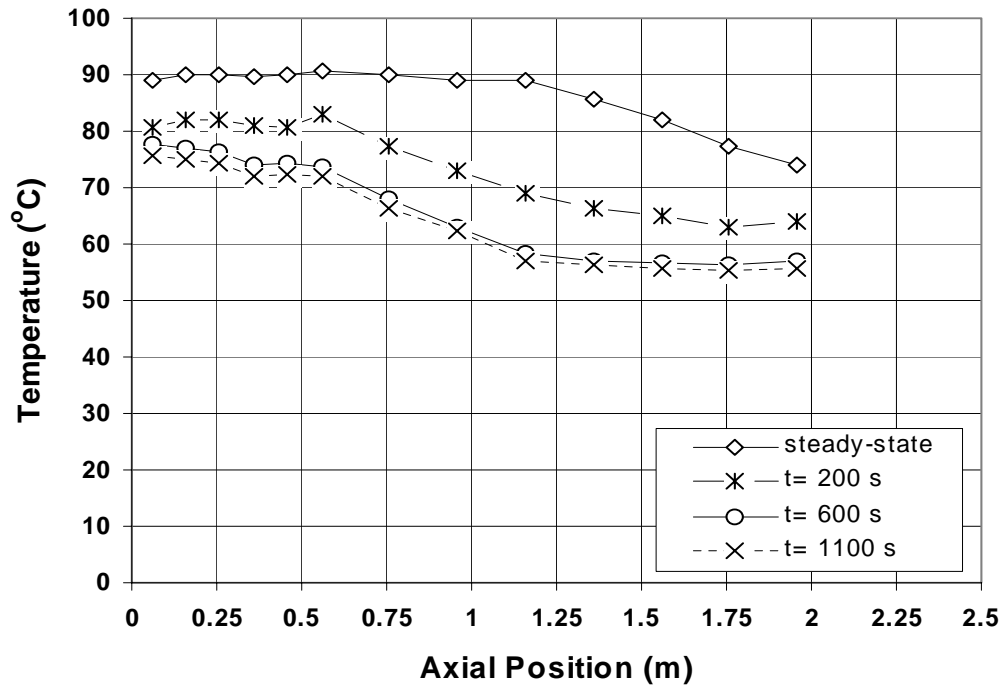


Figure 2.5-4 Inner Wall Temperature Profile for Loss of Coolant Transient (Pure Vapor)

The heat flow direction changes as time progresses and this can be best understood by comparing Figure and Figure . The temperature difference between inner wall and coolant (dT_{wc}) is about 60°C for steady-state case and it drops drastically during transient (Figure). The maximum dT_{wc} value is 25°C at 1100 s. The heat flow direction reverses at a distance of 0.25 m and 0.85 m (from top of the condenser), for times 200 s, and 600–1100 s, respectively. The trend of dT_{wc} towards the end of condenser test section is such that it converges to a value between $30\text{--}40^{\circ}\text{C}$. Thus, heat removal from primary side changes to heat addition to the primary side, possibly by condensation of vapor at the jacket pipe, at the top of the test section and the length of heat flow reversal increases as mixture level in secondary side decreases. This is another evidence for how effective condensation length is affected by boil-off rate of coolant in the secondary side. It is implied from Figure that the effective condensation rate is considerably decreased as time progresses from end of BCM (100 s) to the end of transient period (1100 s).

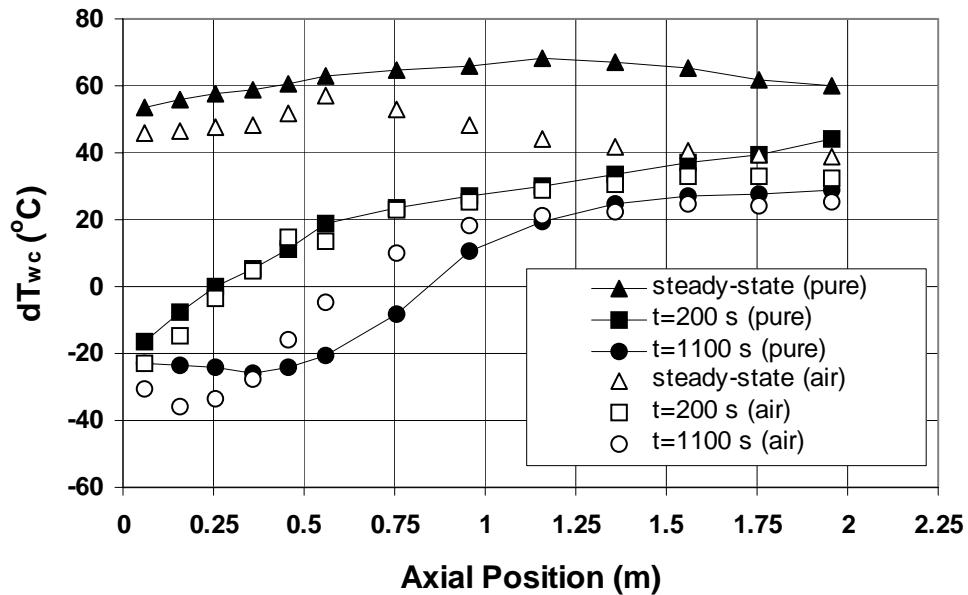


Figure 2.5-5 Temperature Difference Across Inner Wall And Coolant

The temperature profiles for coolant and inner wall of the condenser tube are presented in Figure and Figure , for air/vapor mixture transient case. The active condensation length is shortened by the presence of air, as indicated by coolant temperature profiles, compared to the pure vapor case. It is interesting to note that the effective condensation length is about 0.75 m from top, for steady state, and heat transfer rate dies off towards bottom keeping coolant temperature almost constant ($\sim 15^{\circ}\text{C}$) at the rest of the channel. Hence, the effective condensation length is affected by two factors: drop of coolant mixture level due to boil-off and increased diffusion resistance of air towards bottom of the condenser tube. As can be seen in Figure , the heat flow direction reversal is observed for 0.25 m and 0.62 m (from top of the condenser) for 200 s and 600–1100 s, respectively. The shorter heat flow direction reversal for $t \geq 600$ s, compared to the pure vapor case, is the result of less boil-off rate in air/vapor mixture transient that leads to higher mixture level in secondary side. This is the indication of how boil-off rate could be affected from presence of air in the system. The inner wall temperatures (Figure) clearly

indicate air accumulation towards bottom of the tube. Even in steady state run, the temperature starts to fall at length 0.6 m whereas it is 1.25 m in pure vapor run. Moreover, the inner wall temperatures drop below 50°C in air/vapor mixture transient while they remain above that value for pure vapor run. Here it is worth to mention that the inner wall temperature is suppressed along the tube, due to existence of air inside, and comparison with corresponding pure vapor results gives a temperature difference of 15°C and 30°C at 0.6 m and 1.4 m from top, respectively, for steady state. For transient (t=1100 s), the temperature difference is 18°C and 13°C, at the same axial location. The temperature suppression, for lower half of the tube, is smaller in transient period when compared to the steady state period. This can be attributed to the accumulation of condensate inside the tube.

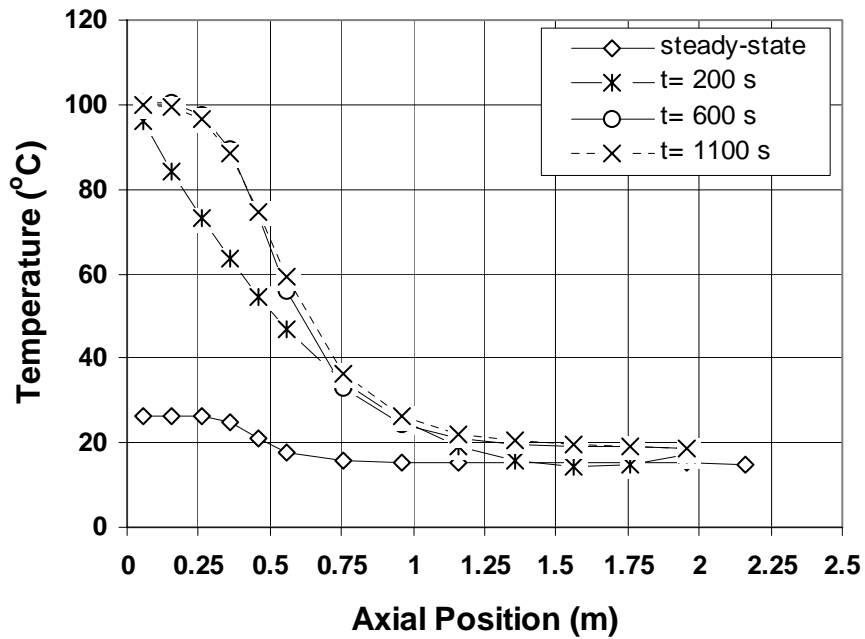


Figure 2.5-6 Coolant Temperature Profile for Loss of Coolant Transient (Air/Vapor Mixture)

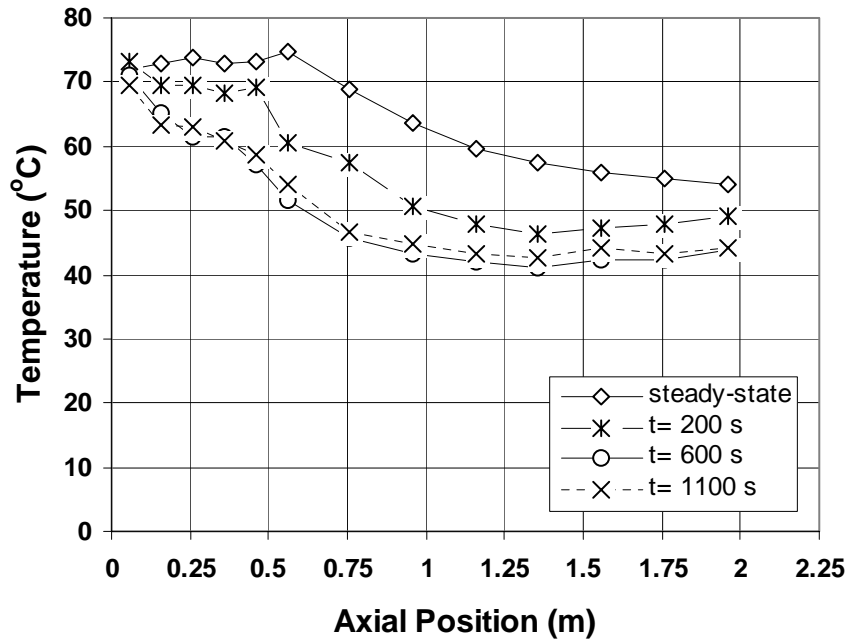


Figure 2.5-7 Inner Wall Temperature for Loss of Coolant Transient (Air/Vapor Mixture)

The effect of air on coolant and inner wall temperatures can be best observed in Figure , Figure , Figure and Figure . At steady-state period, the variation of both temperatures exhibits a characteristic trend indicating how accumulated air inside the condenser tube could adversely affect the heat transfer process in a heat exchanger. At first glance we see that both temperatures (coolant and inner wall) are suppressed due to existence of air inside the tube: The decreases in coolant and inner wall temperatures are as high as 10°C and 30°C, respectively. But more interesting is the shape of the coolant temperature variation of the case with air/steam mixture compared to the corresponding pure steam case. The heat transfer to coolant dies off below 0.75 m (from the top) in case with air while it decreases almost linearly towards the bottom of channel in pure steam case. In other words, the effective heat transfer –presumably by condensation– length seems to be about 0.5 m (

Figure) in the mixture case, which is much shorter than that of pure steam. The temperature profiles of coolant and inner wall for transient case ($t=200$ s and 1100 s) are presented in Figure and Figure . There are two outcomes when the figures of coolant temperature are referred to: First, the boil-off rate decreases in case of air/steam mixture due to weaker heat transfer rate to the secondary side ($t=1100$ s in respective figure); second, the coolant temperatures are suppressed towards the end of condenser due to presence of air in tube. It is interesting to note that the coolant temperatures of air/steam mixture experiment corresponding to times of 200 s and 1100 s, get closer at 0.75 m from top. However, the same occurrence is observed at 1.13 m for pure steam experiment. These nodes of equal temperature can be considered as the axial positions of loss of heat transfer effectiveness. Though gets diminished at the end of condenser tube the effect of air is still observable towards the end tube. For example, the temperature suppression measured is as high as 10°C, at 1.5 m from the top. The suppression of inner wall temperatures due to effect of air could also be observed from Figure . The inner wall temperatures approaches to an approximate value of 60°C and 45°C for pure steam and mixture cases, respectively.

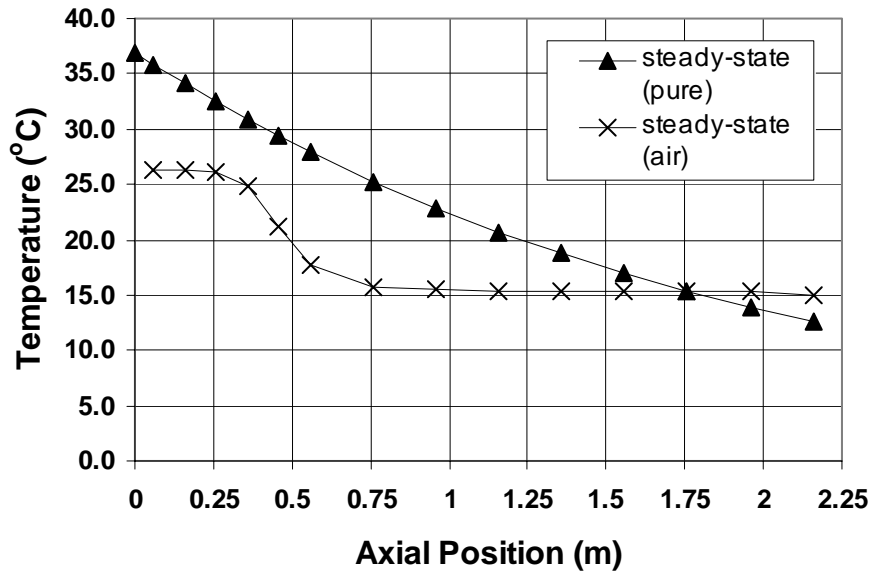


Figure 2.5-8 Comparison of Coolant Temperature Profiles for Steady-state

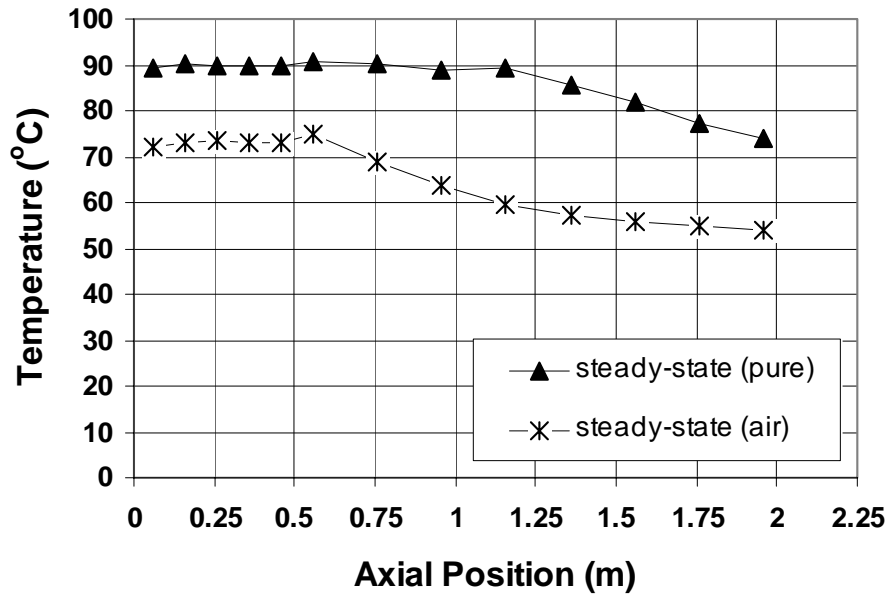


Figure 2.5-9 Comparison of Inner Wall Temperature Profiles for Steady-state

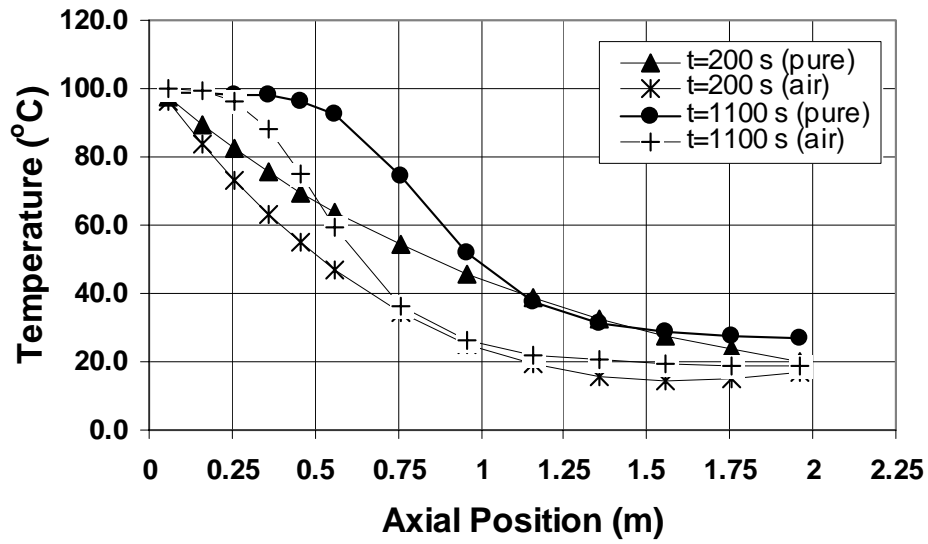


Figure 2.5-10 Comparison of Coolant Temperature Profiles for Transient

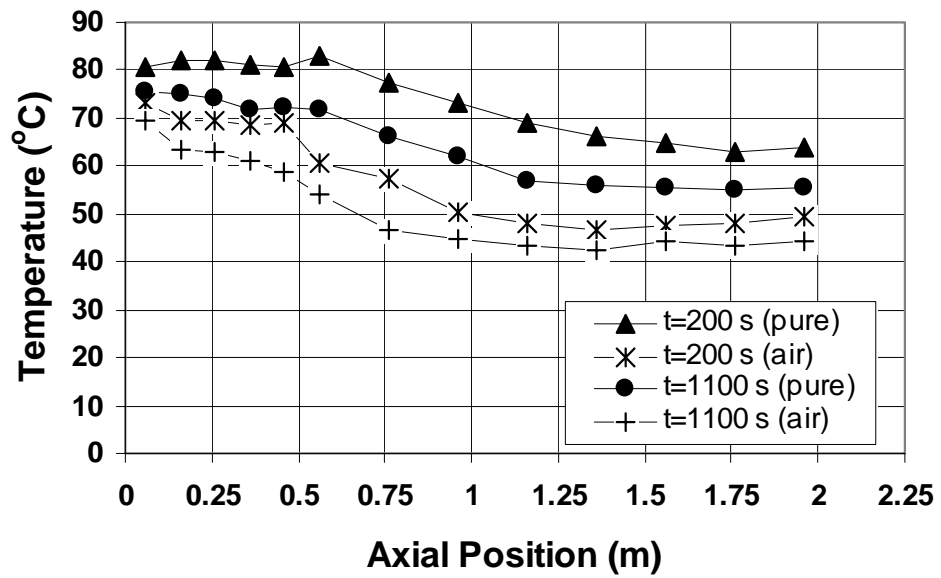


Figure 2.5-11 Comparison of Inner Wall Temperature Profiles for Transient

2.6 RESULTS OF RELAP5 SIMULATIONS

In this section, the results of the simulations performed by using the RELAP5/mod3.3 (beta version) code [7] are presented. The RELAP5 model (Figure) consists of 43 volumes, 41 junctions and 17 heat structures with total mesh points of 221. The input model is given in Appendix A. The model for condenser tube consists of 17 volumes. The volume heights were adjusted according to the elevations of thermocouples used for inner wall and coolant temperatures so that they are at the volumetric centers. Two sets of runs, which correspond to pure steam and air/steam mixture cases, were done. In each run, the mass flow rate was set to “zero” in time dependent junction (TJ-412) to simulate “no flow” condition at the outlet of the condenser tube. The total transient period in calculations is 1000 s as in experiments, however the steady-state period (100 s in experiment) that corresponds to the Boiler-Condenser Mode (BCM) of operation has been adjusted till an agreement was achieved for the coolant temperature distribution in the jacket pipe for both BCM and transient periods. It should be pointed out that this kind of simulations is very sensitive to the length of period of BCM prior to transient (loss of coolant to the secondary side) since steam flow to the condenser tube initiates condensation and accumulation of condensate due to heat removal to the secondary side. An optimum length of time for BCM should be selected in calculations to be able to get a realistic coolant temperature distribution in the jacket pipe, for both BCM and transient periods. After some trial runs the optimum BCM periods was found to be 200 s and 300 s for pure steam and air/steam mixture runs, respectively. In general, longer BCM period in calculations results in suppression of coolant temperatures with shorter length of saturation distance at the top for transient period. The BCM period for air/steam mixture run has an exceptional importance since air accumulation and hence distribution is directly affected by the rate of condensation and air suction. In other words, if BCM period gets longer air inside of tube can be suppressed more prior to the transient. In this transient the distribution of air mass fraction plays a central role for secondary side temperature distribution and boil-off rate.

Besides these, two sets of calculations (one for in-tube conditions without the jacket pipe and one for coolant side conditions without primary side) were performed by using measured inner wall temperatures as the boundary condition to be able to find heat transfer rate from primary side, coolant temperature, static quality, air quality, and saturation temperature distributions for air/steam mixture case. The details of results of these calculations performed by using RELAP5 code are presented in the following subsections.

2.6.1 Pure Steam Runs

The primary parameter for understanding the capability of RELAP5 for simulating the experiments of METU-CTF transients is the temperature of coolant inside the jacket pipe. After some trial runs it was found that the run with BCM period of 200 s yielded best fit to the experimental data, as could be seen in Figure . The results presented in Figure , Figure and Figure are from the RELAP5 model given in Figure , with jacket pipe. Times given in legend are times after the loss of coolant (feed-water) to the secondary side and “axial position” in X-axis stands for length measured from top. The pressure history measured in the experiment (see

Figure) was given as boundary condition (time versus pressure and quality) for TV-003 in Figure . There is a general agreement between RELAP5 results and data for coolant temperature trends (Figure) both qualitatively and quantitatively. A deviation is observed at 200 s such that the coolant temperature is underestimated at the exit of coolant channel. It is clear from figure that the coolant temperature measured at the exit of the

channel is about 96°C (almost saturated) while it is predicted to be about 80°C. However, the boil-off rate at time 1100 s was predicted almost correctly by the code although the length of channel in which saturated vapor exists seems to be shorter (~15 cm) in experiment. Although the coolant temperatures are in agreement with the data, an underestimation for local heat flux is observed, as given in Figure for steady state. According to the prediction of RELAP5 termination of condensation occurs at 1.2 m from top. As will be discussed below, better heat flux prediction was obtained when the measured inner wall temperature was given as boundary condition. The cumulative heat transfer rate as predicted by the model with the jacket pipe is presented in Figure . Heat transfer rate diminishes towards the bottom of the jacket pipe (coolant entrance) as expected, however the calculated heat transfer rate is highly underestimated (36%) towards the exit of the jacket pipe, especially at the last 1 m. This is evident from the coolant temperatures at steady state as well and the underestimation is as high as 6–10%. The code predicts heat transfer regime as condensation for the primary side volumes (first 12 volumes) in steady state condition. The heat transfer mode in the jacket pipe for steady state is predicted to be single-phase liquid convection, for all volumes. It is to be noted at this point that the wires of thermocouples in the jacket pipe could lead some uncertainties in prevailing flow and heat transfer regimes that is not possible for to code to predict. The flow and heat transfer regimes in secondary side play an important role for simulation of this kind of transients.

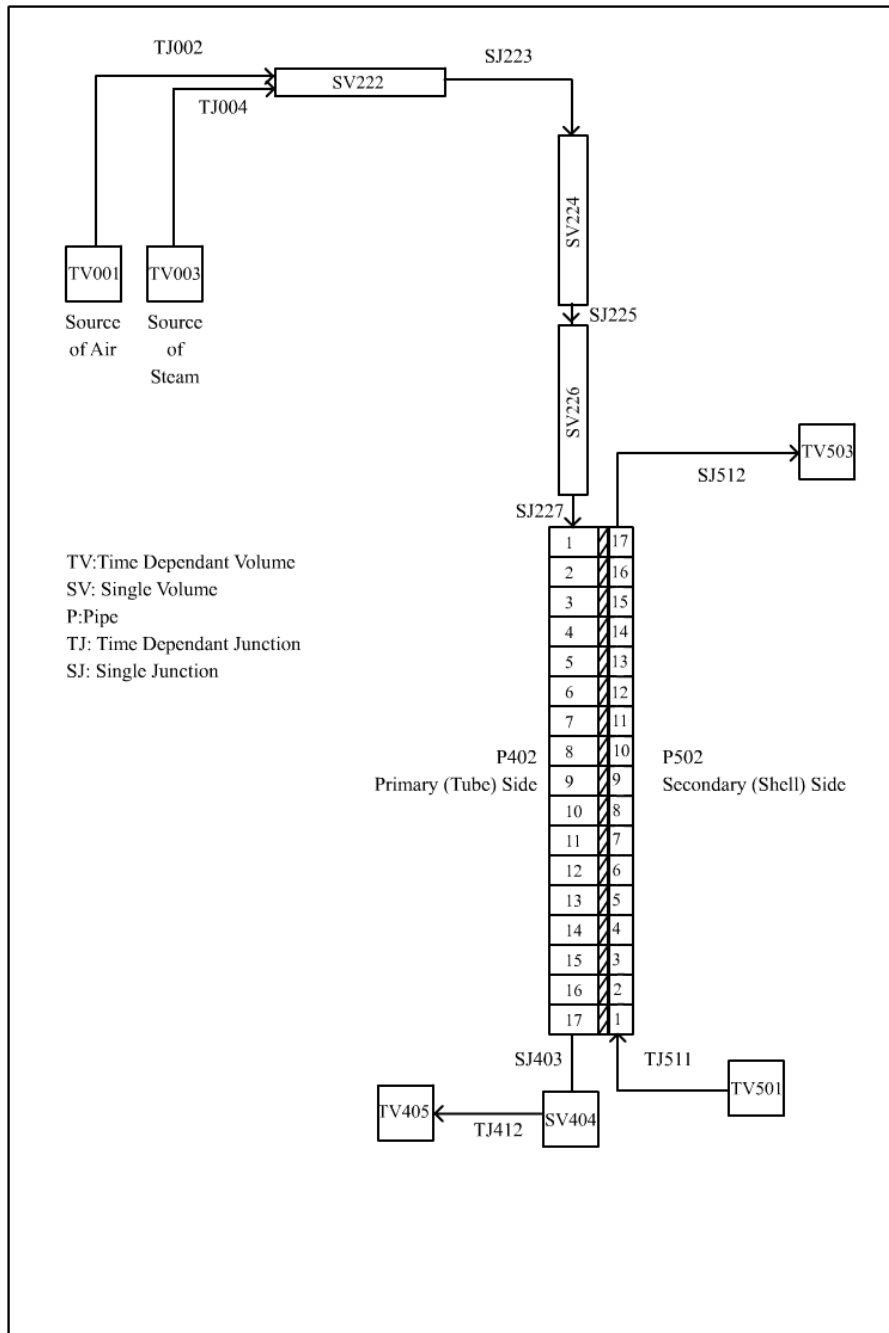


Figure 2.6-1 Nodalization Scheme of the METU-CTF for RELAP5 Computer Code

The calculated coolant temperatures under steady state and transient are seen in Figure for three axial positions of thermocouples (TC-2, TC-6 and TC-12) corresponding to 0.4 m, 1.2 m and 2 m from the bottom of jacket pipe, respectively. The comparison of RELAP5 results with the experimental data shows that the coolant temperature for steady state (BCM) is in agreement with the data while it yields an overestimation of about 8–10°C, for the thermocouple (TC-6) during transient ($t > 200$ s). The same overestimation can be seen in Figure at the axial location of about 1 m from top. However, calculated temperatures for TC-2 and TC-12 are much closer to the data with a difference of about 2–5°C and this is quite acceptable.

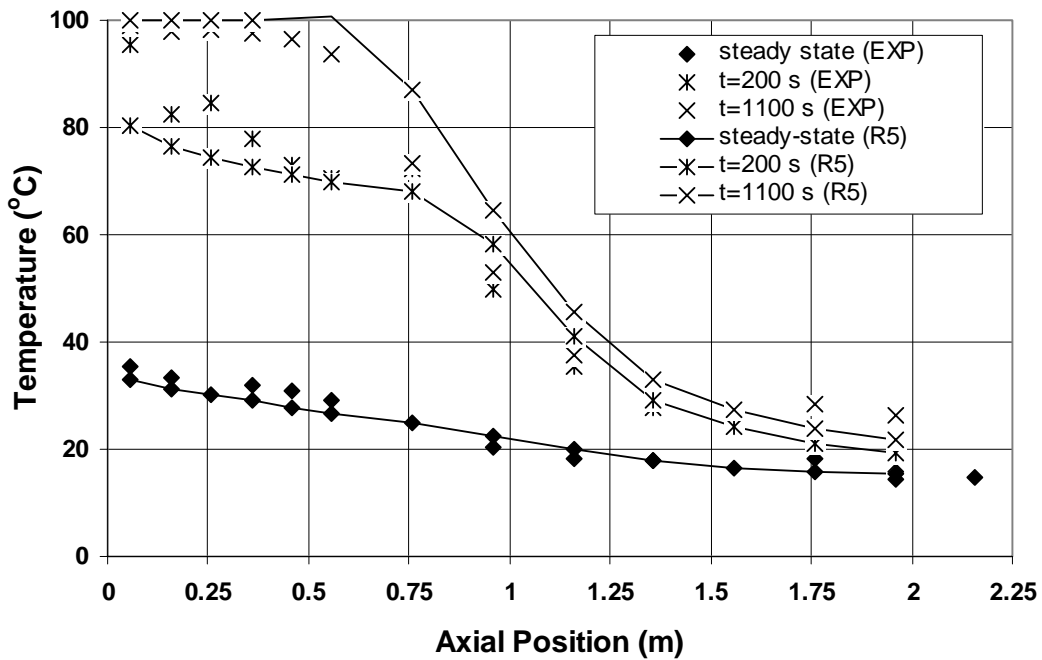


Figure 2.6-2 Experimental and RELAP5 Results for Coolant Temperature

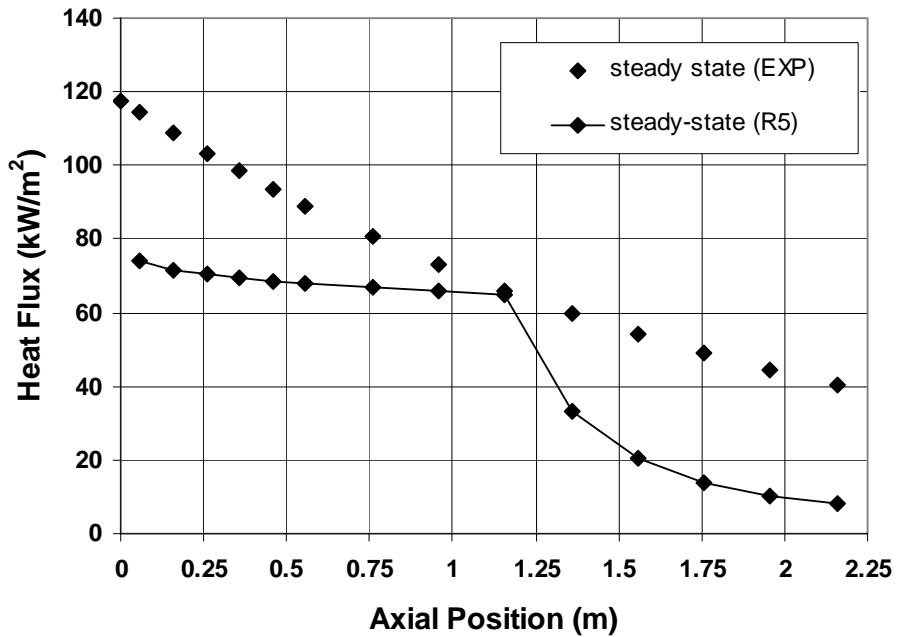


Figure 2.6-3 Experimental and RELAP5 Results for Local Heat Flux Distributions

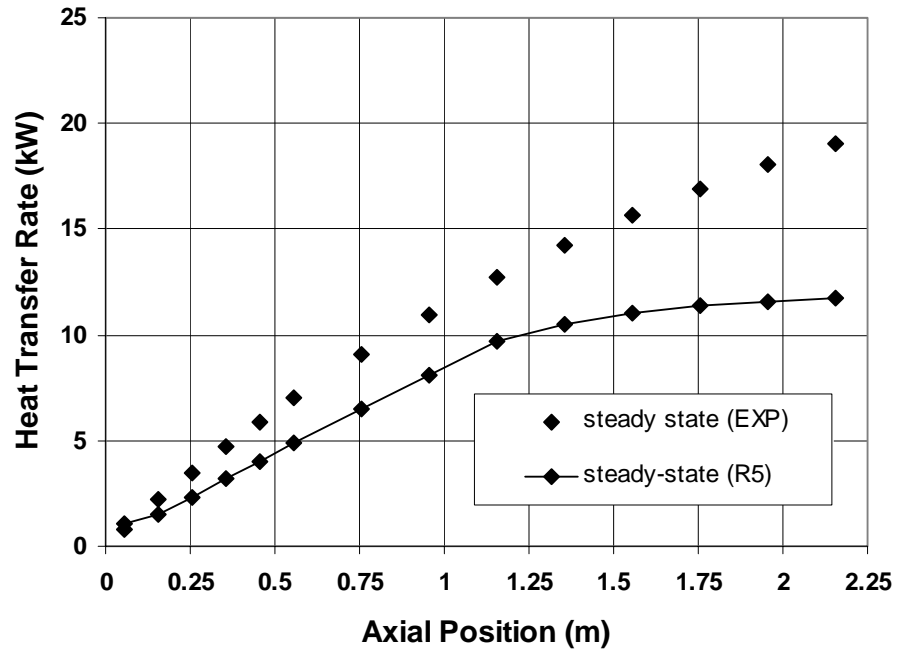


Figure 2.6-4 Experimental and RELAP5 Results for Cumulative Heat Transfer Rate

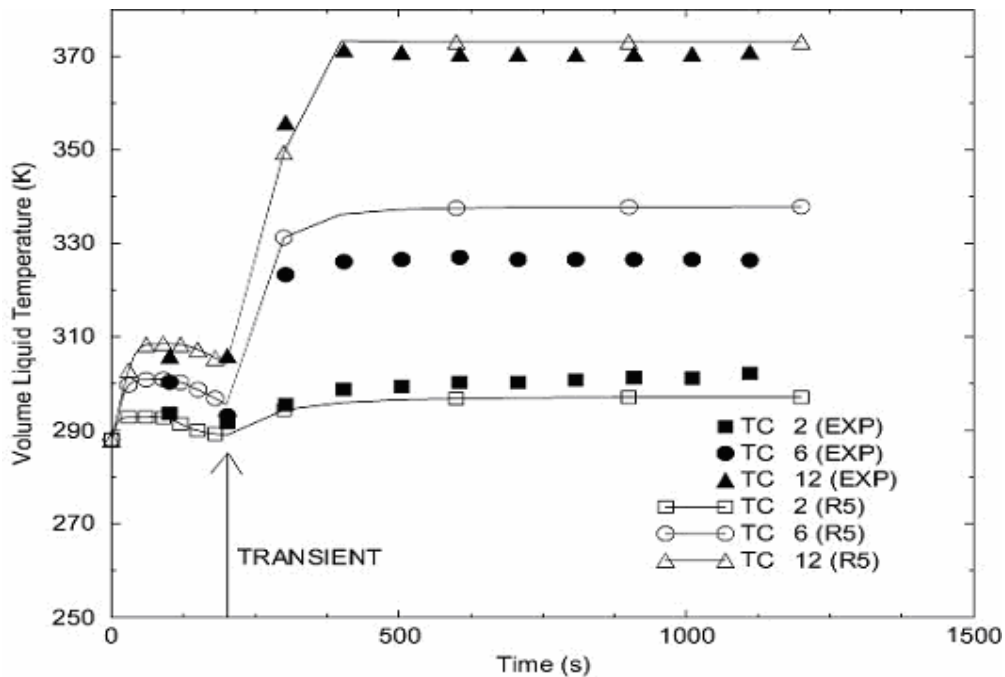


Figure 2.6-5 Experimental and RELAP5 Results for Coolant Temperature (0.4 m, 1.2 m and 2 m from bottom)

RELAP5 calculations were also repeated by using the measured inner wall temperatures since it is known that inner wall temperatures are subjected to some uncertainty with respect to film developed at the inner surface of the condenser tube. In ideal situation –or in theoretical approach– the condensate film is expected to develop at the entrance of the tube with zero film thickness at $Z=0$ m which may not be true in reality since condensate accumulation could be started before the entrance of the test section where environmental heat loss is possible. In METU-CTF, the vertical pipe with D_i of 38.1 and 33.5 mm and total length of 0.33 m were not thermally insulated and due to this reason some uncertainties (such as irregular film development or even dropwise condensation) associated with the liquid film development at the entrance of the condenser tube are expected to occur in this region. In Figure and Figure , the comparison of experimental data and RELAP5 calculations performed by using measured inner wall temperatures as boundary condition were presented. Since local heat flux and total heat transfer rate were not calculated in experimental data due to lack of measurement for coolant flow rate in jacket pipe during transient, only the results of steady state are presented in Figure and Figure . The jacket pipe was not taken into account in calculations presented here so that only the left surface values of local heat flux and cumulative heat transfer rate were considered. As could be seen in Figure , the local heat flux trend for steady state exhibits an underestimation of about 20% down to 1.25 m and then the heat flux dies off towards the bottom of tube with a considerable underestimation compared to the data. In RELAP5 run, the condensation terminates after 1.25 m and single-phase liquid convection prevails inside. However, the cumulative heat transfer rate prediction of the code for steady state is better than that of Figure (the model with the jacket pipe) and follows the trend of the data with an overestimation. The total heat load of the condenser, which is about 19 kW, is calculated with an error of less than 1%.

For the sake of understanding the capability of the code to simulate the coolant temperature profile by imposing the measured inner wall temperatures, a model for jacket pipe was used

and the coolant temperature profile, as given in Figure , was obtained. The predicted coolant temperature is not as good as the one presented in Figure (calculation with primary and secondary side) and exhibits an underestimation of about 3–5°C for the first 0.5 m of the tube. However, there is an overestimation of 4°C (maximum) at the rest of the channel. The heat transfer mode in the jacket pipe for steady state is predicted to be single-phase liquid convection, for all volumes.

The effect of fine-node model was also tested since it was expected that the condensation took place in condenser tube could be sensitive to the number of volumes modeled. A run performed by a model of 27 volumes for condenser tube and 27 volumes for jacket pipe revealed the fact that the analysis is not sensitive to the number of volumes, at least for volume number greater than 17.

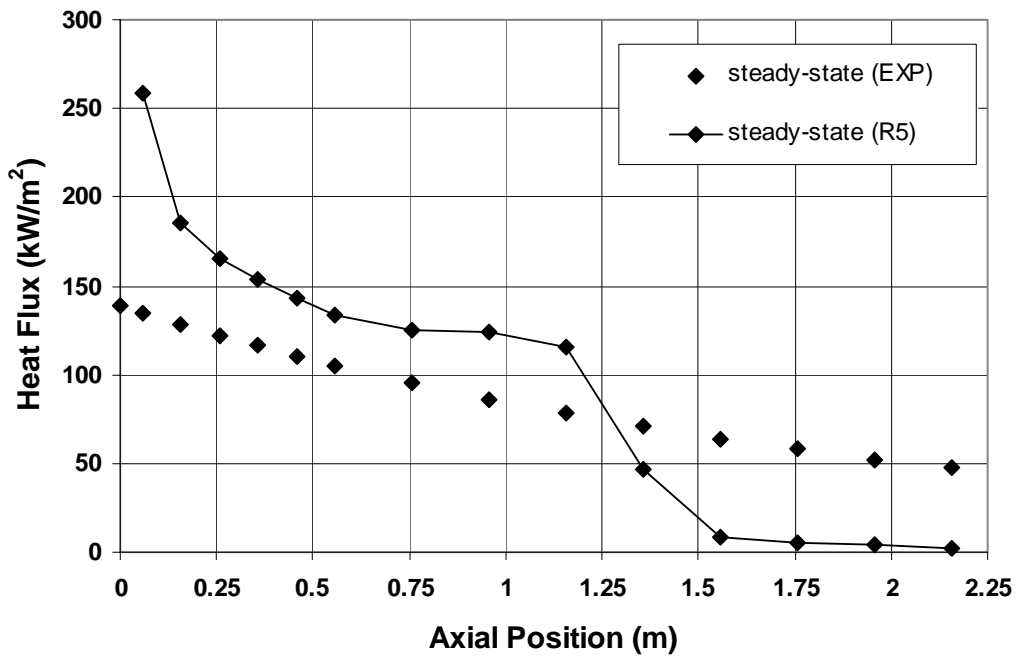


Figure 2.6-6 Experimental and RELAP5 Results for Local Heat Flux Distributions

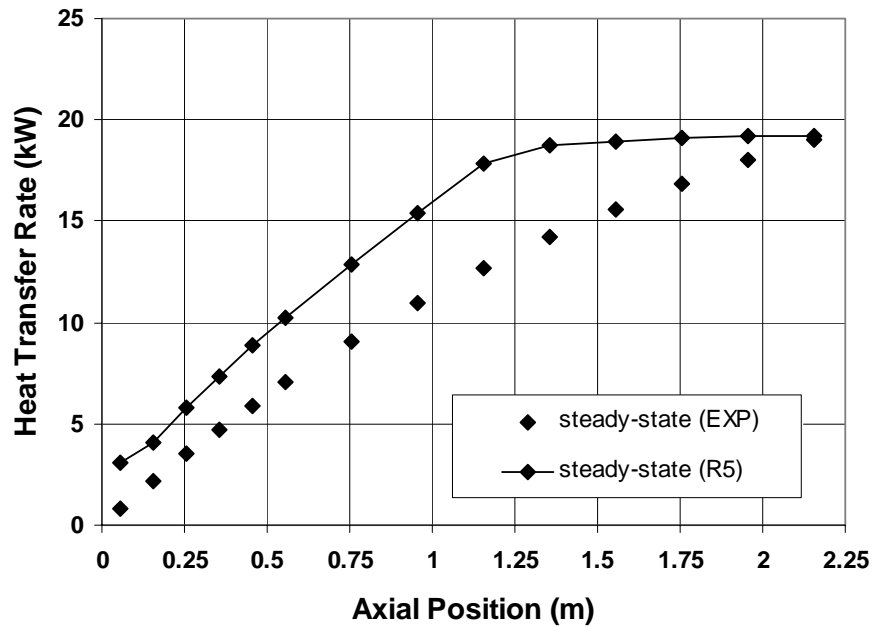


Figure 2.6-7 Experimental and RELAP5 Results for Cummulative Heat Transfer Rate

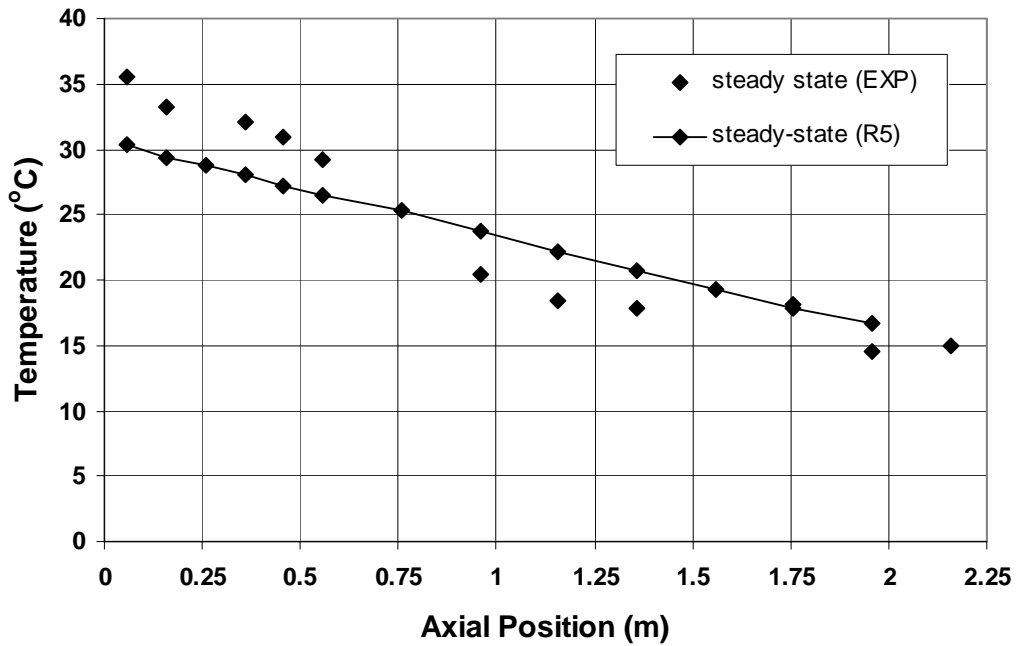


Figure 2.6-8 Experimental and RELAP5 Results for Coolant Temperature

The performance of the condenser as the function of time, under pure steam operating condition, can be apparently understood by referring to the Figure , Figure and Figure . It

is clear from Figure and Figure that the performance diminishes considerably after 500 s and goes down to almost zero power at the end of the transient. The governing factors to be considered for performance degradation are the prevailing heat transfer modes in primary and secondary sides, and condensate and coolant levels in primary and secondary sides, respectively.

The first 200 s represents the steady state period in RELAP5 calculations, as explained before. The heat transfer modes selected by the code at 200 s are condensation in primary side (1.2 m from top), single-phase liquid convection at the rest of the tube and single-phase liquid convection for all secondary side volumes. After the initiation of transient (loss of coolant to the secondary side) condensation is still the dominating mode of heat transfer, till 600 s. However, the heat transfer mode rapidly changes in secondary side: While heat is removed by single-phase liquid convection at 200 s, it turned to subcooled nucleate boiling at 300 s, for 0.8 m from top. Then, at 400 s, saturated nucleate boiling dominates heat removal from top (0.4 m). Single-phase vapor convection starts at about 500 s at which condenser performance considerably decreases. The degradation of the condenser performance is also clear from Figure : collapsed levels as calculated by RELAP5 come closer at about 500 s. The experimental data given in Figure does not directly represent the secondary side collapsed level since thermocouple elevations, normalized to the total length, at which measured temperature was 97–98°C (saturation temperature at the elevation of Ankara) were plotted to this figure. However, it is better to consider this data as a saturation line, which does not fully fit to the method of collapsed level calculation by RELAP5 based on a control variable technique considering “volume length x (1 – void fraction)” at each cell. In experiment, the saturation level is about 78.8% from 475 s till the end of the measurement.

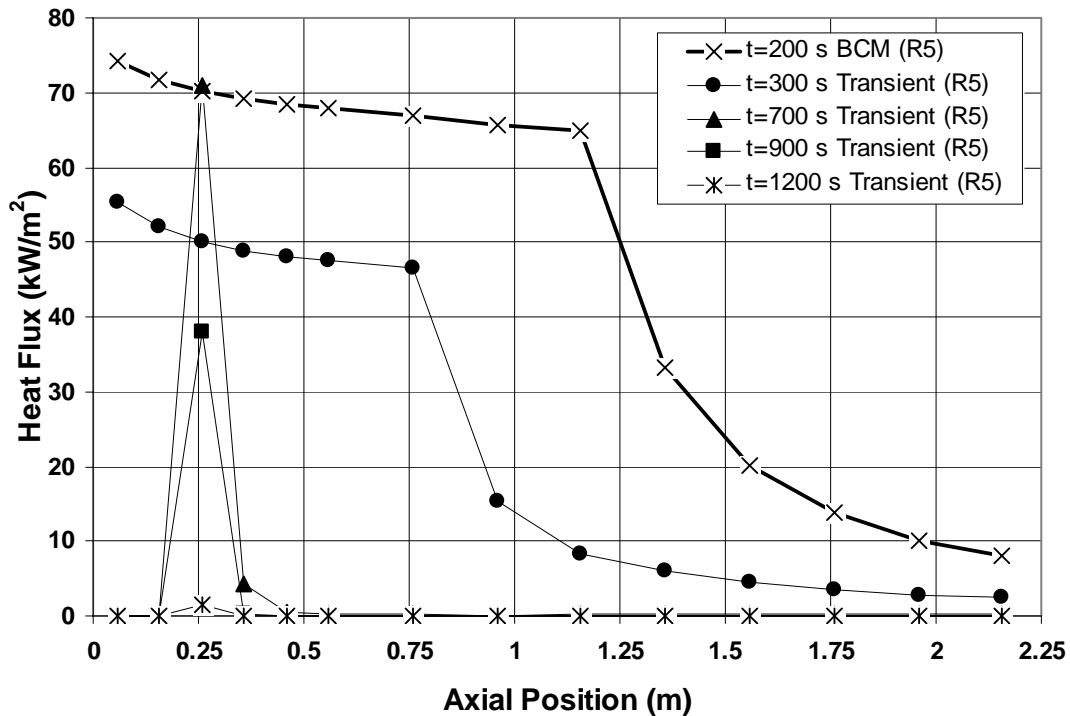


Figure 2.6-9 RELAP5 Results for Local Flux at Different Times

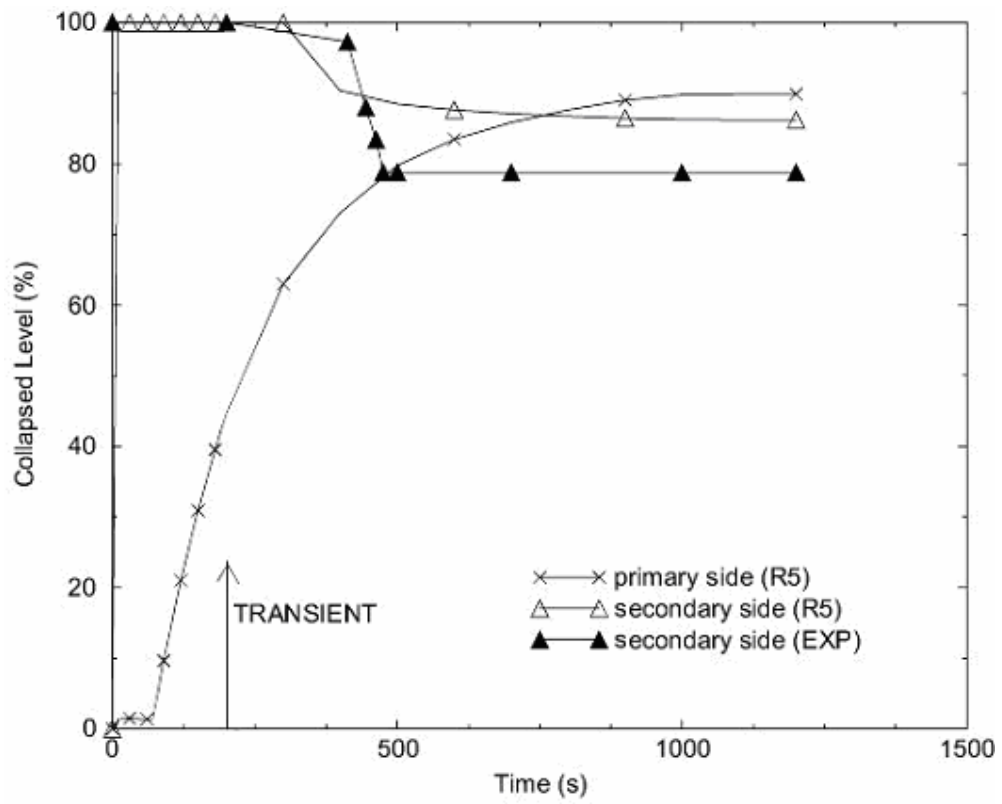


Figure 2.6-10 Liquid Collapsed Level in Primary and Secondary Sides

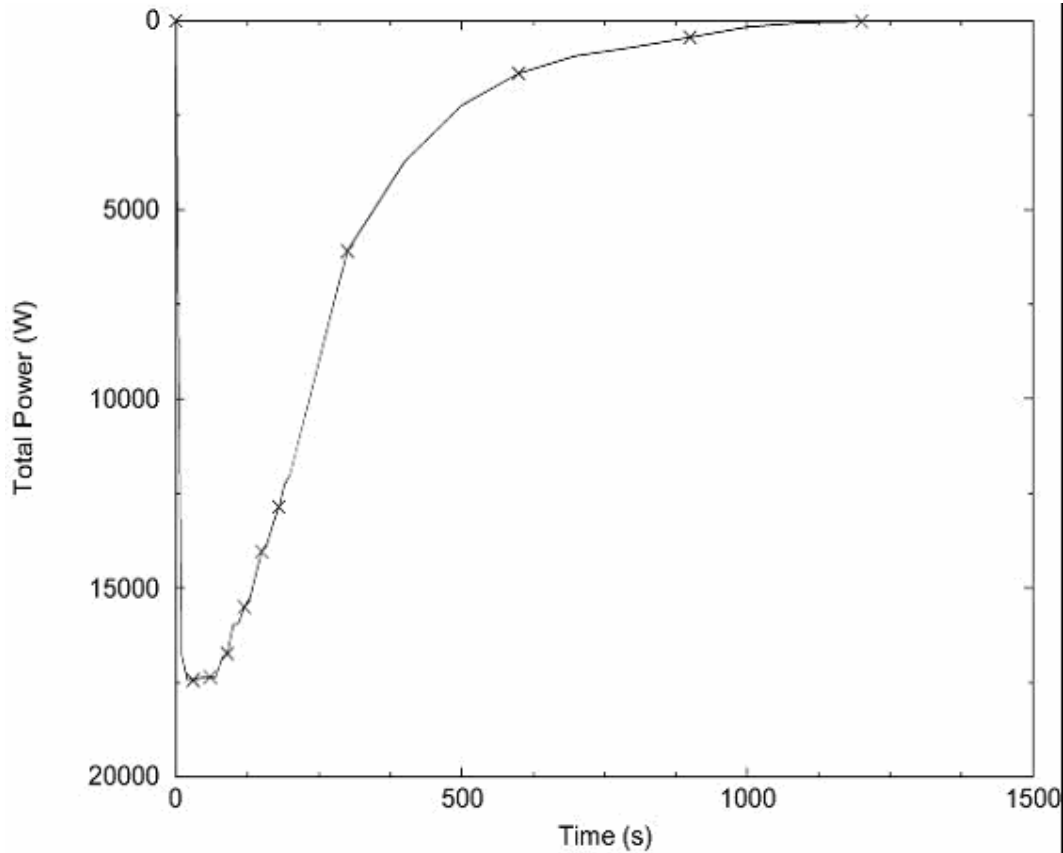


Figure 2.6-11 RELAP5 Result for Total Power of the Condenser

2.6.2 Air/steam Mixture Runs

As described in Section 0, the primary parameter for understanding the capability of RELAP5 for simulating the experiments of METU-CTF transients is the temperature of coolant inside the jacket pipe. In case the steady state (or at least quasi steady state which is named as BCM) calculation is to be performed for air/steam mixture, the length of the BCM period is important. In air/steam mixture case, the importance of the BCM period in simulation is due to two main factors: condensate accumulation and suppression of air inside the tube due to incoming steam (or suction due to condensation). It should be reminded that the bottom of the condenser tube was closed prior to data recording in experiments. So, incoming steam, condensate formed inside the tube due to condensation and air are enclosed inside the tube in BCM and transient periods. Hence the BCM periods should be well adjusted to be able to obtain acceptable results compared to the experimental data. Another parameter that affects the results is the mass of air inside the tube at the beginning of the calculation (BCM period), which is unknown in experiment. However saturated air mixed with steam was a reasonable assumption for the calculation and it is proved so. After some trial runs it was found that the run with BCM period of 300 s yields best fit to the experimental data.

In this section, the results of the base calculations performed by use of standard input model (with primary and secondary sides of the METU-CTF) will be presented. In this model, thermodynamic state of volumes representing the condenser tube was defined by flag "105" and input given for these volumes consists of pressure, static quality and air quality. The thermodynamic state of these volumes was calculated prior to the base calculation by an

input model, without the jacket pipe, with the time dependent measured inner wall temperature distribution given as boundary condition for heat structures. In this model, the state of primary side was set to saturated condition (i.e. flag “104” for volume initial condition and $X_s=1.0$). Then the saturated temperature, static quality and air quality distribution was obtained. In Figure static and air qualities obtained by use of measured inner wall temperature are shown. It is clear from this figure that air accumulation drastically occurs at the bottom of tube (approx. 0.8 m). The air quality (X_{air}) and static quality (X_s) is defined in Equations (2.11) and 2.12).

$$X_{air} = \frac{M_{air}}{M_{air} + M_v} \quad (2.11)$$

$$X_s = \frac{M_{air} + M_v}{M_{air} + M_v + M_l} \quad (2.12)$$

By referring to these definitions, it is apparent from Figure that the lower part of the condenser tube (1 m from the bottom) is predicted to be full of condensate with some minor amount of air accumulated inside. In other words air dominates gas phase at the bottom of tube however static quality is very close to zero, which means there is no vapor left to be condensed there.

Since thermodynamic state during BCM was forced by the input model, the BCM period was kept very short, i.e. 20 s. However, overall evaluation reveals the fact that the aforementioned input model with forced thermodynamic state inside the tube and the input with BCM period of 300 s plus all saturated air/steam mixture inside of condenser yield very close results. Moreover, the effect of fine-node model was also tested: A run performed by a model of 27 volumes for condenser tube and 27 volumes for jacket pipe revealed the fact that the analysis is not sensitive to the number of volumes, at least for volume number greater than 17.

The comparison of RELAP5 results obtained by use of standard model with jacket pipe and the experimental data for coolant temperature is given in Figure . Generally, the code prediction is in agreement with the data qualitatively and smallest deviation (most of the values deviates less than 10%) from the data is obtained for the steady state condition. However, the trend of coolant temperature does not strictly follow the data for steady state condition, which implies that the air mass distribution trend is somehow different from the experimental condition. Similar to the pure steam case, a deviation is observed at 200 s such that the coolant temperature is underestimated at the exit of coolant channel. It is clear from figure that the coolant temperature measured at the exit of the channel is about 96°C (almost saturated) while it is predicted to be about 76°C. However, the boil-off rate at time 1100 s was predicted almost correctly by the code although the length of channel in which saturated vapor exists is shorter (~10 cm) in experiment. Moreover, the temperature increase at times 200 s and 1100 s is steeper in experiment than that of code prediction, which results in higher deviations for prediction (+47% and +35%, respectively) between 0.26–0.76 m.

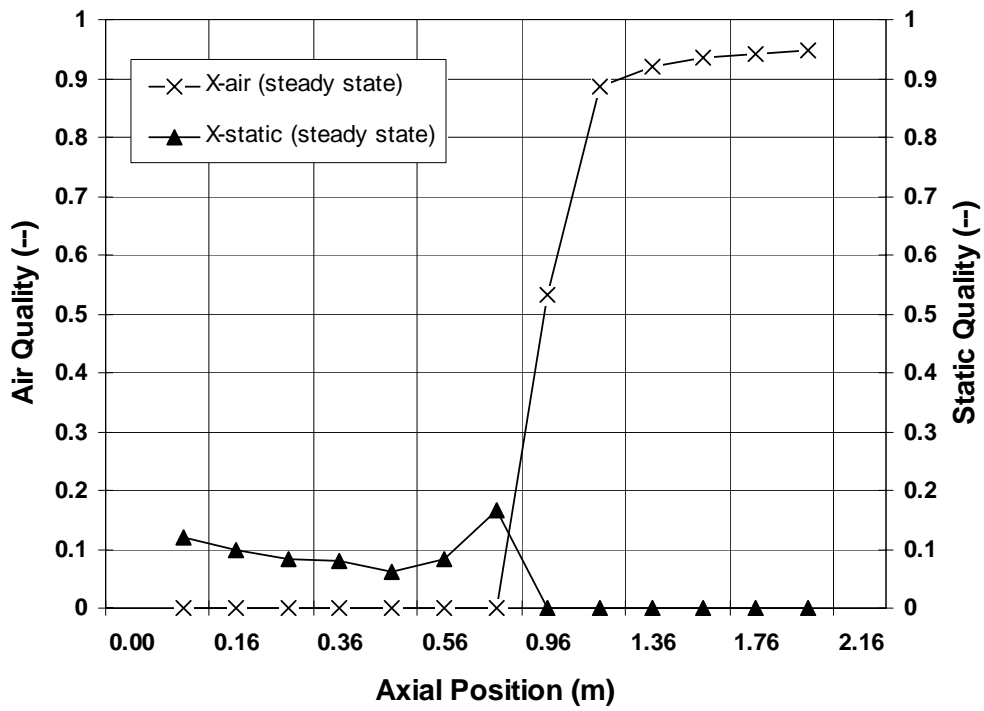


Figure 2.6-12 RELAP5 Results for Air and Static Qualities obtained by Measured T_{wi}

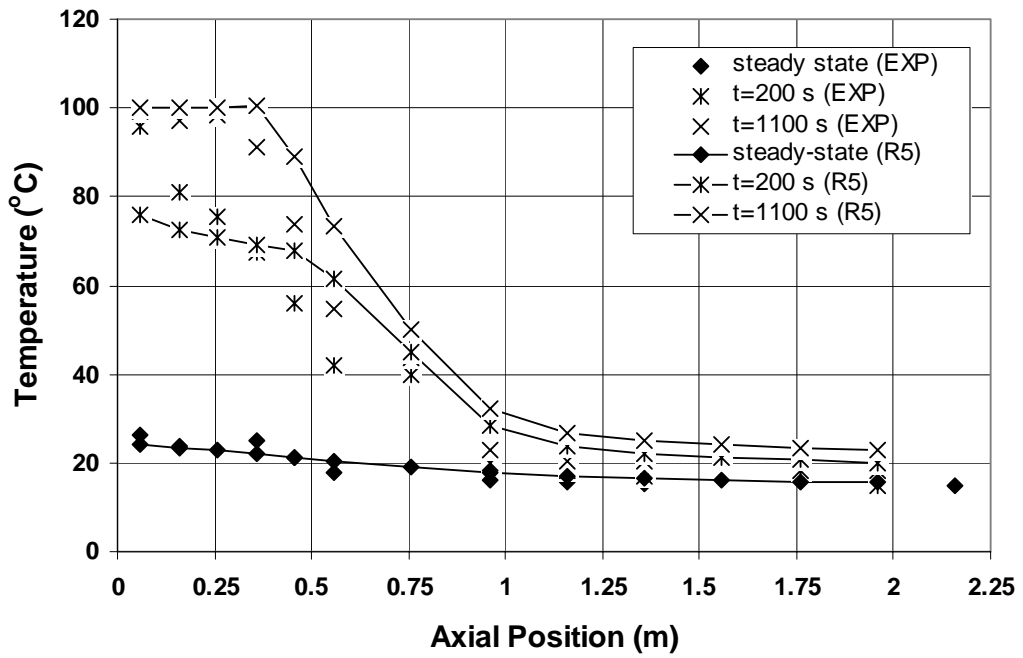


Figure 2.6-13 Experimental and RELAP5 Results for Coolant Temperature

The local heat flux distribution for steady state (BCM) is presented in Figure and main discrepancy comes from the peak at 0.5 m from the top of the condenser. This peak observed in the experimental data is due to the measured coolant temperature profile, which exhibits a very steep increase between 0.4–0.6 m (Figure). It is interesting to note that the coolant temperature remains almost constant from 0.37 m to the entrance (0 m) and this peculiar trend leads to a heat flux that sharply dies off towards the top of the condenser where steam enters. The observation made for the experimental data leads to a conclusion that there is a weak heat transfer by condensation at the first 0.37 m of the condenser tube. However it should be kept in mind that there is a higher uncertainty for the coolant temperature measurement at the exit of the jacket (inlet of the condenser tube) due to possible error in the thermocouple at the uppermost elevation (TJ-13, refer to Figure). But the measurements made by the thermocouples (TJ-12 and TJ-10) confirm the aforementioned weak heat transfer in this short entrance region. The weak heat transfer at the entrance region obtained in experiment is also observable in Figure . The code prediction for heat flux and total heat transfer rate does not imply accumulation of air as strong as the experiment does when the active heat transfer length is referred to. However the experimental result of coolant temperature, local heat flux and total heat transfer rate confirm the prediction of RELAP5 for the trends of local air and static qualities, as shown in Figure , i.e. there is no heat transfer at the lower half of the condenser of about 1 m from the bottom end. Moreover, the total heat load (8.3 kW) is predicted well by the code with a deviation of +4.6%, as could be seen in Figure .

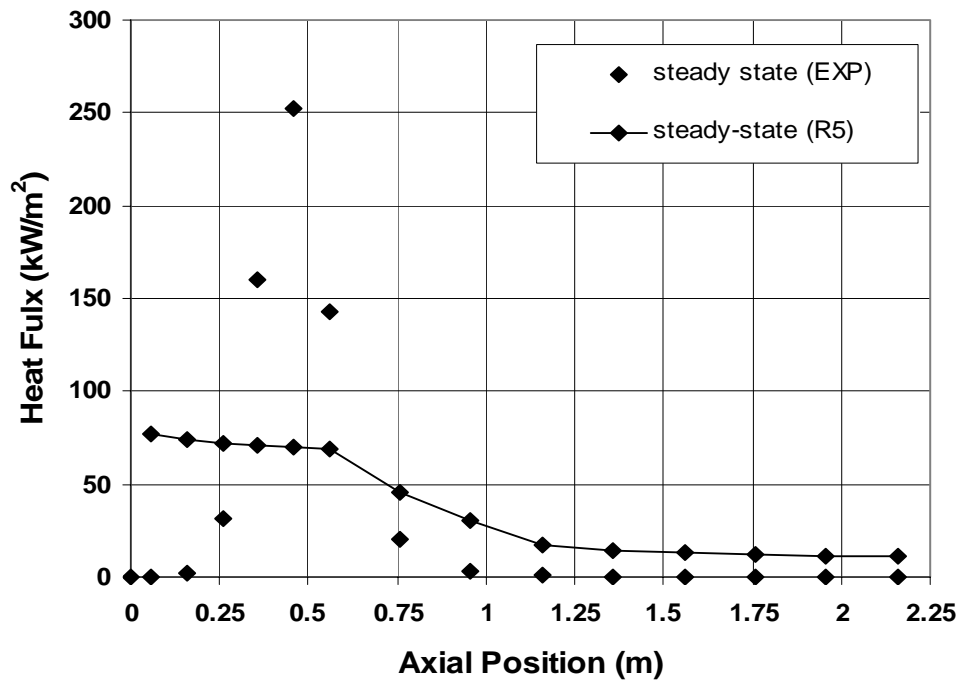


Figure 2.6-14 Experimental and RELAP5 Results for Local Heat Flux Distributions

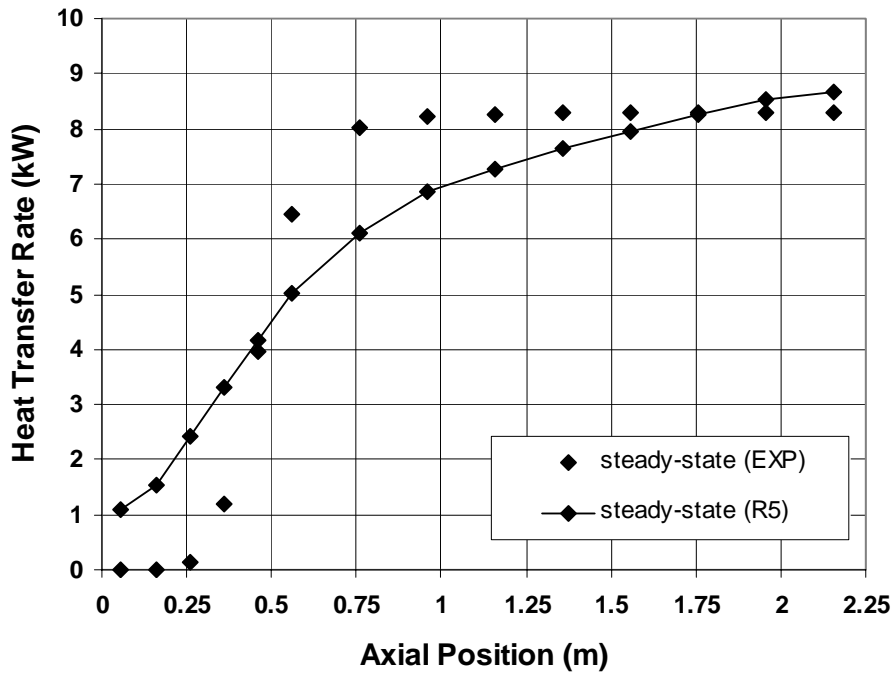


Figure 2.6-15 Experimental and RELAP5 Results for Cumulative Heat Transfer Rate

The calculated coolant temperatures under steady state and transient are seen in Figure for three axial positions of thermocouples (TC-2, TC-8 and TC-12) corresponding to 0.4 m, 1.6 m and 2 m from the bottom of jacket pipe, respectively. The comparison of RELAP5 results with the experimental data shows that the coolant temperatures for steady state (BCM) are in agreement with the data, with a maximum temperature deviation of 3°C, while it yields an overestimation of about 20°C, for the thermocouple (TC-8) during transient ($t \geq 200$ s). The same overestimation can be seen in Figure at the axial location of about 0.6 m from top. However, calculated temperatures for TC-2 and TC-12 are much closer to the data with a difference of about 2–3°C (with the only exception of prediction for TC-12 at 200 s that yields 8°C) and this is quite acceptable. Since temperature measurements at the elevations of 0.4 m and 1.2 m from the bottom (the elevation of TC-2 and TC-6) have yielded close results, the data for higher elevation (1.6 m for TC-8) was taken for Figure . It should be recalled that TC-6 has been taken for Figure (pure steam comparison) previously.

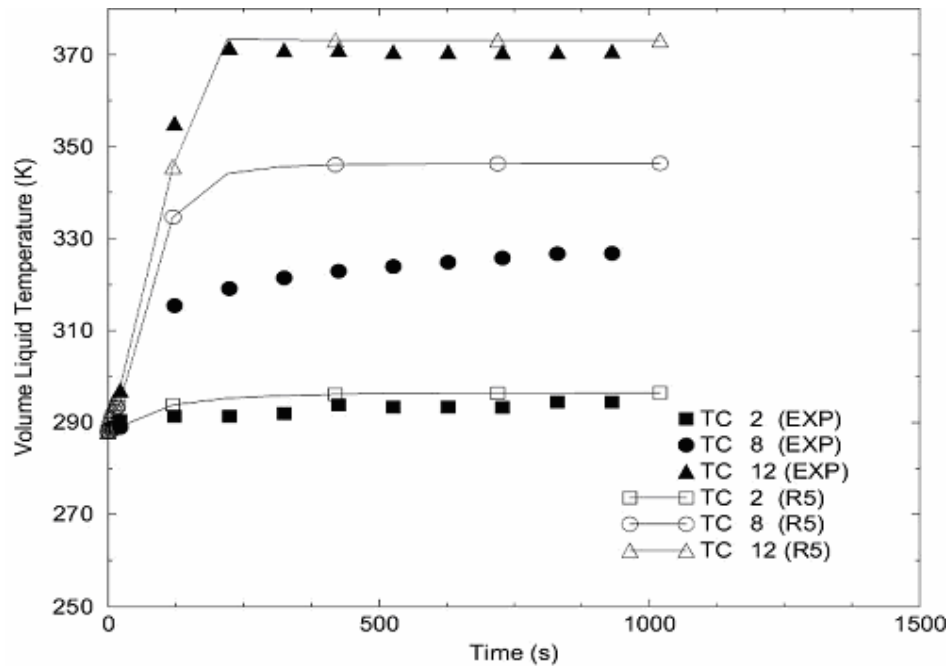


Figure 2.6-16 Experimental and RELAP5 Results for Coolant Temperature (0.4 m, 1.6 m and 2 m from bottom)

For sake of understanding the capability of the code in simulating the coolant temperature profile by imposing the measured inner wall temperatures (T_{wi}), an input model for jacket pipe was used and the coolant temperature profile, as given in Figure , was obtained for steady state. The predicted coolant temperature with T_{wi} used as boundary condition is not as good as the one with primary and secondary side (standard input model) and exhibits an overestimation of about 4°C (+22% deviation) from the experimental data, at the middle of the condenser. However, the standard model yields a maximum deviation from the data of about +9% at the same location. The trend of standard model follows the data in a much better way, which could be the indication of better estimation for local air quality distribution. But it should be pointed out that both models fail in simulating “snake-like” behaviour at the entrance of the condenser. There is a difference in heat transfer regimes (modes) as predicted by RELAP5 for each of the two models: The heat transfer mode in the jacket pipe for steady state is predicted to be single-phase liquid convection (subcooled wall) for all volumes in the model with a jacket pipe only (T_{wi} given as boundary condition) while subcooled nucleate boiling mode is switched on for the exit of the jacket pipe and the rest is single-phase liquid convection in a standard model. The heat transfer mode for the primary side of the tubes is calculated as condensation (void is less than one) for the first 9 volumes from top and condensation for air/steam mixture exists at 10th volume while the rest is single-phase liquid convection plus air.

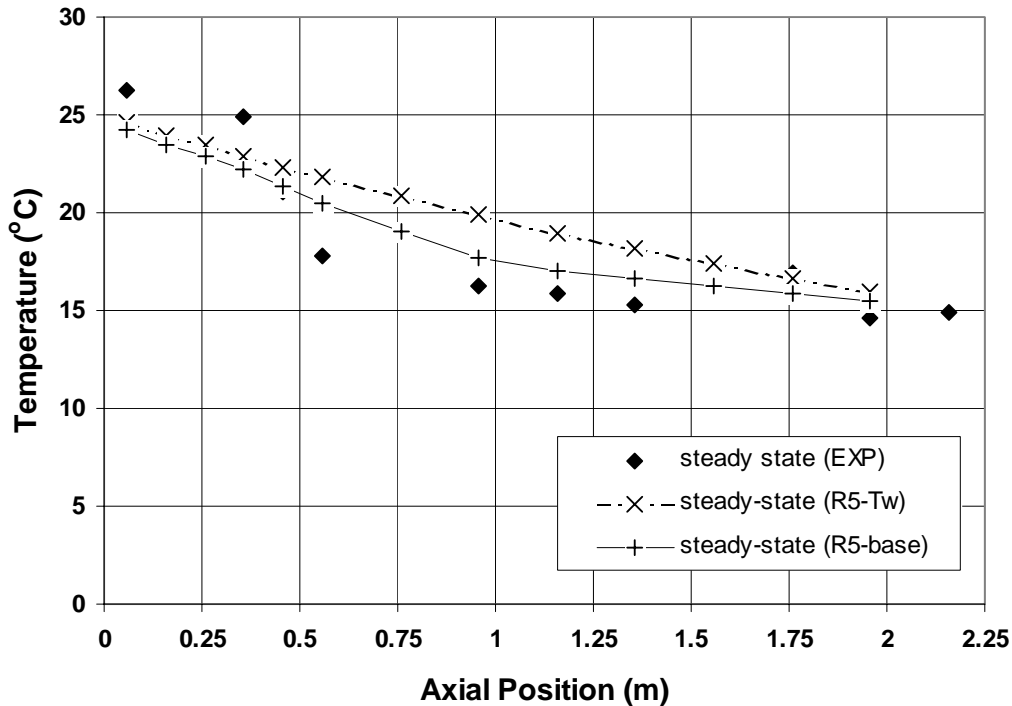


Figure 2.6-17 Experimental and RELAP5 Results for Coolant Temperature (R5-base: standard input, R5-Tw: T_{wi} given as boundary condition)

Since the heat transfer characteristics could be well understood by local heat flux and air quality, the RELAP5 results for 20 s (steady state; BCM), 120 s and 1020 s are presented in Figure Figure and Figure , respectively. The purpose of giving these results is to understand the change in characteristics of heat transfer mechanism in the condenser tube by the progress of time during transient. Since no measurement were done for local heat flux during transient period and for local air mass fraction (air quality) in the condenser tube, only the code predictions are presented in this section. Note that times given in figures, i.e. 20 s, 120 s and 1020 s, correspond to 100 s, 200 s and 1100 s in experiment, respectively. The overall evaluation of these results reveal the fact that the local heat flux along the condenser is depressed drastically by time, which means the heat transfer performance is degraded as coolant in the jacket pipe stagnates and boils off due to loss of coolant to the secondary side. The degradation of performance is quite important during the first 100 s of the transient period as could be seen by comparing the results given in Figure and Figure . The local heat flux values calculated for the first 0.56 m of the condenser are suppressed at 120 s compared to the values of 20 s (steady state) and the percent decrease of local heat flux varies from 20% to 50%. The sole reason for the decrease of heat flux at the top of the condenser is the degraded heat transfer to the secondary side due to coolant flow cut off at 20 s. Hence the calculated mass flow rate drops from 0.181 kg/s to almost 0.0 kg/s, in the secondary side after 20 s. Although the secondary mass flow rate is about zero at 120 s, coolant boil-off does not occur and the heat transfer regime on the secondary side, for the first half meter, is subcooled nucleate boiling which keeps up the heat removal from the primary side to some extent. The suppression of heat flux at lower elevations is also remarkable and the reason of this suppression that is as high as 30% is the increased degradation of heat removal performance by time. The heat transfer regime in the primary

side at time 120 s is condensation for the first 0.5 m ($X_s \sim 0.1-0.2$) and some air mixed with vapor is predicted at the distance of 0.6 m and single-phase liquid convection plus air prevails towards the bottom of tube. Thus, increase in air quality towards the bottom of tube observed for the time interval of 20–120 s, has no any practical implications since no vapor left to be condensed there.

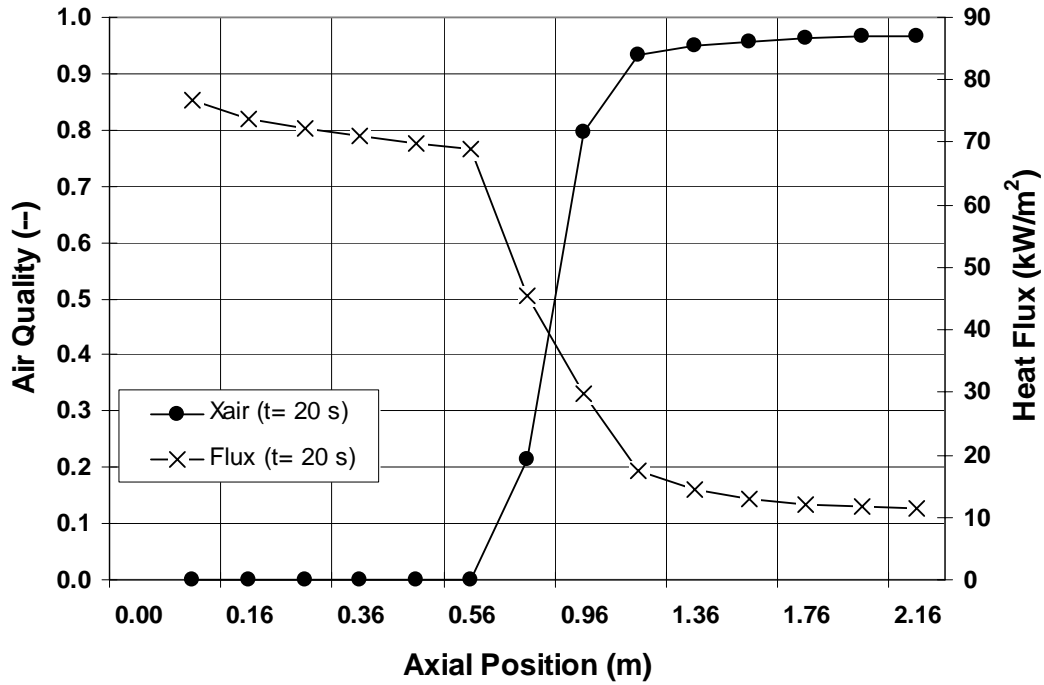


Figure 2.6-18 RELAP5 Results for Air Quality and Heat Flux (t=20 s)

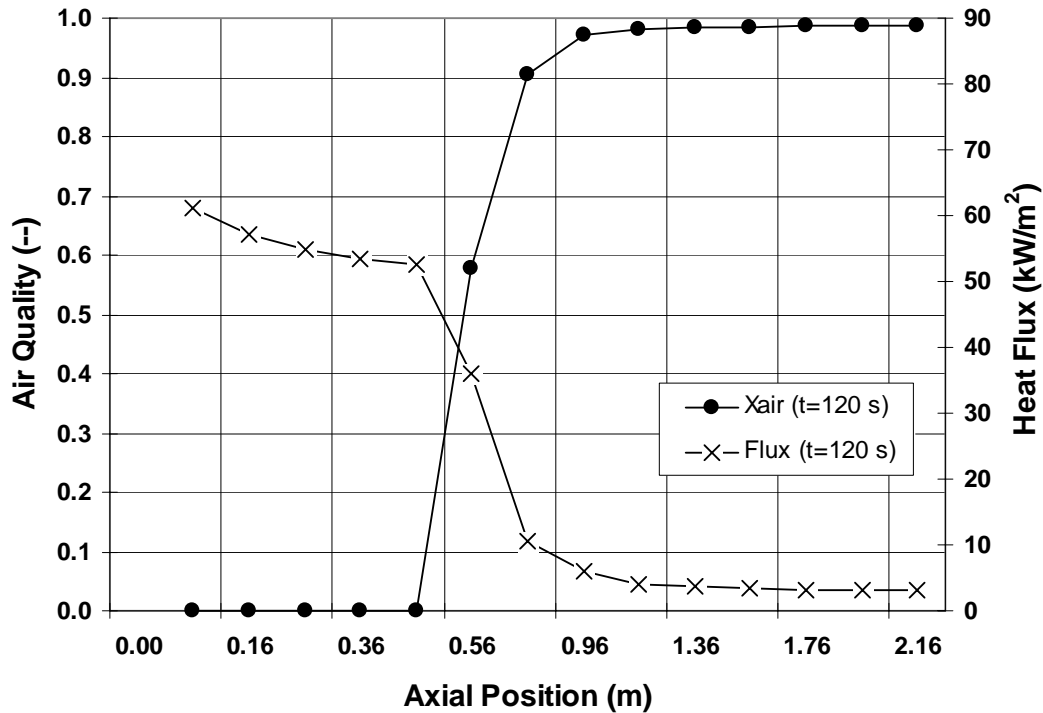


Figure 2.6-19 RELAP5 Results for Air Quality and Heat Flux (t=120 s)

Since the code calculations yield similar results for local heat flux and air quality, for times greater than about 400 s, only the result corresponding to 1020 s is presented. In the end of transient (t=1020 s) the heat transfer performance of the condenser totally dies off, as shown in Figure . However it is interesting to note that the code predicts air quality of 30% at the second node of condenser tube model, which might be due to circulation of air inside the tube. This behaviour was observed in RELAP5 results for times greater than 120 s in volumes towards top in spite of the fact that air tends to accumulate in the bottom. Since the current experimental data is insufficient for investigation of air circulation inside the condenser tube further investigation is needed in this topic of interest. The dominated heat transfer regime is single-phase liquid convection at the secondary side while single-phase vapor convection and saturated nucleate boiling prevails in the very top volumes. However, first 0.16 m of the condenser tube model is predicted to be full of liquid/vapor mixture with a static quality of 0.998 and the rest is either all liquid or liquid/air mixture with the exception of a short distance (0.075 m; corresponding to the second data node in Figure), enclosing air/vapor mixture, just beneath the uppermost volumes that are full of vapor. As could be seen in Figure , there is a sharp increase in local heat flux at the elevation of 0.158 m from the top and this might be due to heat transfer mode selected by the code for the secondary side, which is saturated nucleate boiling. At the same location the heat transfer mode on the primary side is condensation in the presence of air, with an air quality of 30%.

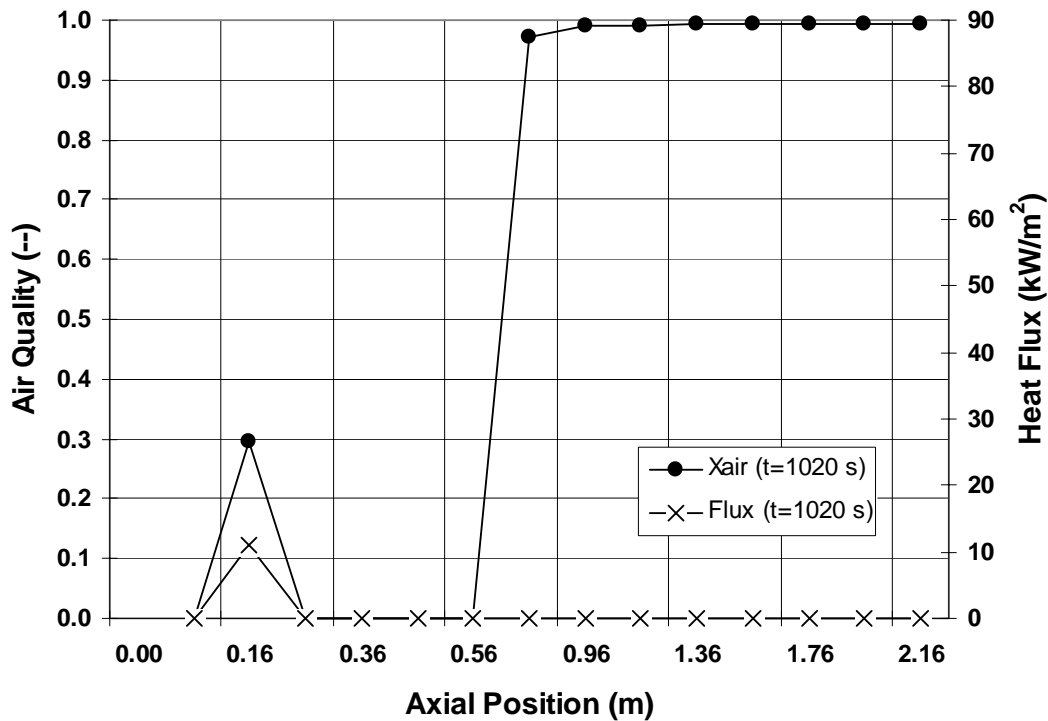


Figure 2.6-20 RELAP5 Results for Air Quality and Heat Flux (t=1020 s)

The decrease of the condenser performance can be understood by referring to the collapsed level in the primary and secondary sides, as presented in Figure . Even at the beginning of the transient, the collapsed level in the condenser tube is about 60% of the total length. This indicates how fast the accumulation of condensate inside of tube is. The collapsed level in the jacket pipe drops sharply after 170 s and remains at a level of 92% till to the end of the transient. Since the collapsed levels come close at about 400 s, one should expect the condenser performance to be weak or even nearly zero after that time. This is proved to be true when Figure is referred to. The total power as predicted by RELAP5 reveals the fact that the condenser performance weakens after 400 s and then totally dies-off. The aforementioned local flux versus axial position calculations also confirms this time dependency of condenser performance, as discussed earlier. The experimental data given in Figure is simply a prediction for secondary side level by considering thermocouple elevations at which measured temperature was 97–98°C (saturation temperature at the elevation of Ankara). Hence the data do not directly represent the collapsed level and better to consider this data as a saturation line, which does not fully fit to the method of collapsed level calculated by RELAP5 based on a control variable technique considering “volume length x (1 – void fraction)” for each cell. In experiment, the saturation level is about 88% from 270 s till the end of the measurement.

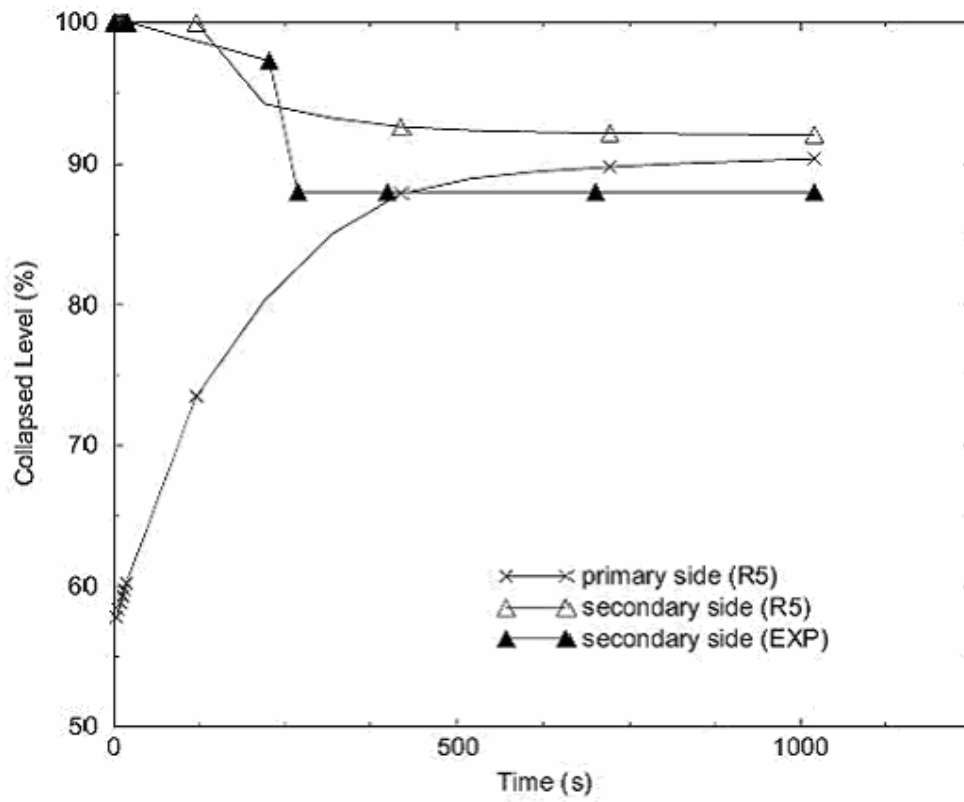


Figure 2.6-21 Liquid Collapsed Level in Primary and Secondary Sides

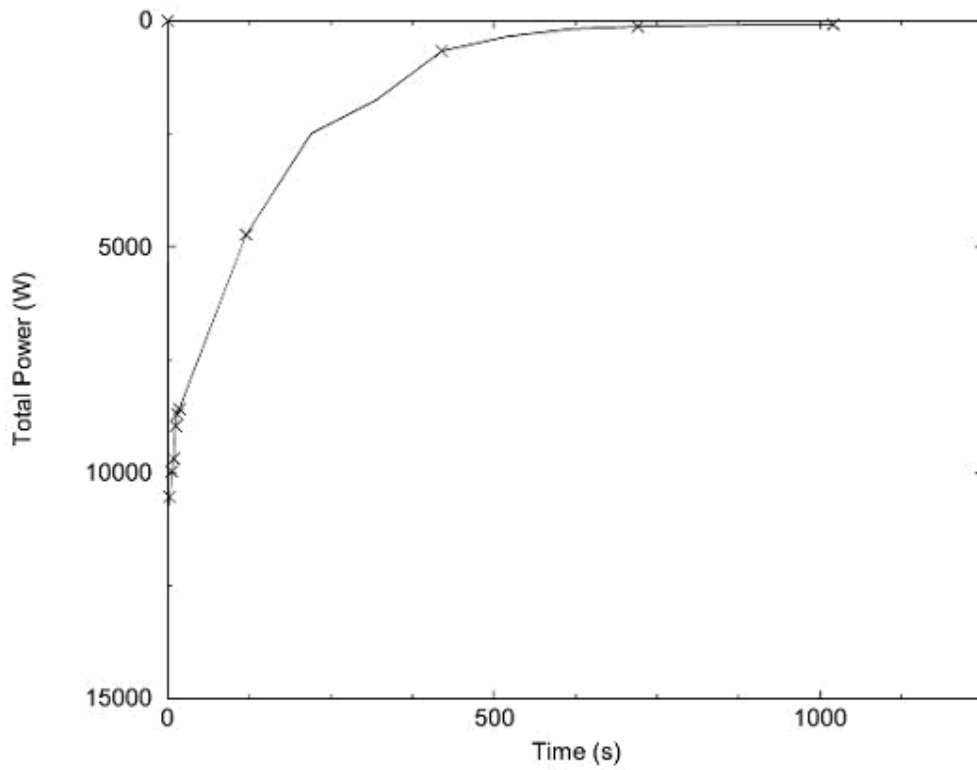


Figure 2.6-22 RELAP5 Result for Total Power of the Condenser

3 EXPERIMENTAL INVESTIGATION OF COOLING EFFECTIVENESS UNDER COLD SHUTDOWN CONDITION AND RELAP5 SIMULATION

3.1 GENERAL

A computational investigation of the experiment concerning the loss of the Residual Heat Removal System (RHRS) during reduced inventory operation was carried out using the RELAP5/mod3.3 (beta version) thermal-hydraulic code [7]. The experiment was conducted at the UMCP 2X4 integral test loop (University of Maryland) and consisted of two parts, loss of RHRS and loss of feed water system [11]. The objective of the work presented in this part of the report is to assess the capability of RELAP5 code to capture the phenomena observed in the experiment during the Boiler-Condenser Mode (BCM) and the Loss Of Feed Water (LOFW) transient.

3.2 DESCRIPTION OF THE UMCP 2X4 TEST FACILITY

The UMCP (The University of Maryland, College Park) facility [10] is shown schematically in Figure . The facility is an integral one and consists of a vessel with an internal downcomer, a pressurizer, two hot legs, two 28 tube Once Through type of Steam Generator (OTSG) simulators, and four cold legs. The UMCP facility does not have coolant circulating pumps. The vessel contains 16 electrical heater rods to provide a maximum of 203 kW heat input to the loop. Eight hinged vent valves are installed internally in the vessel to simulate the full scale reactor vessel vent valves. By volume, UMCP facility is about 1/500 of the volume of a Pressurized Water Reactor (PWR) with 177 fuel assemblies. Unlike the MIST facility, the UMCP facility is not full height. The UMCP hardware is capable of operating at a maximum pressure of 2.07 MPa. The stated objectives of the tests to be conducted at the facility were to study small break loss-of-coolant accident and phenomena associated with natural circulation in a Babcock and Wilcocks (B&W) design plants.

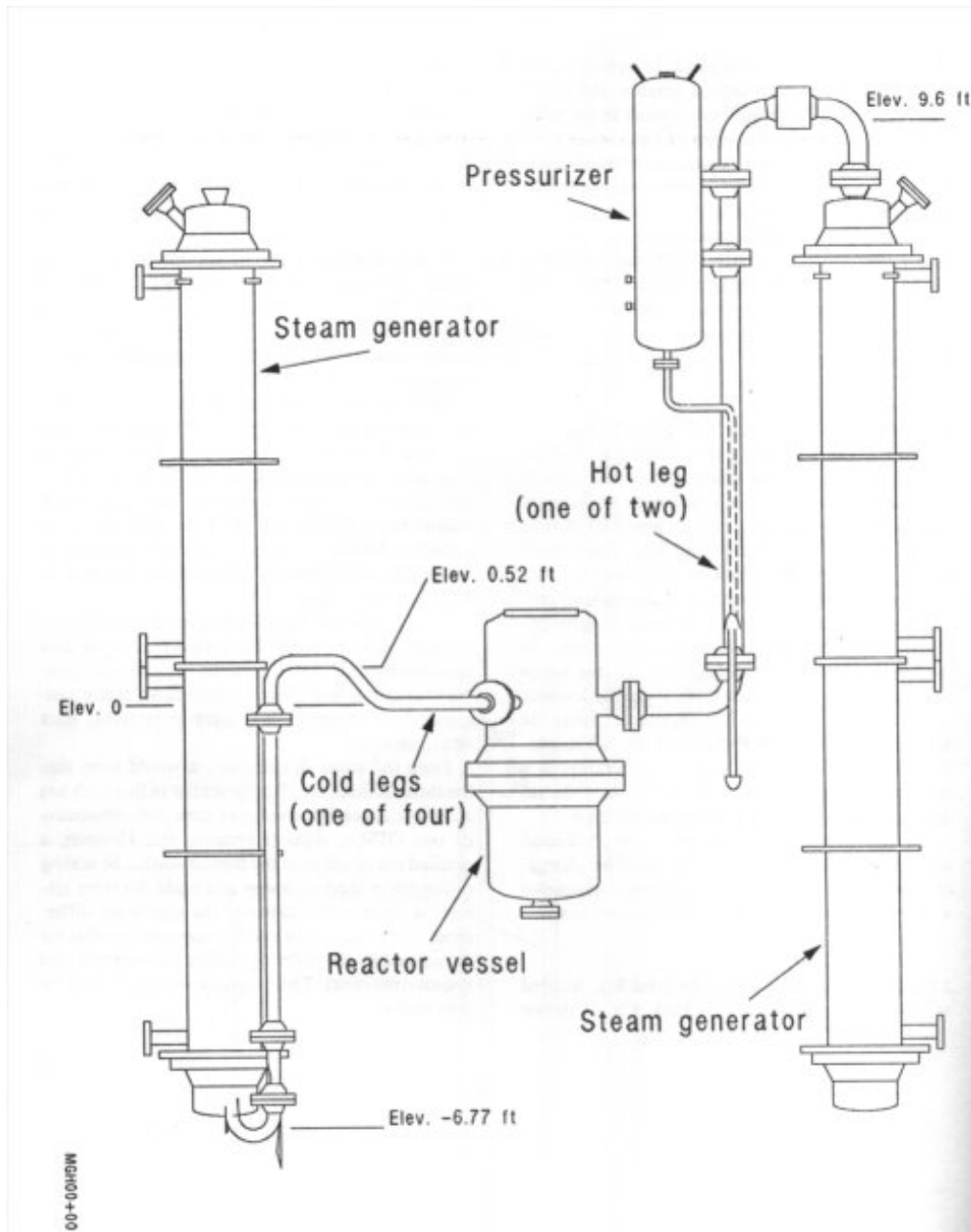


Figure 3.2-1 UMCP Test Facility

3.3 DESCRIPTION OF THE EXPERIMENT AND RELAP5 ANALYSIS

The test facility is a 1/500 scaled model of a typical B&W type of PWR having a once-through type of Steam Generator (SG). The experiment [11] was performed with a constant core power (34.9 kW) of 0.6% of the scaled nominal power. The facility consists of two loops: Loop-A and loop-B. Loop-B was blocked at the pump suction side and SG-B was kept inactive by empty secondary side. The initial system pressure and temperature, corresponding to cold shutdown condition at time 0 s, were 1 bar and 303 K, respectively. The coolant level in the vessel was 95% and the corresponding primary side levels in the SG-A and SG-B were 53% and 42%, respectively. The parts of the system above the

coolant level were full of air. The secondary side of the SG-A was full and the feedwater flow rate was 0.115 kg/s.

The RELAP5 model is shown in Figure . The model consists of 106 volumes, 106 junctions and 78 heat structures with 262 mesh points. The input model is given in Appendix B. Loop-B was blocked at the cold leg by using “zero flow time dependent junctions”. The simulation was initialized at the system parameters given above. The liquid levels were adjusted according to the initial condition of the experiment, and the state in the volumes above the liquid level was initialized by vapor/air mixture in saturated condition. The flag used for initial conditions of the volumes containing air is “104”, which means the state is defined by pressure, temperature and static quality. To initialize the problem with saturated air condition, static quality was set to “1.0” for all volumes above the coolant level. The heater power was adjusted by a power table (time versus power) and was assumed to reach the nominal decay power (34.9 kW) in 280 s. In the RELAP5 input model, the environmental heat losses were also modeled by constant environmental temperature (24°C) and convection heat transfer coefficient (7 W/m²/K) for SG-A secondary side, pressurizer tank and surge line, hot leg and cold leg piping. No information on environmental heat losses for the UMCP tests were provided at the technical report. The collapsed levels were calculated by control variable technique.

The period of calculation till the initiation of LOFW transient is 9000 s. After the establishment of steady-state conditions by the BCM, the feedwater flow rate to the secondary side of the SG-A was turned off and the LOFW analysis was initiated. The total problem time is 18,000 s. The new steam table (tpfh2onew) was used in calculations by RELAP5/mod3.3 (beta version).

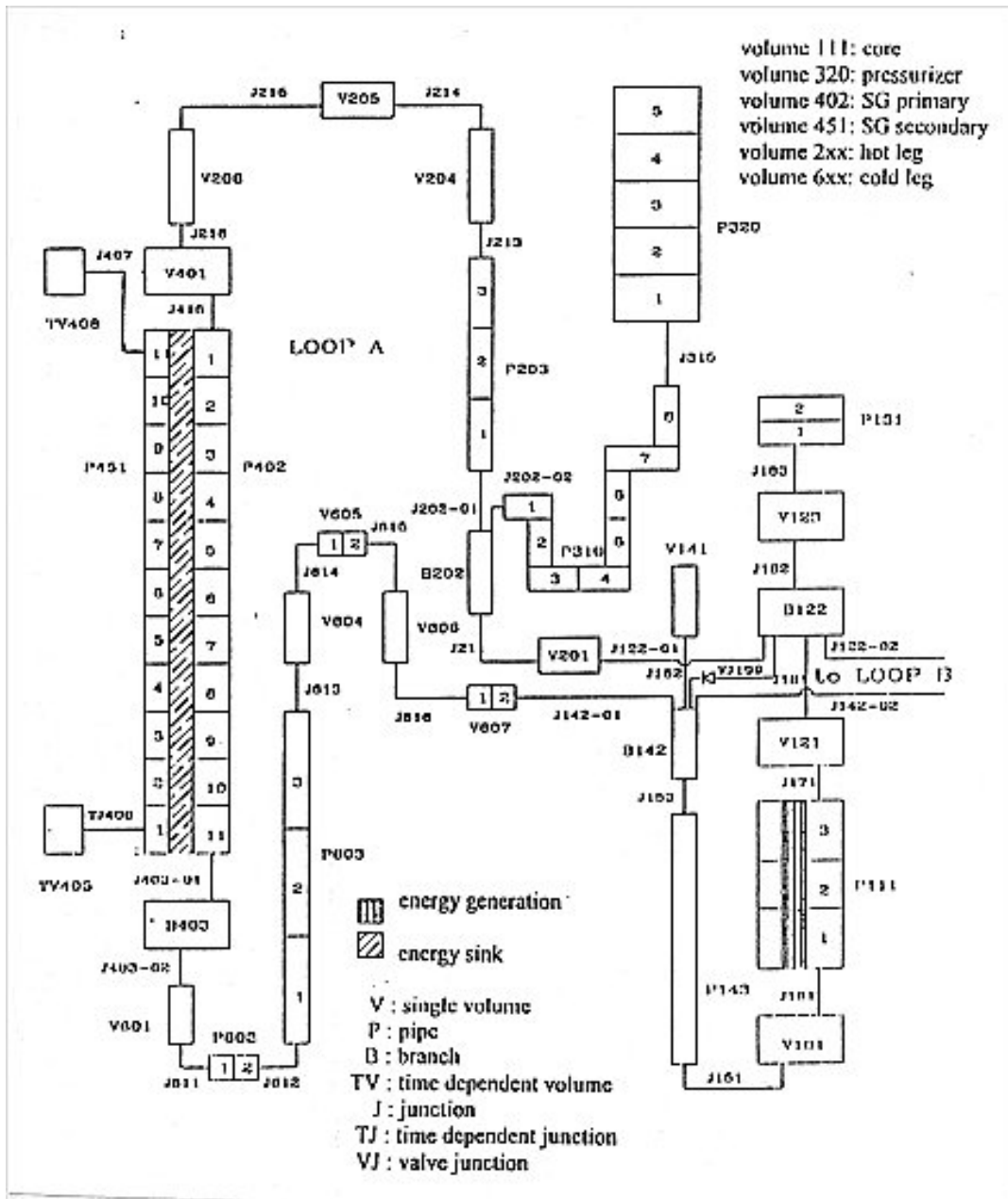


Figure 3.3-1 RELAP5 Model of UMCP Test Facility

3.4 RESULTS AND DISCUSSION

Since there was not any experimental data recording from the time of cold shutdown conditions ($t=0$ s) until the time when the BCM has already been established ($t=7620$ s), only the code prediction was presented for this time interval, as shown in Figure . First, voiding in the core.

Figure) was started at 700 s due to the lack of residual heat removal capability, and then the pressure was considerably increased at about 2000 s as the result of expansion of coolant in the upper part of the vessel. The heat transfer rate in SG-A could not take over the residual heat load till 2000 s, as could be seen in Figure , since the condensation could not be sufficient due to air accumulation at the top of the hot leg (candy cane). The heat transfer mode as predicted by the code is presented in Figure , for the first and the fifth volumes of

SG-A tubes, i.e. P402-01 and P402-05 given in Figure . The selected heat transfer mode is 30 (condensation in the presence of air when the void is less than one) from time 1570 s till the end of the problem. It is apparently clear from the Figure that establishment of BCM, which leads to a plateau region in system pressure (Figure), is directly affected by the condensation of vapor inside the first SG-A tube volume (402-01) only. The heat transfer is dominated by the topmost volume simulating the SG-A tubes, with an average heat flux of 25–30 kW/m² during the period of 2,400–10,000 s., The heat transfer in the topmost one dominates the other lower ones in this period though heat transfer by condensation is initiated after 2400 s in almost all 5 volumes from the top. However the heat flux remains very low in lower volumes and even in the second volume the heat flux is about 3 kW/m², during the same period. It is again clear from Figure that the heat load of SG-A shifts from top volume (402-01) to the fifth one by passing each volume in between, in the progress of time due to boiloff in the secondary side as the result of LOFW. The effective heat transfer by condensation in the second volume is at 10,000–12,000 s, third volume is at 12,000–14,000 s, fourth volume is at 14,000–16,000 s and fifth volume is at 16,000–18,000 s. Hence, it can be concluded that effectiveness of condensation after 10,000 s remains in one tube volume, beginning from the second one from the top, for about 2,000 s. This directly implies that the boiloff rate of the secondary coolant is about 2×10^{-4} m/s. The secondary side level of SG-A is presented in Figure . The level is 100% till the initiation of LOFW transient (9,000 s). The level decreases in the experiment at a slower rate than that of RELAP5 result. However, it is to be noted that the level given in the figure for RELAP5 is the collapsed level and it is questionable whether the data exactly correspond to the code prediction using control variable technique. In code calculation the collapsed level was calculated as “length of volume multiplied by (1–void fraction)” for each volume and the results summed up to calculate the collapsed level. According to the result of RELAP5 the collapsed level drops to half the full height of the secondary side at the end of the analysis while it remains at about 70% in experiment.

After condensation prevails in the top volume of the SG-A tube as the result of decrease of air inside due to system pressure increase, which pushed down air down to the SG tubes, the BCM was established at about 416 kPa (Figure). The code underpredicts the pressure by 6% compared to the experimental data. The liquid temperature at the upper plenum of the vessel (Figure) also follows the trend of the system pressure, as expected. The result of the code is in agreement with the data, except there is an overestimation after 15,000 s. The Reactor Vessel Vent Valve (RVVV) model, which connects the upper plenum of the vessel and the downcomer, was also modeled to relieve the pressure when pressure at the upper plenum exceeds that of the downcomer by 510 Pa.

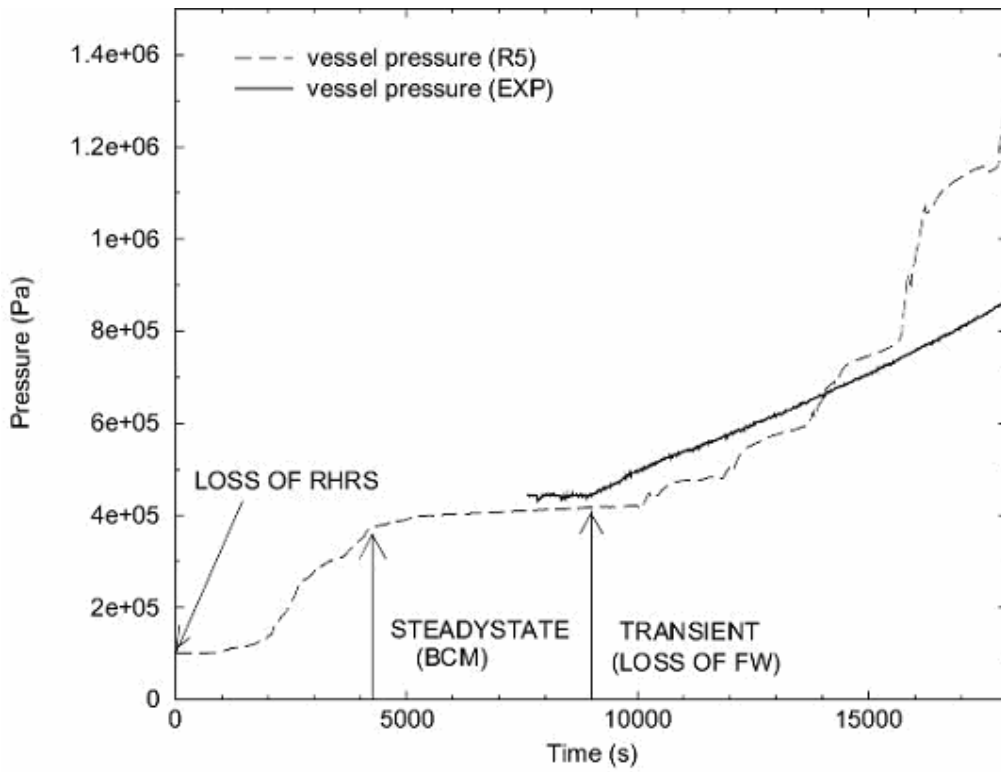


Figure 3.4-1 Upper Plenum Pressure

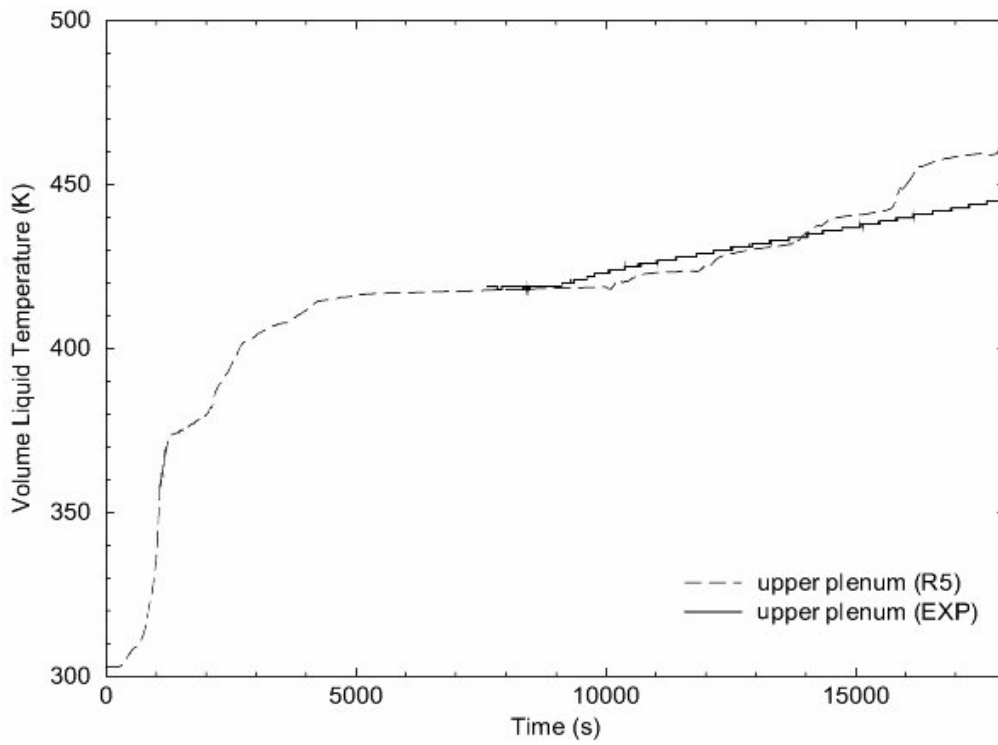


Figure 3.4-2 Liquid Temperature at the Upper Plenum of Vessel

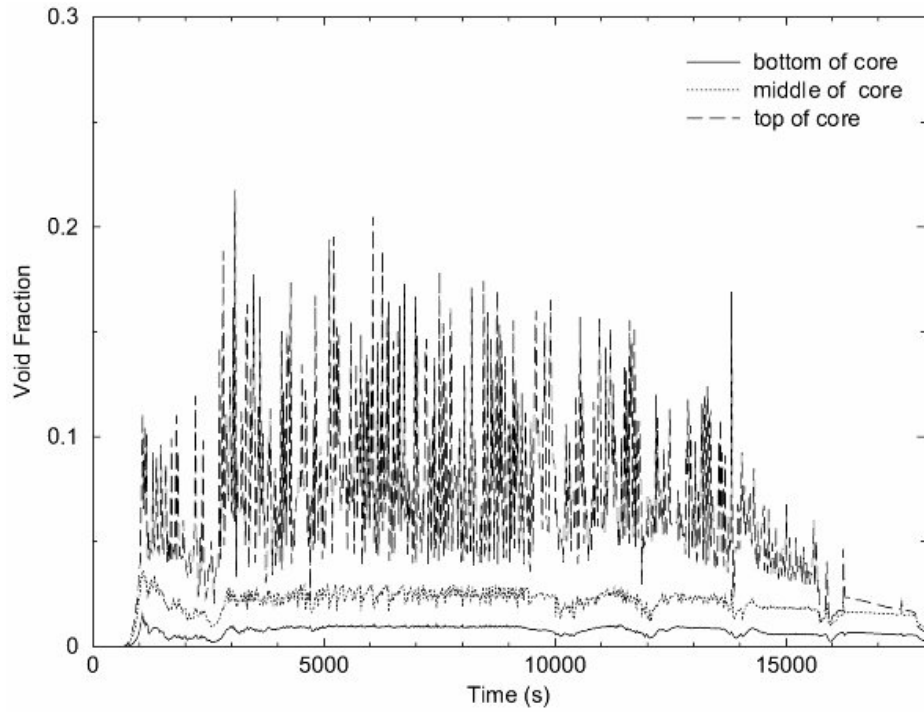


Figure 3.4-3 Void Fractions in Core

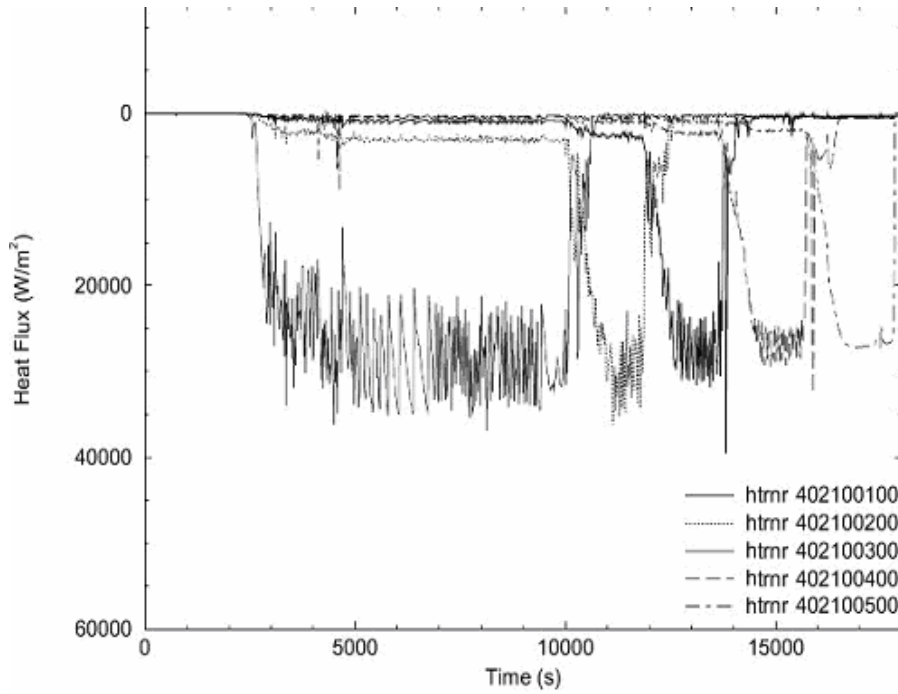


Figure 3.4-4 Heat Flux in Tubes of SG-A

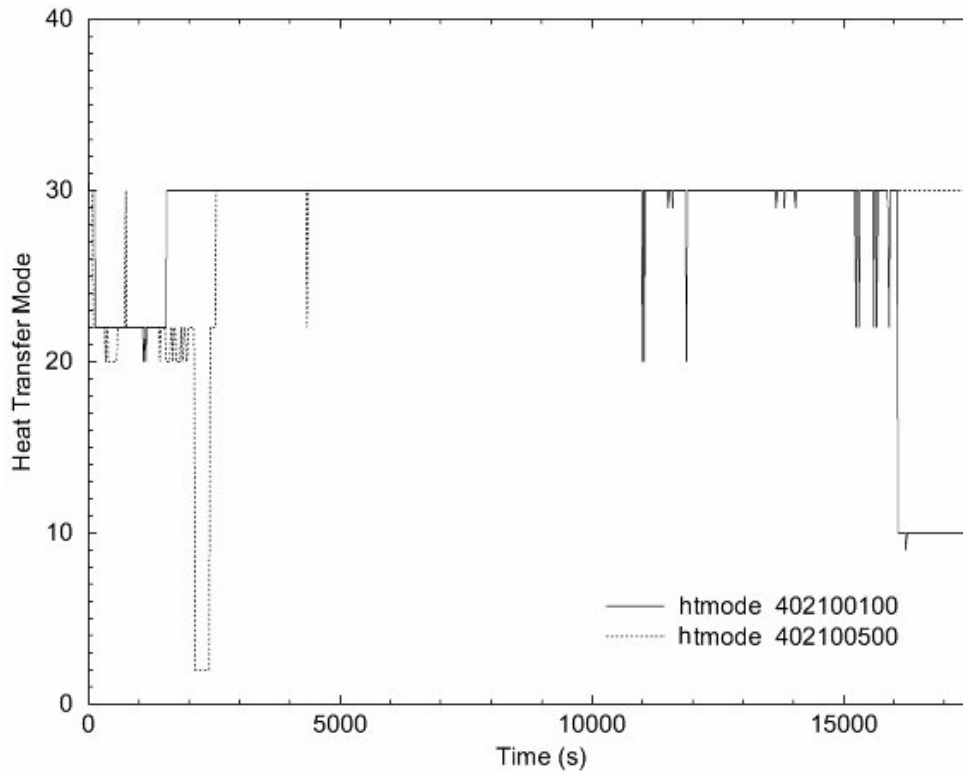


Figure 3.4-4 Heat Transfer Modes in Tubes of SG-A

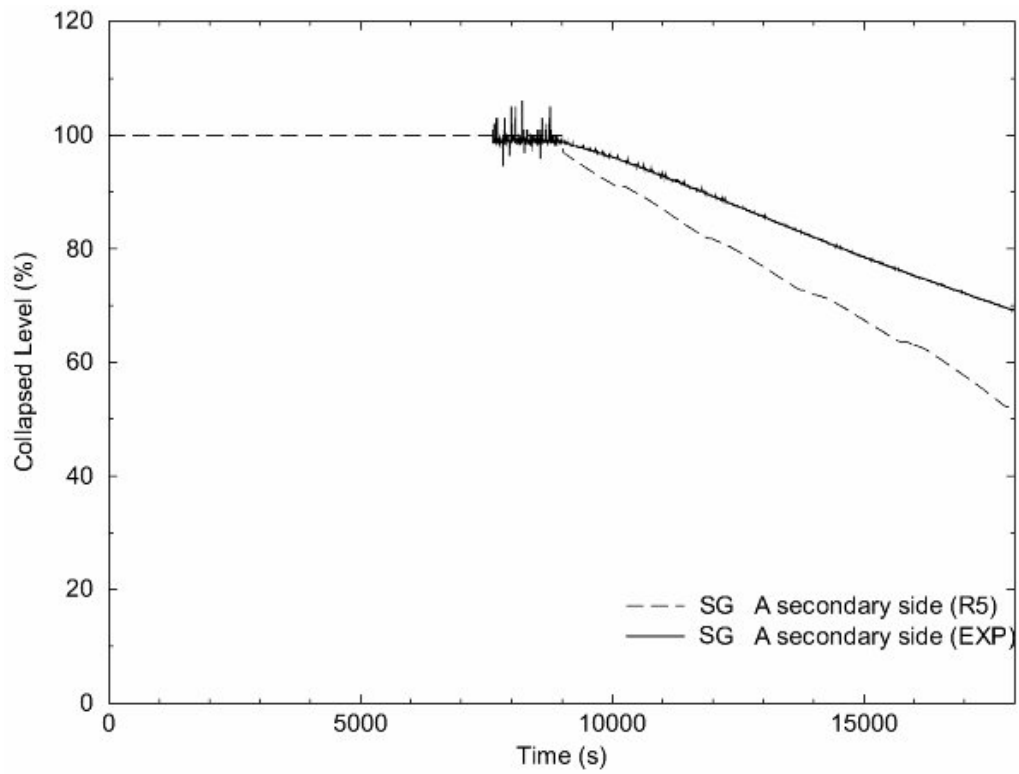


Figure 3.4-6 Secondary Side Level of SG-A

The change in heat transfer characteristics of the SG-A by the progress of time can be best understood by referring to the local heat flux and air quality trends with respect to the axial position, at certain times. The dominant heat transfer mechanism is condensation in almost all times, as discussed earlier (Figure) and the rate of condensation was governed mainly by axial air mass distribution and secondary side level. After feedwater flow was terminated to the secondary side of the SG-A, coolant at the secondary side started to boil-off and this resulted in a shift of condensation to the lower volumes along with the level decrease in the secondary side. The air inside the tubes was also forced to accumulate in lower volumes in the progress of time. The heat transfer rate from the uppermost SG tube volume (P402-01 in Figure) is ~78% of the total power in the end of BCM ($t=9000$ s). The total heat power load of the SG-A is 34,239 W at this time. It is interesting to note that only one volume in the RELAP5 model of the SG-A takes over the heat load to be transferred to the secondary side and that volume shifts downwards in the progress of time. This behaviour can clearly be seen in axial trends of local heat flux in SG-A as presented in Figure , Figure , Figure and Figure , for times 9000 s, 10,500 s, 15,000 s and 18,000 s, respectively, which also confirms the trend in Figure for heat flux. Another interesting observation made from these figures and Figure is that the heat power load of SG-A slowly decreases by time after the LOFW transient was initiated and condensation that persists in one hydrodynamic volume at a time is always a dominating heat transfer mechanism throughout the analysis. At the end of the analysis at 18,000 s, the first 5 volumes of the SG-A secondary side is full of vapor with X_s of 1.0, which makes it impossible to transfer energy from corresponding primary side volumes by condensation. This also caused failure in calculation just after 18,000 s. Another observation made is for the air quality behaviour by time: Air is continuously accumulated downwards as time progresses due to suction effect of condensation that shifts downward along with boiloff of secondary side coolant, which is also observed at METU-CTF analyses (see Section 0).

As discussed in Section 0 for METU-CTF air/steam mixture experiment, even at the beginning of the transient the collapsed level in condenser tube was about 60% of the total length. This was the indication for how fast the accumulation of condensate inside of tube is. At the time which collapsed levels of primary and secondary sides has got close to each other the condenser performance became weak or even nearly zero. However the situation is different in UMCP case: The power of the SG-A slowly degrades till to the time at which secondary side level drops to the level inside of tubes, as can be seen in Figure and Figure . It is to be noted that the collapsed level in primary side of the SG-A remains at an almost constant level (~50%) during BCM steady state for the period of 5,000–9,000 s, contrary to the situation observed for the METU-CTF. It should be recalled that the calculated collapsed level at the METU-CTF was drastically increasing during transient and approaching to about 90% in 1000 s. This simply shows the difference in conducting experiments in an integral and separate effect test facilities. In the former one the loop behaviour could affect the parameters of primary importance (in this case it is the collapsed level in SG tubes), which then lead to important differences in system behaviour compared to the separate effect test facilities. The result of RELAP5 code for the primary side level in steady state BCM period is underestimated compared to the data, i.e. levels calculated and measured are about 50% and 75%, respectively. However, the level measured exhibits a linear decrease by time after LOFW transient initiation and the slope of decrease predicted by the code is in agreement by the data. The level in primary side (tubes) of the SG-B, which is not active, remains unchanged throughout the experiment and simulation (~47%).

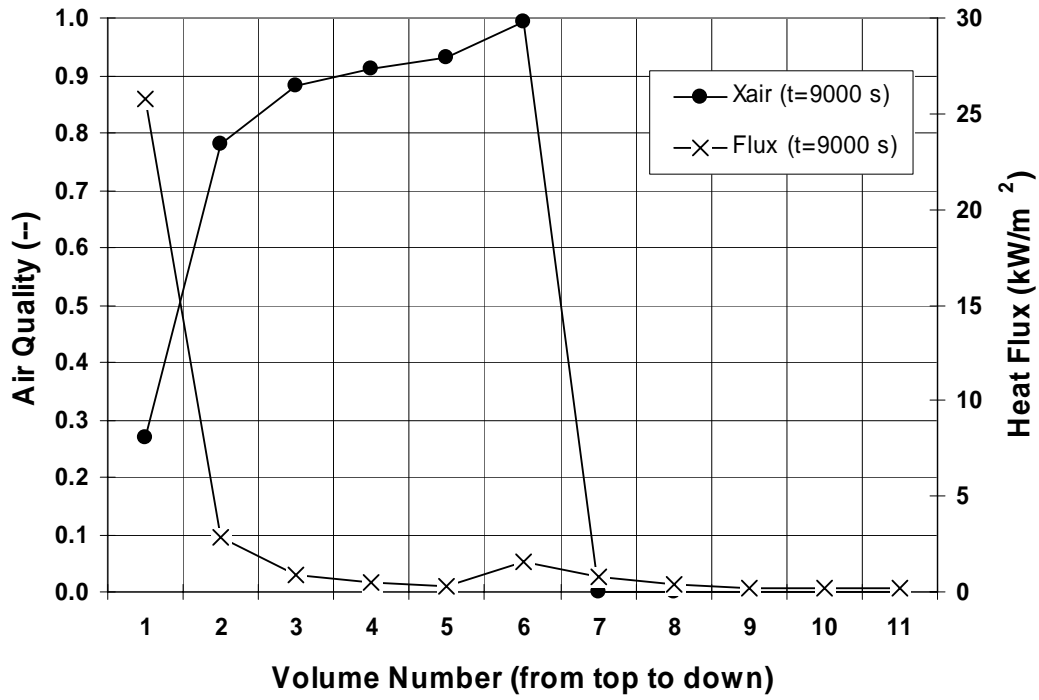


Figure 3.4-7 RELAP5 Results for Air Quality and Heat Flux (t=9000 s)

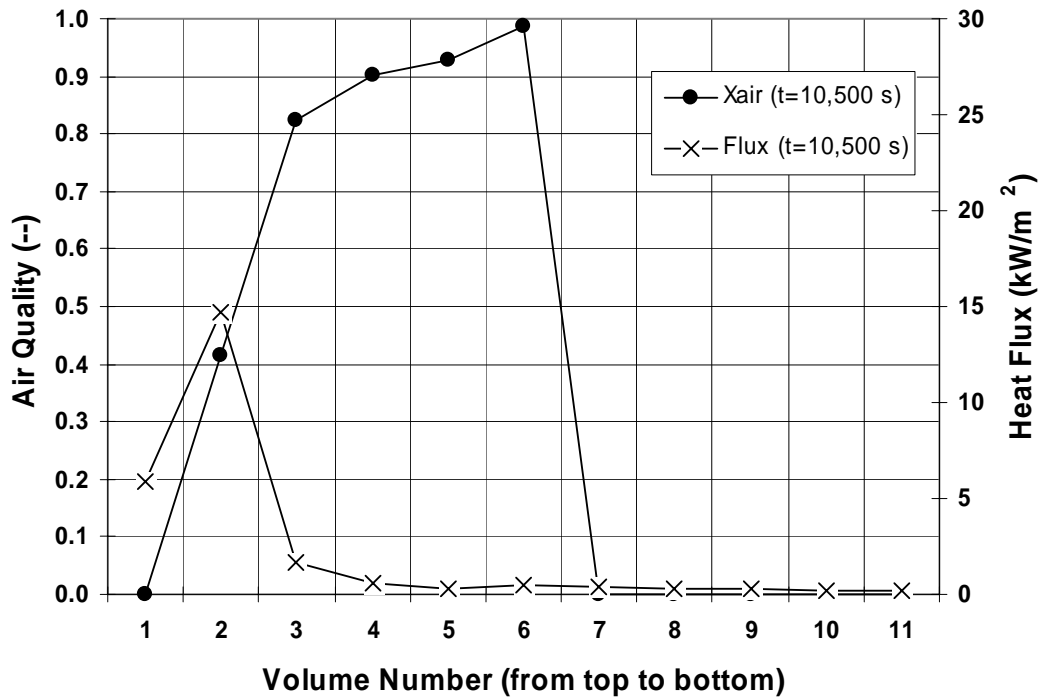


Figure 3.4-8 RELAP5 Results for Air Quality and Heat Flux (t=10,500 s)

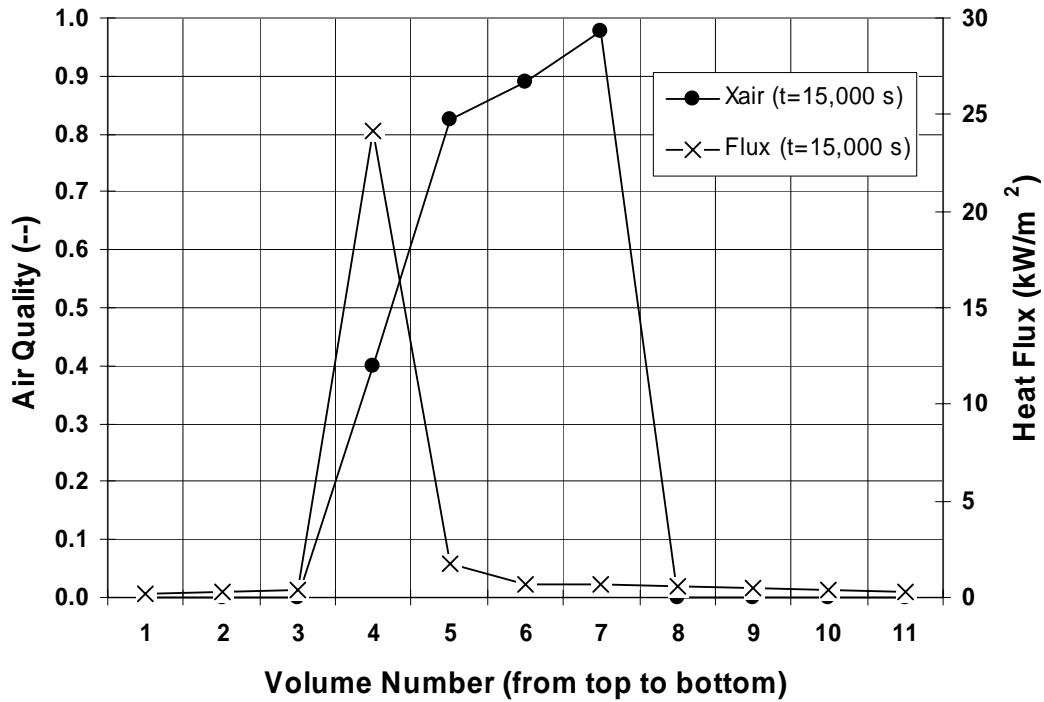


Figure 3.4-9 RELAP5 Results for Air Quality and Heat Flux (t=15,000 s)

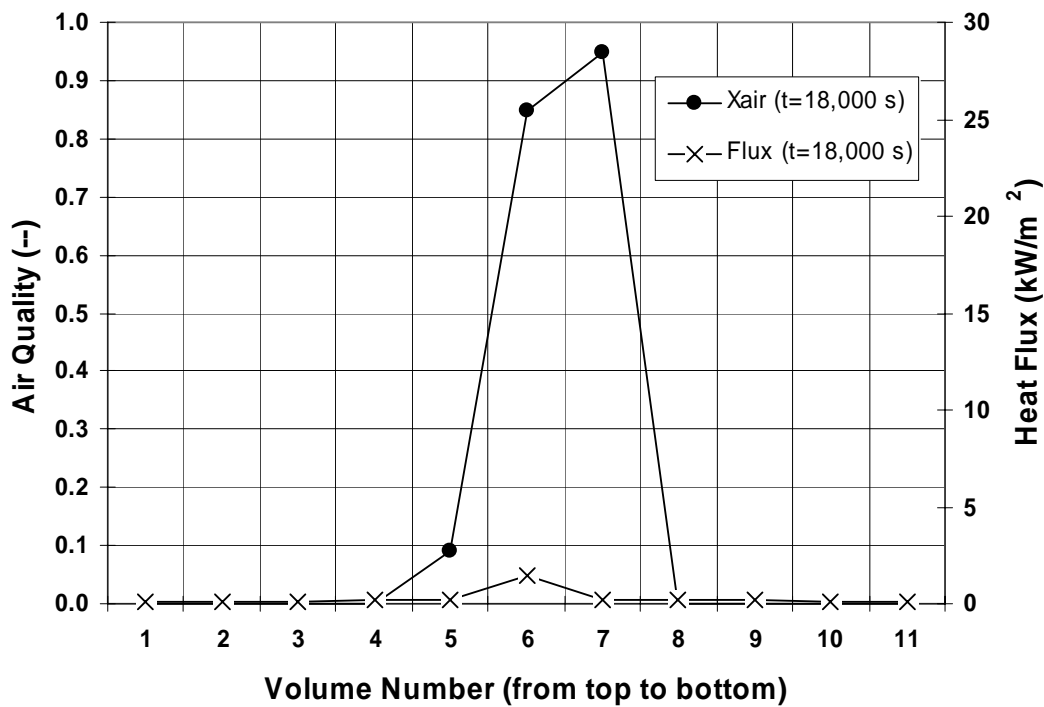


Figure 3.4-10 RELAP5 Results for Air Quality and Heat Flux (t=18,000 s)

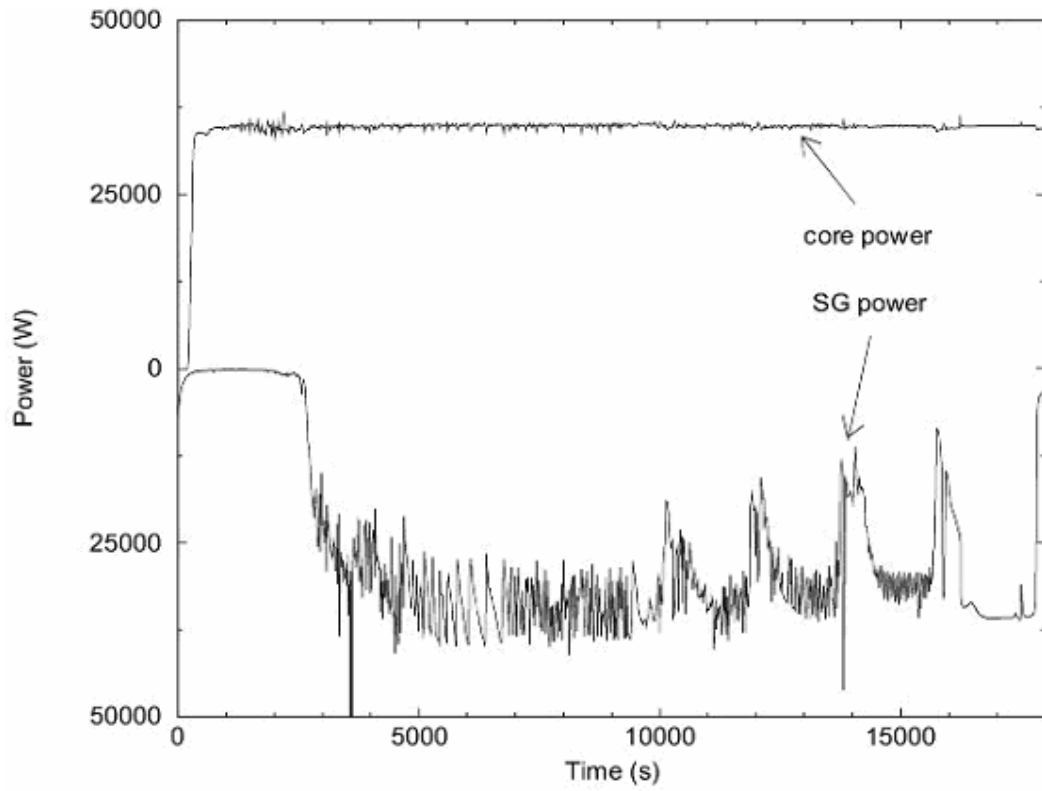


Figure 3.4-11 RELAP5 Results for Core and SG-A Power

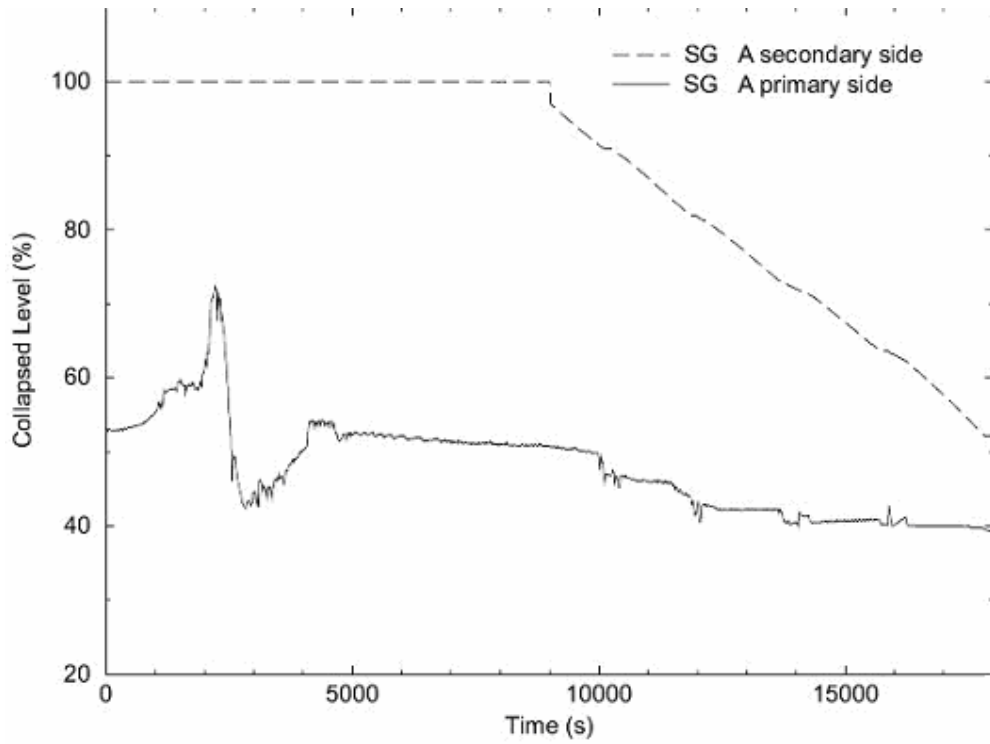


Figure 3.4-12 RELAP5 Results for Collapsed Level in SG-A

The code calculation has yielded close results for the vessel and pressurizer collapsed levels, as can be seen in Figure . Maximum deviation of the calculated vessel level is about -10%, compared to the data while it matches almost exactly with the data for the pressurizer level. This figure also reveals the fact that the start of condensation, at about 2000 s, in the SG-A tubes leads to a sudden insurge of coolant into the pressurizer tank, which is initially empty, and decrease in level of the vessel. Then both levels stabilize at about 60–63% during steady state BCM of operation. After the initiation of LOFW transient, the pressurizer tank starts to fill further more due to system pressurization. However the vessel level remains unchanged within the same period. To demonstrate the effect of initiation of condensation at the SG-A, mass flow rate at the inlet of the SG-A plenum is presented in Figure . The mass flow rate suddenly increases at 2000 s by the suction effect of condensation and remains almost same (~0.012 kg/s) till the end of the analysis. Although there is a positive flow towards SG-A tubes, the flow in core exhibits an oscillatory behavior around “zero” flow axis, as could be seen in Figure , due to existence of air in the system.

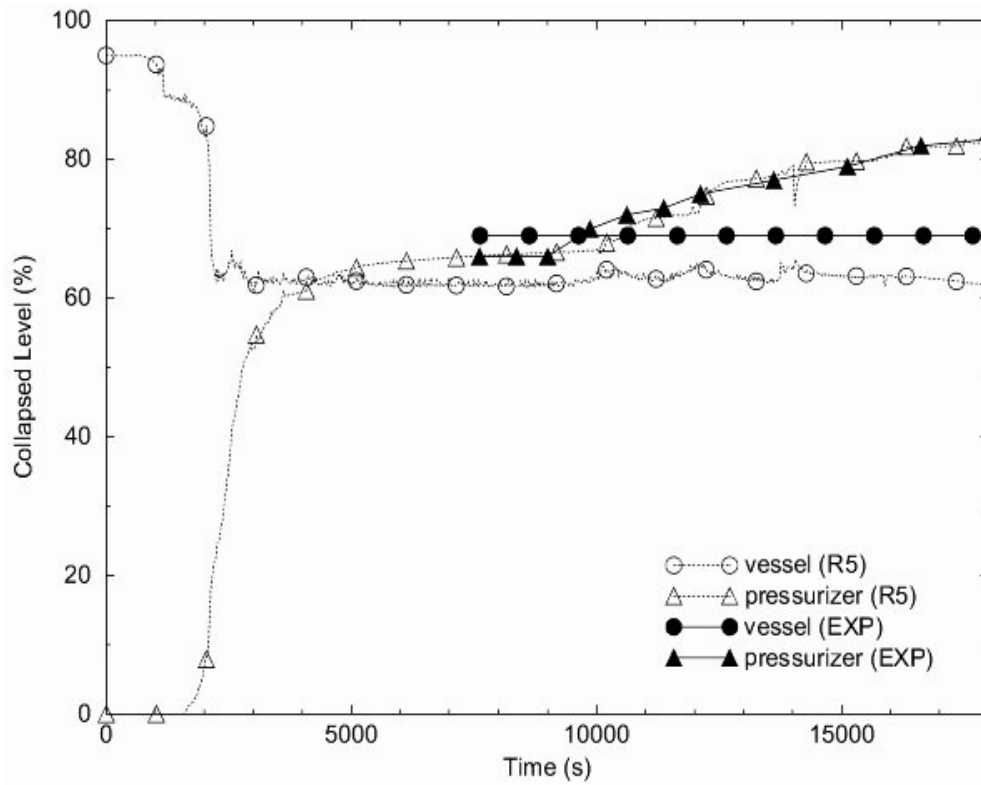


Figure 3.4-13 RELAP5 Results for Collapsed Level in Vessel and Pressurizer

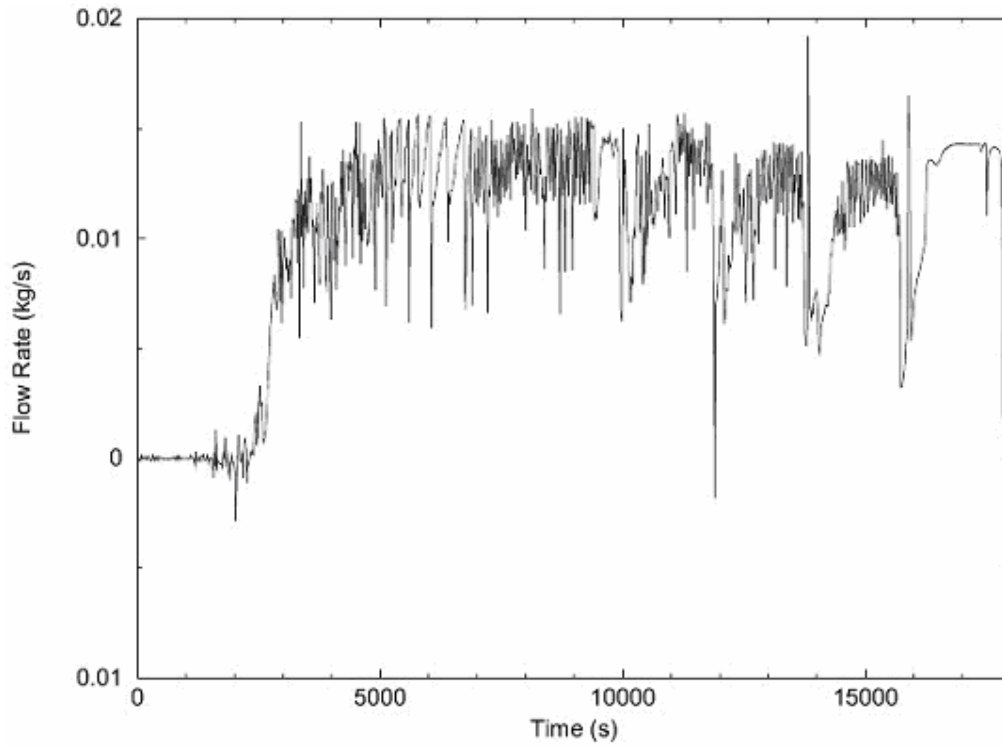


Figure 3.4-14 RELAP5 Result for Flow at the inlet of SG-A Primary Side

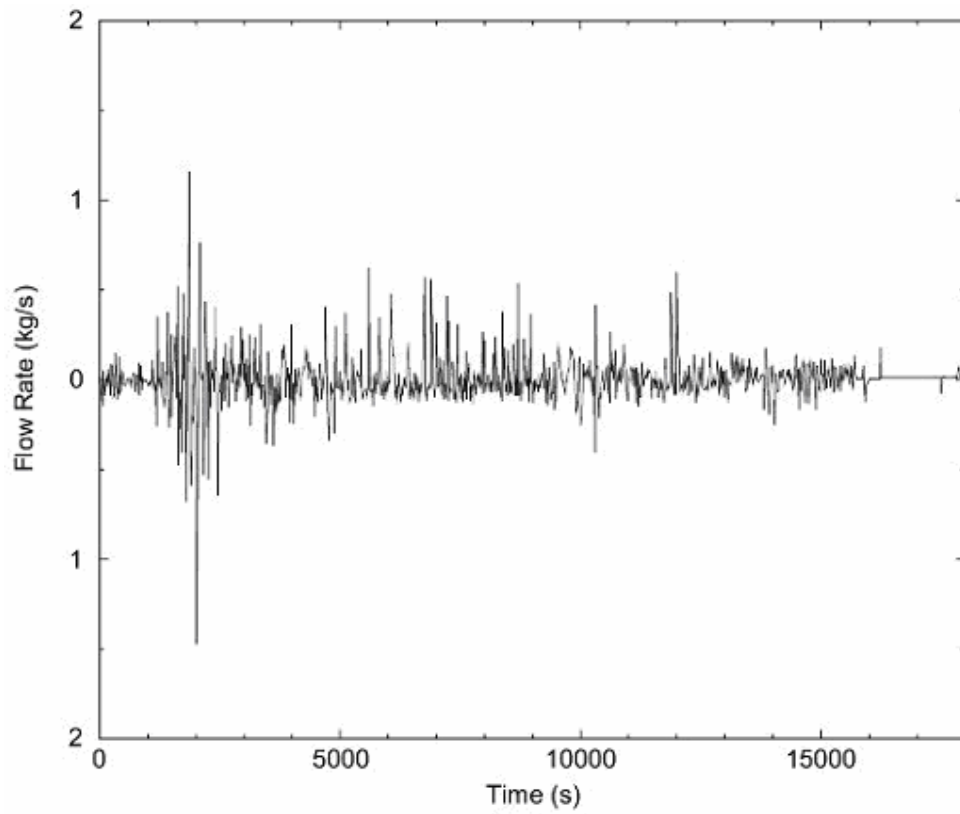


Figure 3.4-15 RELAP5 Result for Core Flow

3.4.1 Effect of SG-A Fine Node Modelling

Since condensation plays an important role for reaching to BCM of operation after loss of RHR system and for system pressure increase rate after LOFW transient initiation, effect of fine node model of the SG-A on condensation in primary side was tested. For this purpose, the volume lengths of SG-A tube bundle (P402) and associated secondary side volumes (P451) were halved and number of volumes was doubled, i.e. increased to 22 volumes in both primary and secondary side volumes. As described earlier and given in Appendix B, the base model consists of 11 volumes.

Since the transient is not so fast, the fine node model yielded similar results to those of base model with coarse node modeling for SG-A, as could be seen in Figure , Figure and Figure . Interesting point is that the heat flux of 10 tube volumes (Figure) exhibits a similar trend as in the case of coarse node model with the exception that there are 10 peaks compared to 5 peaks obtained in coarse model (Figure). This simply shows that the effective condensation length remains invariant with respect to volume number. The collapsed level in the secondary side also proves it to be true, which is almost same in two models, as presented in Figure . These results show that the simulation is not affected by the node number in SG-A model and this finding also confirms that of METU-CTF simulations concerning the effect of volume number on condensation.

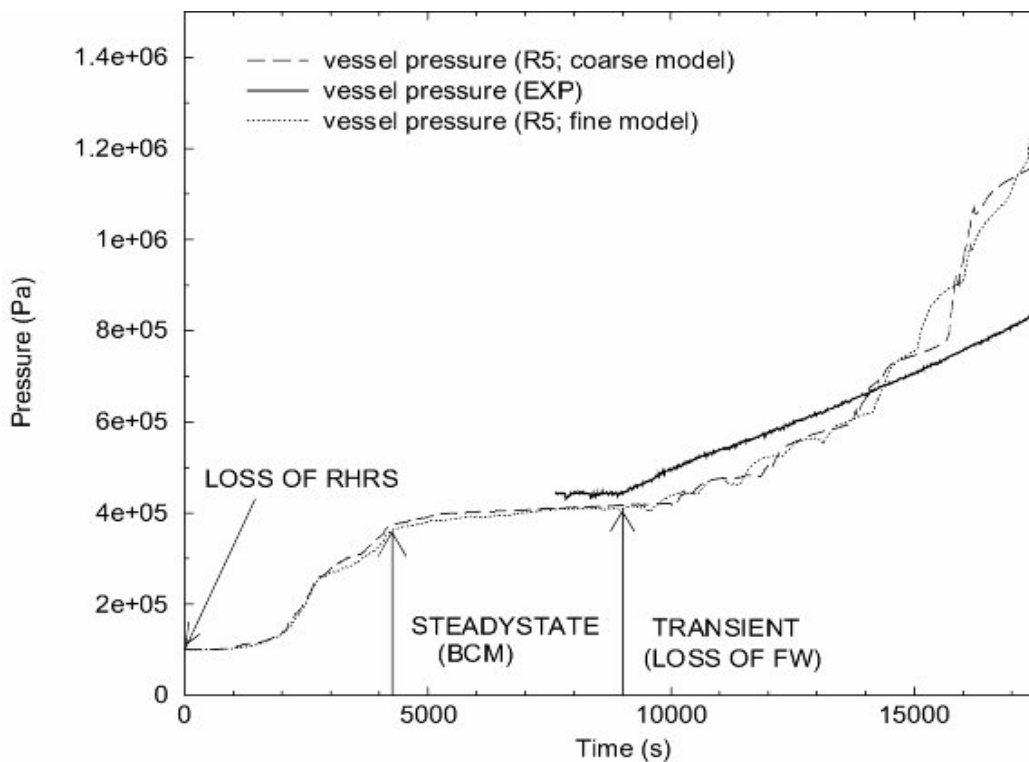


Figure 3.4-16 Comparison of System Pressure for Coarse and Fine Node Modeling

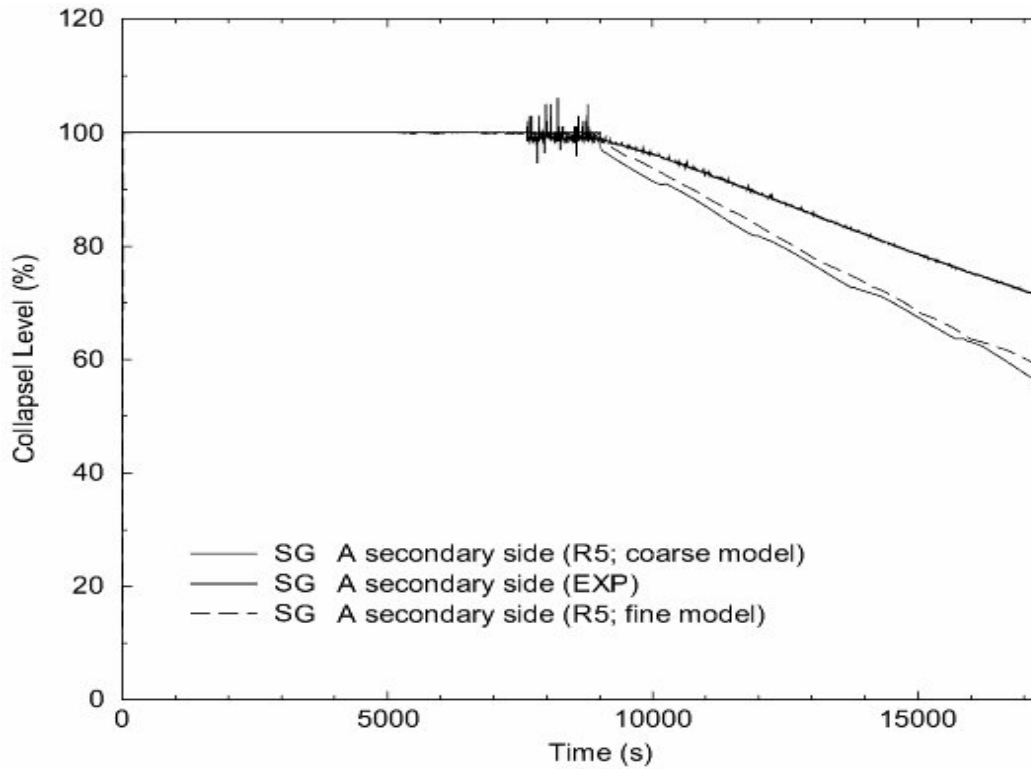


Figure 3.4-17 Comparison of SG-A Level for Coarse and Fine Node Modeling

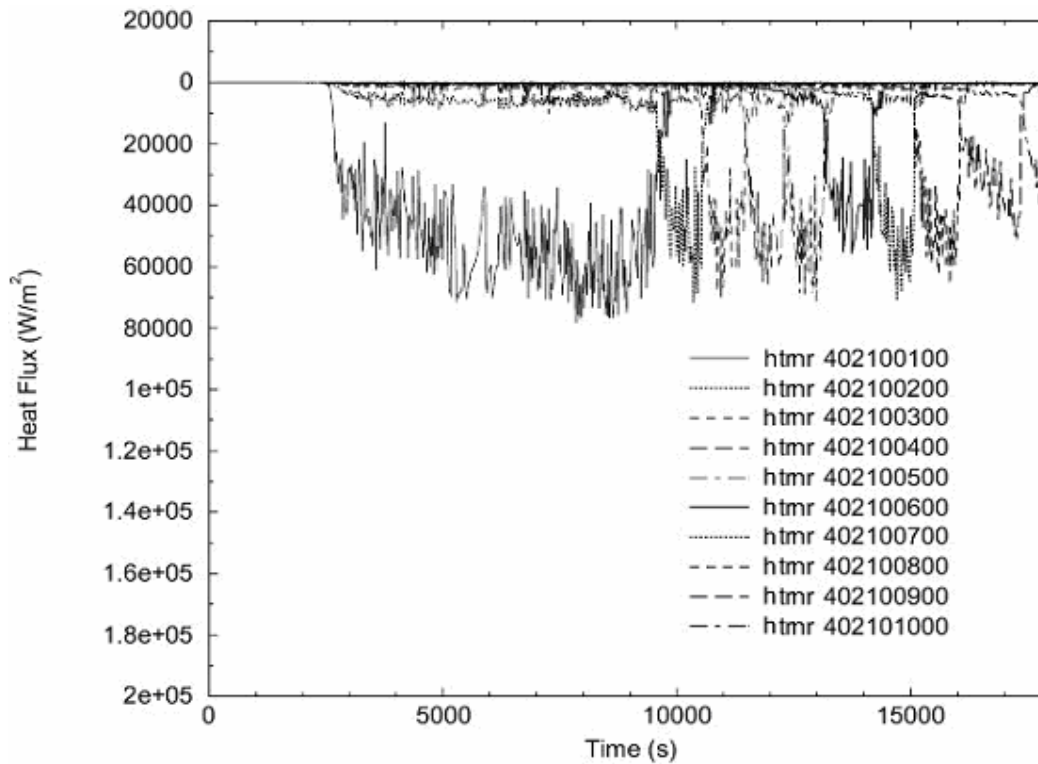


Figure 3.4-18 Heat Flux in SG-A Tubes for Fine Node Modeling

3.4.2 Computational Aspect of the Analysis

The maximum time steps given as input for the analysis are 0.005 s and 0.01 s till 9000 s (loss of RHR+BCM part) and 0.0025 s for the LOFW transient part ($t > 9000$ s). The time steps selected by the code during the calculation and Courant time step are presented in Figure . It is clear that the maximum time steps given as input are used by the code without any need for forcing smaller steps. There is enough margin for the Courant limit throughout the whole analysis period. The RELAP5 code was run on COMPAQ XP1000 with Tru64 UNIX operating system and ALPHA processor. The code (RELAP5/mod3.3 beta version) was installed with default options. The calculation took 12,659 s for 9,000 s period for loss of RHR system and BCM period, as could be seen in Figure . This means calculation time is about 1.5 times of the problem time. However, CPU time increased for transient period, i.e. 34,277 s for 9,000 s transient time that is about 3.8 times the problem time. The mass error (Figure) is very low compared to the total mass of the system. Maximum error is -0.03 kg at 9,000 s which is acceptable compared to the total system mass (622 kg). The mass error remains stable (approx. -0.005 kg) during transient.

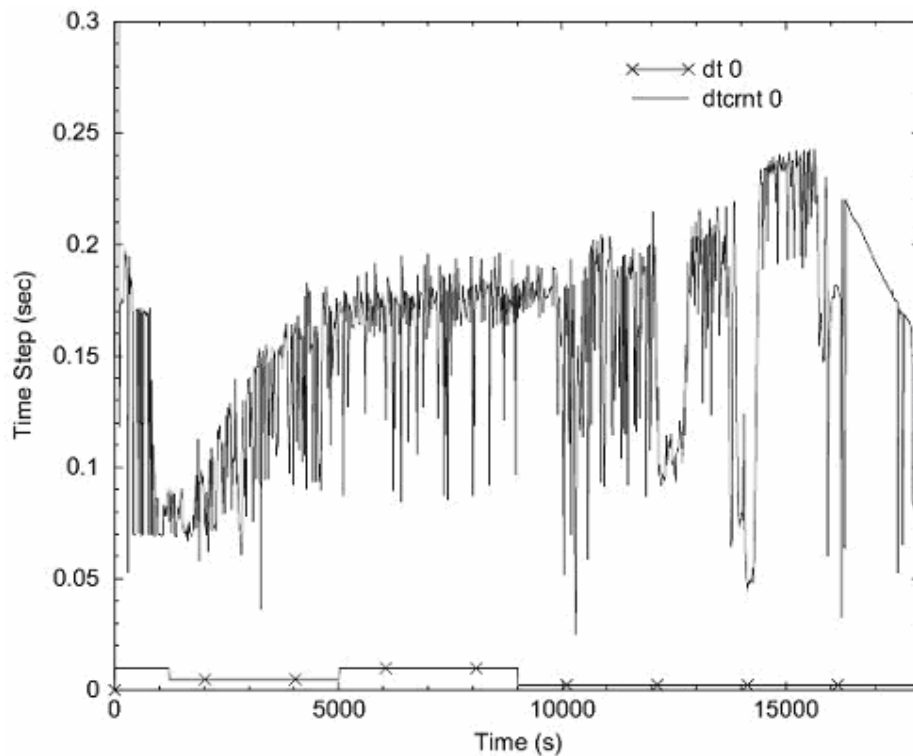


Figure 3.4-19 Time Step and Courant Time Step of the RELAP5 Calculation

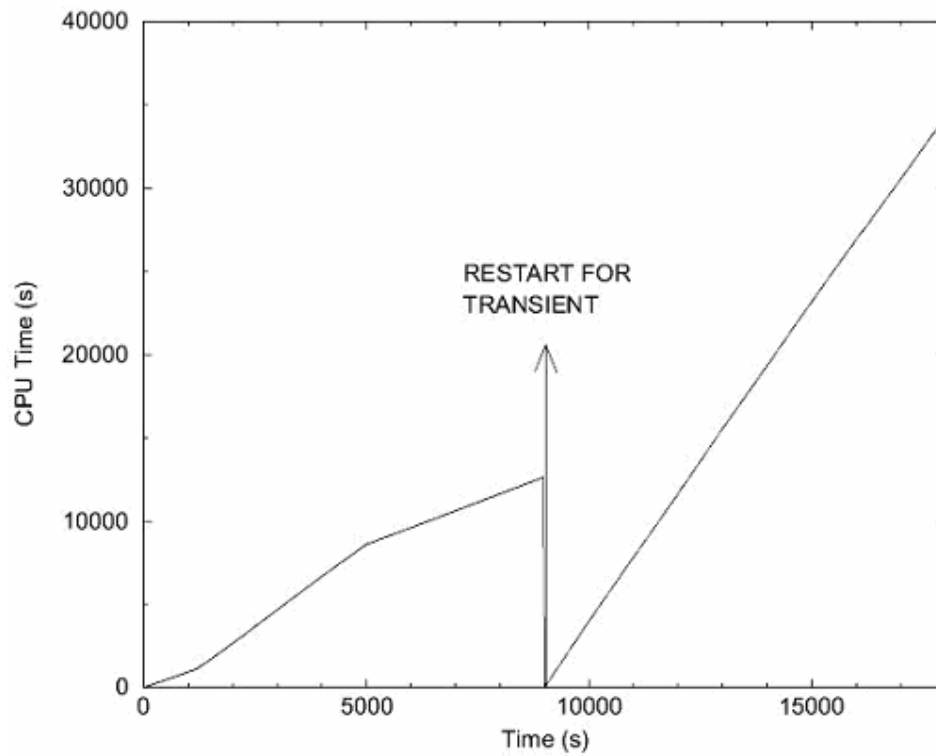


Figure 3.4-20 CPU Time of the RELAP5 Calculation

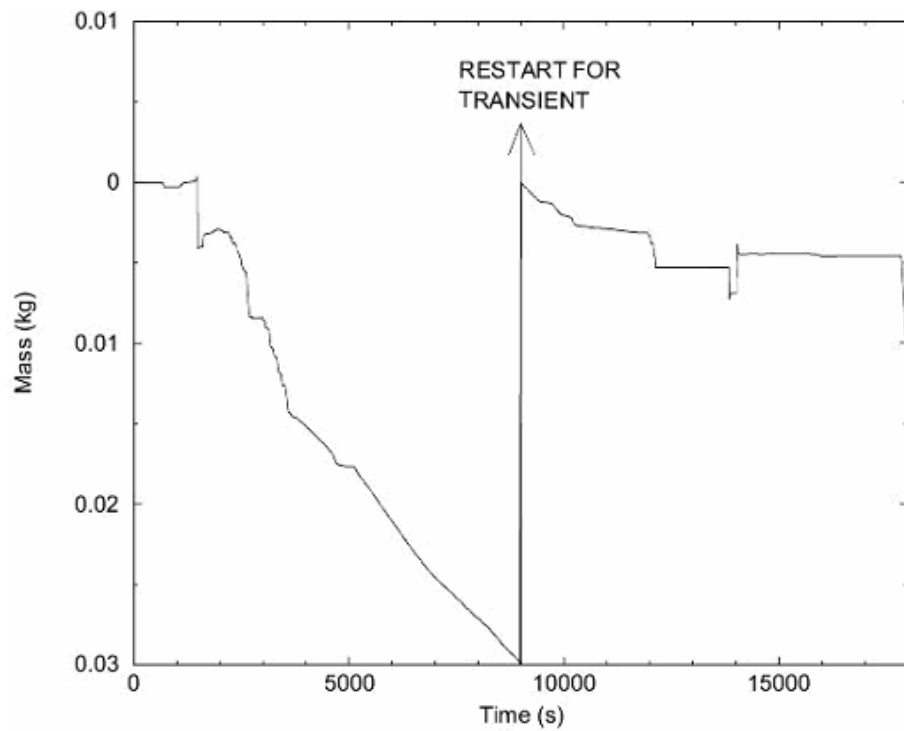


Figure 3.4-21 Mass Error of RELAP5 Calculation

3.4.3 Comparison of METU-CTF and UMCP Data with respect to Geometry and Hydrodynamics

Since main idea for designing the METU-CTF Facility and experimental test matrix came from the simulation of the loss of residual heat removal and feedwater systems on UMCP Test Facility, it could be worth to compare the main design and experimental parameters of two test facilities, i.e. METU-CTF and the steam generator model of the UMCP Facility. Note that only one tube is considered for the primary side of the steam generator model of the UMCP.

Primary Side:

Parameter	METU-CTF	UMCP ¹
D_i (m)	0.033	0.02997
D_o (m)	0.039	0.03175
t_m (mm)	3	0.89
A_{flow} (m ²)	8.553×10^{-4}	7.055×10^{-4}
L (m)	2.158	3.90525
L_{active} (m) prior transient	0.9	1.99
\dot{m} (kg/s) steady state in BCM	0.0028	0.0005
Re_{mix} (at entrance) steady state in BCM	8,000	800
P (bar) steady state in BCM	2.25	4.18

¹ Data applies to one SG tube

Secondary Side:

Parameter	METU-CTF	UMCP
D_i (m)	0.0812	0.311
D_h (m)	0.0422	0.0543
A_{flow} (m ²)	3.984×10^{-3}	5.15×10^{-2}
L (m)	2.158	3.90525 (tube length)
Tube heat transfer area (m ²)	0.2644	0.3895
\dot{m} (kg/s) steady state in BCM	0.181	0.115
Re _{coolant} range steady state in BCM	1,700–2,100	133–413
P (bar)	1.013	1.013

3.4.4 Comparison of RELAP5/mod3.2 and RELAP5/mod3.3 versions

In this section, the results obtained by the RELAP5/mod3.3 (beta version) code is compared to those of the earliest version of the RELAP5 code given to the TAEA under the CAMP Agreement, which is RELAP5/mod3.2. The mod3.2 version was installed on DEC ALPHA OSF/1 in 1996 with the Fortran OSF/1 compiler (Fortran 77; version 1.3) and the same executable “relap5.x” file was used for the comparison given in this section.

In Figure the upper plenum pressure is presented. It is clear from this figure that the system pressure is highly overestimated by RELAP5/m3.2 with a peak at 6,000 s. The overshooting yields a pressure of about 13 bars at 6,000 s, which is three times that of RELAP5/mod3.3 and experimental data during BCM period. This unrealistic result continues till the end of the transient with an overestimation of 100% compared to the result of mod3.3 at time 18,000 s. As discussed in previous sections, the coolant level in the secondary side of the SG-A is important for the correct prediction of heat transfer mechanism from the primary side. Both code versions yielded almost same results for the collapsed level in the secondary side of the SG-A, as seen in Figure . This simply proves that the heat transfer from primary to secondary side calculated by both code versions is almost same for transient period ($t > 9,000$ s). Since heat transfer by condensation is dominated by the first SG-A tube volume (P402-01 in Figure), the heat transfer modes are compared in Figure . The heat transfer modes predictions are almost same in both code versions. Although the mode of heat transfer, i.e. condensation in the presence of air, is predicted correctly by the earliest version of RELAP5, the heat flux at the same location exhibits important differences in two code versions, as shown in Figure . In spite of correct timing for condensation ($t \sim 2,000$ s), the heat removal from primary side initiates at about 4,000 s in calculation by mod3.2, which means 2,000 s delay compared to the mod3.3 result. This delay in heat transfer resulted in system pressure overestimation in mod3.2. The heat flux get closer at 7,000–9,000 s interval. For times greater than 9,000 s (LOFW transient), the heat flux is similar in both code versions.

Another remarkable result worth to mention is the mass error in two code versions (Figure): The mass error in RELAP5/mod3.2 calculation escalates to about +2.6 kg at 9,000 s (end of BCM steady state period) while it is –0.03 kg in RELAP5/mod3.3. The mass error calculated by mod3.2 version increases almost linearly during transient ($t > 9,000$ s) and reaches to +2.7 kg. As discussed previously, the mass error in transient period remains almost stable in mod3.3 calculation, which is –0.005 kg. However, the CPU time of mod3.3 is higher than that of mod3.2, as could be seen in Figure .

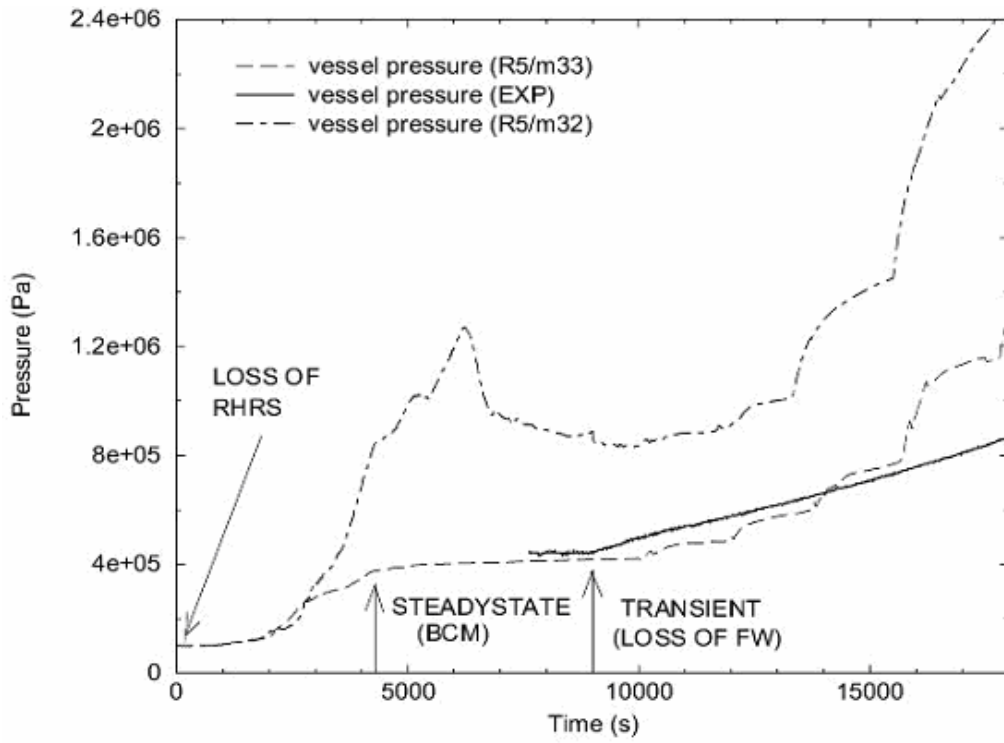


Figure 3.4-22 Upper Plenum Pressure (R5/m32 and R5/m33)

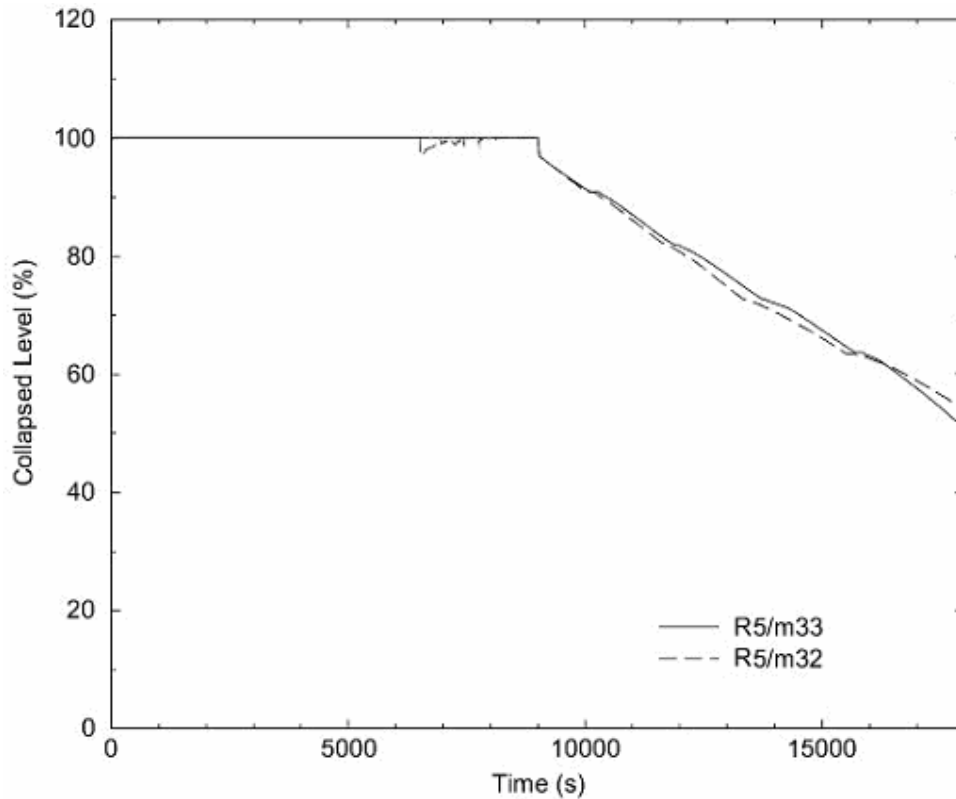


Figure 3.4-23 Secondary Side Level of SG-A (R5/m32 and R5/m33)

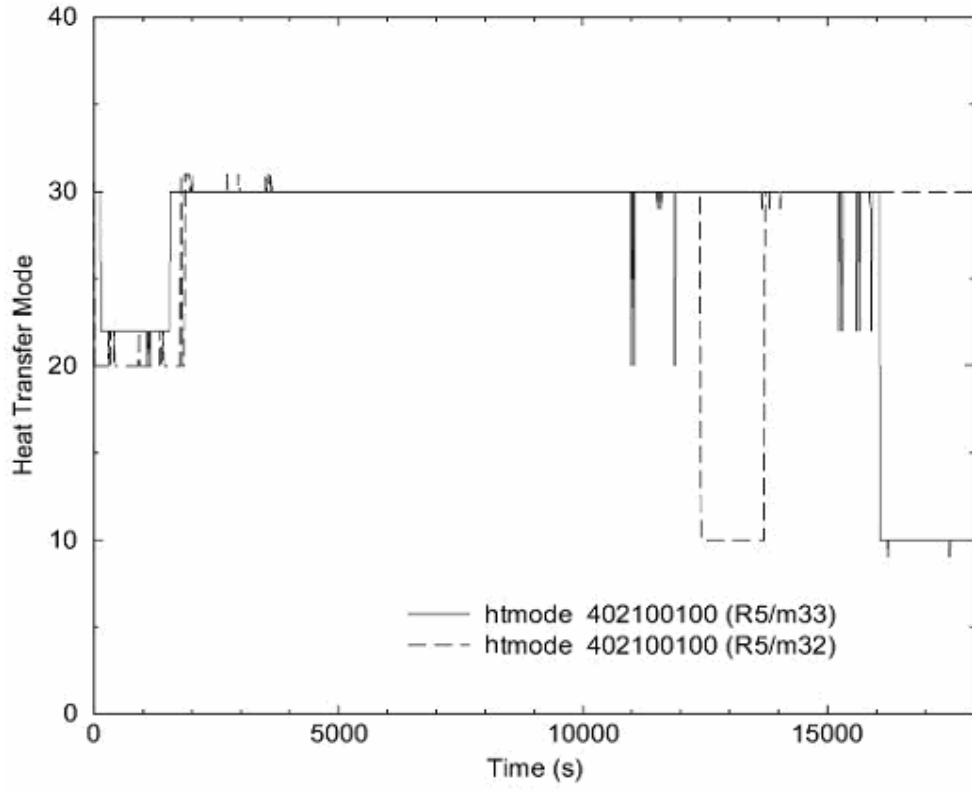


Figure 3.4-24 Heat Transfer Modes in Tubes of SG-A (R5/m32 and R5/m33)

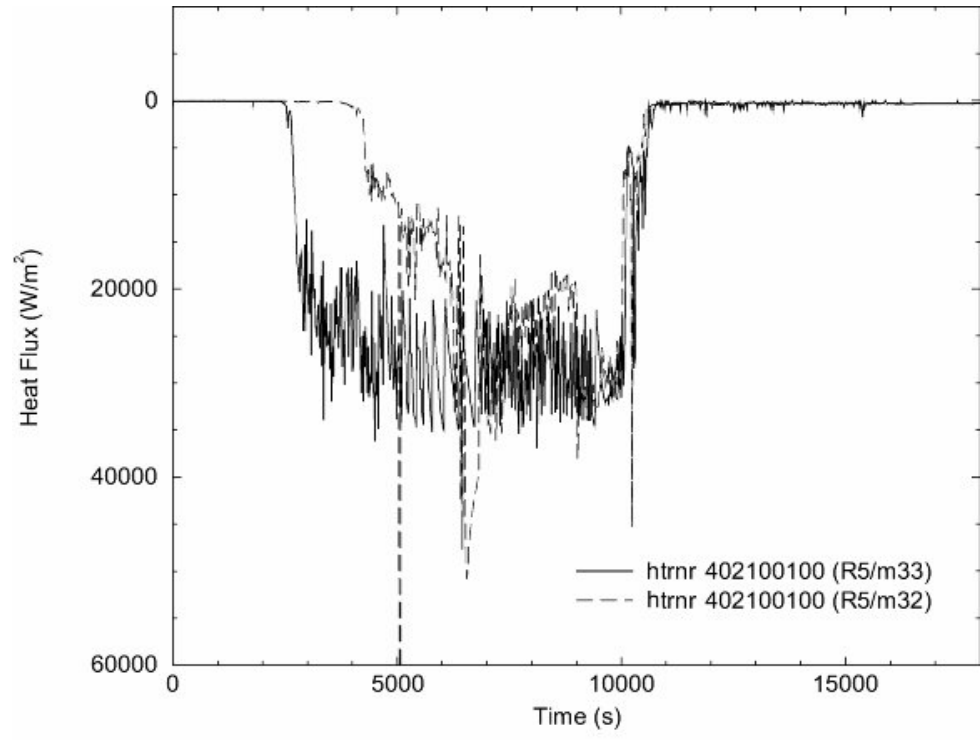


Figure 3.4-25 Heat Flux in Tubes of SG-A (R5/m32 and R5/m33)

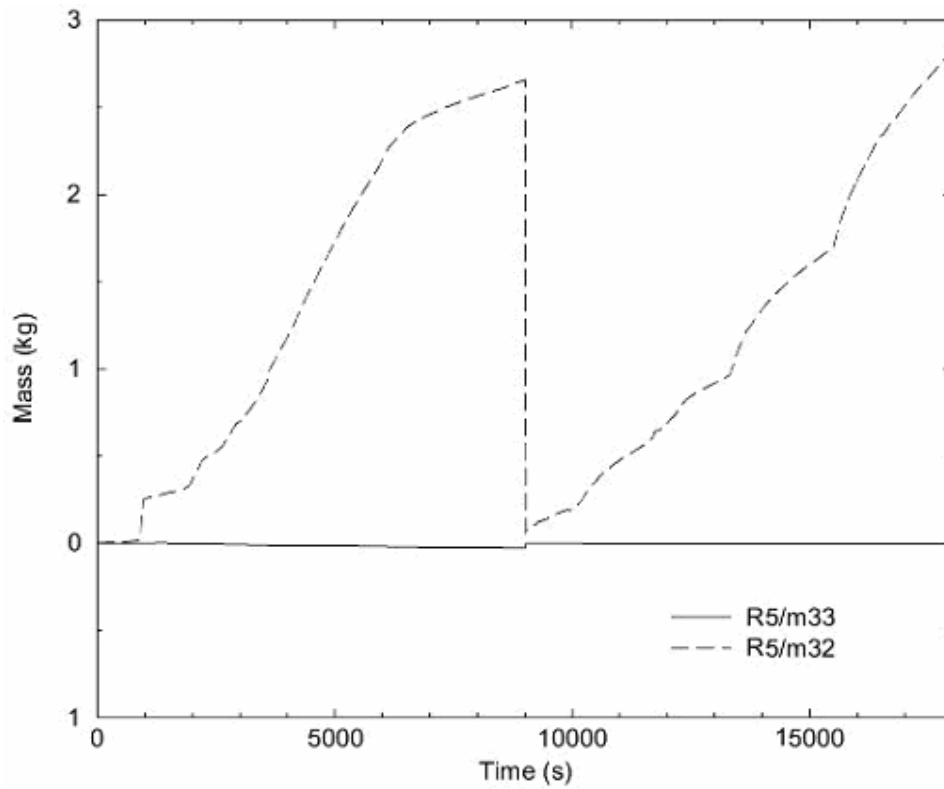


Figure 3.4-26 Mass Error of RELAP5 Calculation (R5/m32 and R5/m33)

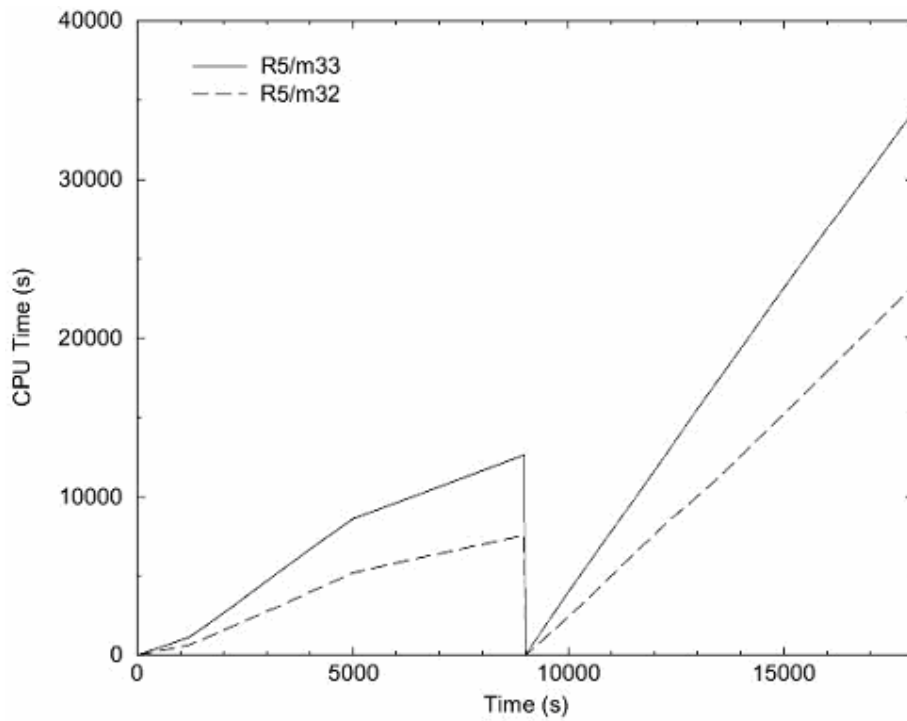


Figure 3.4-27 CPU Time of the RELAP5 Calculation (R5/m32 and R5/m33)

CONCLUSION

The following conclusions are drawn based on the experimental investigation of condensation in the presence of air, performed at the METU-CTF and UMCP test facilities, under transient conditions:

- (1) The pressure increase upon loss of coolant transient at the METU-CTF is almost linear by time and the rate of increase is about 0.6 mbar/s, for both pure vapor and air/vapor mixture cases. Vapor suction rate during BCM decreases considerably when some amount of air is trapped in the condenser tube prior to the start of experiment. The effective condensation length is the function of boil-off rate of coolant and air mass fraction in condenser tube. It is evident from the coolant temperature profiles at the secondary side that overall heat transfer rate is suppressed in transient with air/vapor mixture, which results in less boil-off rate compared to the corresponding pure vapor transient. It is clear that the rate of vapor suction is the function of condensation rate and hence a comparison of total heat transfer rates in cases with and without air exhibits this clearly, i.e. during BCM mode of operation in pure vapor case the total heat transfer rate is 19 kW which is as twice as that of air/vapor mixture case, i.e. 8 kW.
- (2) There is a general agreement between RELAP5 results and data for coolant temperature trends for pure steam case at the METU-CTF, both qualitatively and quantitatively. A deviation is observed at 200 s such that the coolant temperature is underestimated at the exit of coolant channel. However, the boil-off rate at time 1100 s was predicted almost correctly by the code although the length of channel in which saturated vapor exists seems to be shorter (~15 cm) in experiment. The comparison of RELAP5 results with the experimental data shows that the coolant temperature for steady state (BCM) is in agreement with the data while it yields an overestimation of about 8–10°C for the thermocouple TC-6 (above mid-plane of the jacket pipe) during transient ($t > 200$ s). However, calculated temperatures for TC-2 (bottom) and TC-12 (top) are much closer to the data with a difference of about 2–5°C and this is quite acceptable.
- (3) Although the coolant temperatures are in agreement with the data for pure steam case in METU-CTF simulation, an underestimation for local heat flux is observed for the calculation performed by using standard input model with jacket pipe, at steady state condition. However, a better heat flux prediction was obtained when the measured inner wall temperature was given as boundary condition. The cumulative heat transfer rate prediction of the code for steady state is better when measured inner wall temperatures are given as boundary condition and follows the trend of the data with an overestimation. The total heat load of the condenser, which is about 19 kW, is calculated with an error of less than 1%. The flow and heat transfer regimes in secondary side play an important role for simulation of this kind of transients.
- (4) The code prediction for coolant temperature at the secondary side is in agreement with the data of air/steam mixture case of METU-CTF qualitatively and smallest deviation (most of the values deviates less than 10%) from the data is obtained for steady state condition. However, the trend of coolant temperature does not strictly follow the data for steady state condition, which implies that the air mass distribution trend may be somehow different from the experimental condition. Similar to the pure steam case, a deviation is observed at 200 s such that the coolant temperature is underestimated at the exit of coolant channel. However, the boil-off rate at time 1100 s was predicted almost correctly by the code although the length of channel in which saturated vapor exists is shorter (~10 cm) in experiment. The comparison of RELAP5

results with the experimental data shows that the coolant temperatures for steady state (BCM) are in agreement with the data, with a maximum temperature deviation of 3°C, while it yields an overestimation of about 20°C, for the thermocouple TC-8 (above mid plane of the jacket pipe) during transient ($t \geq 200$ s). However, calculated temperatures for TC-2 (bottom) and TC-12 (top) are much closer to the data with a difference of about 2–3°C and this is quite acceptable.

- (5) The total heat load (8.3 kW) of METU-CTF condenser in air/steam case is predicted well by the code with a deviation of +4.6%. As in the case of pure steam case, the flow and heat transfer regimes in secondary side play an important role for simulation of this kind of transients.
- (6) This kind of simulations is very sensitive to the length of period of BCM prior to transient (loss of coolant to the secondary side) since steam flow to the condenser tube initiates condensation and accumulation of condensate due to heat removal to the secondary side. An optimum length of time for BCM should be selected in calculations to be able to get a realistic coolant temperature distribution in the jacket pipe, for both BCM and transient periods or otherwise the experiment should be well controlled with respect to condensate accumulation inside.
- (7) The thermodynamic state defined as saturated condition (flag 104 for volume control and X_s set to 1.0) for air/steam mixture simulations yielded better results in METU-CTF runs compared to dry air option.
- (8) The runs performed by a METU-CTF model of 27 volumes for condenser tube and 27 volumes for jacket pipe revealed the fact that the analyses for pure steam and air/steam mixture cases are not sensitive to the number of volumes, at least for volume number greater than 17.
- (9) In simulation of loss of RHRS and LOFW transients at the UMCP Test Facility, the RELAP5 code is in general successful and the results are in agreement with the data. The code underpredicts the system pressure during BCM steady state by 6% compared to the experimental data. The liquid temperature at the upper plenum of the vessel also follows the trend of the system pressure, as expected. The result of the code is in agreement with the data with the exception that there is an overestimation after 15,000 s for both system pressure and liquid temperature.
- (10) The lack of experimental data for the period between loss of RHRS and BCM steady state makes it impossible to assess the capability of the RELAP5 code for this period of analysis. However the general findings from the analysis are as follows: After loss of RHRS with SG-A active, voiding in core leads to a system pressure increase due to expansion of coolant in the vessel and then SG-A takes over the heat removal from primary system by condensation after pushing air in candy cane into the SG tubes as the result of upstream pressure increase. Occurance timing of these phenomena governs the parametric behaviour of the transient. During BCM steady state period, condensation of steam in the first SG-A tube volume of the RELAP5 model always dominates other volumes irrespective to the number of volumes whether it is 11 or 22. The heat transfer rate from the uppermost SG tube volume is ~78% of the total power, in the end of BCM ($t=9000$ s).
- (11) After feedwater flow was terminated to the secondary side (LOFW transient) of the SG-A (UMCP), coolant at the secondary side started to boil-off and this resulted in a shift of condensation to the lower volumes along with the level decrease in the secondary side. The air inside the tubes was also forced to accumulate in lower volumes in the progress of time. Another interesting observation made is that the heat power load of SG-A slowly decreases by time after the LOFW transient was initiated and condensation that persists in one hydrodynamic volume at a time is always a dominating heat transfer mechanism throughout the analysis. The dominating condensation process shifts to lower volumes as coolant level in the secondary side decreases.

- (12) Since the transient is not so fast, the fine node model of UMCP SG-A tubes with 22 volumes yielded similar results to those of the base model with coarse node modeling for SG-A with 11 volumes. It is important to note that the effective condensation length remains invariant with respect to volume number, at least for number of volumes greater than 11.
- (13) The mass error is improved in RELAP5/mod3.3 (beta version) and this is best understood by comparing to the earliest version (RELAP5/mod3.2). The mass error in RELAP5/mod3.2 calculation escalates to about +2.6 kg at 9,000 s (end of the BCM steady state period) while it is -0.03 kg in RELAP5/mod3.3. The mass error calculated by mod3.2 version increases almost linearly to a value of +2.7 kg, during transient ($t > 9,000$ s). As discussed previously, the mass error in transient period remains almost stable in mod3.3 calculation, which is -0.005 kg.

LIST OF REFERENCES

1. Tanrikut, A and Heper, H.H., "RELAP5/MOD3 Simulation of Loss of Residual Heat Removal System after Reactor Shutdown," American Nuclear Society 1995 Annual Meeting, Philadelphia, Pennsylvania (USA), 25–29 June 1995.
2. Tanrikut, A., Yesin, O., "An Experimental Research on In-tube Condensation in the Presence of Air," 2nd International Symposium on Two-phase Flow and Experimentation, Pisa (Italy), 23–26 May 1999.
3. Tanrikut, A., "An Assessment of RELAP5 Code for Pure Steam Condensation and Condensation in the Presence of Air," Annual Meeting for Nuclear Technology, Mannheim (Germany), 21–24 May 1996.
4. Tanrikut, A., Aybar, H. S., "RELAP5/MOD3 Simulation for Steam Condensation Under Forced Convection Conditions," American Nuclear Society 1995 Annual Meeting, Philadelphia, Pennsylvania (USA), 25–29 June 1995.
5. Tanrikut, A., "In-Tube Condensation in the Presence of Air," Ph.D. Thesis, Mechanical Engineering Department, Middle East Technical University, Ankara, 1998.
6. Tanrikut, A., Yesin, O., "In-Tube Steam Condensation in the Presence of Air," NUREG/IA-0184, USNRC, Washington, 2000.
7. RELAP5/MOD3.3Beta Code Manual Volume I: Code Structure, System Models and Solution Methods, Idaho National Engineering Laboratory, NUREG/CR-5535, 2001.
8. Methods of Measurements of Fluid in Closed Conduits, British Standard Institution, BS-1042, Section 1.1, 1981.
9. Popp, M., "The Simulation of Thermohydraulic Phenomena in a Pressurized Water Reactor Primary Loop," NUREG/CR-4789, University of Maryland, 1987.
10. Larson, T. K., "An Investigation of Integral Scaling and Data Relation Methods (Integral System Test Program)," NUREG/CR-4531, EGG-2440, INEL, 1987.
11. Heper, H. H., di Marzo, M. and Almenas, K. K., "Experimental Investigation of a B&W Test Facility Cooling Effectiveness Under Cold Shutdown Conditions," Technical Report, University of Maryland, 1991.
12. Brinkworth, B. J., *An Introduction to Experimentation*, The English Universities Press Ltd., 1968.

APPENDIX A

RELAP5 INPUT OF THE METU-CTF

```

*****
*
*
*       A RELAP5/MOD3.3 (beta) Model of the METU-CTF
*
*
*   * Model includes a vertical tube with the shell side *
*   * for the investigation of in-tube condensation *
*   * in the presence of noncondensables *
*
*   Ref: Design Data of the Test Facility (Ali Tanrikut)
*****
*
= METU-CTF Model, BCM air/steam mixture, FW Loss
*
***** steady-state period is just 20 s since the state of primary side (for SS)
***** of tube was taken from den3.out (Tw given as BCs)..!!!
*
100 new  transnt
*
110 air  * noncondensible
*
120 402010000 -0.058 h2o primary
121 502010000 0.050 h2o secondry
*
*   time step cards
*   -----
*
201 20.0 1.0-6 0.1 3 10 100 100
202 1020.0 1.0-6 0.1 3 1000 1000 1000
*
*
*****          TRIP CONTROL LOGIC          *****
*
401 time 0 ge null 0 20.0 n
*****
*
*
*          HYDRODYNAMIC COMPONENTS          *
*
*****
*
*   AIR Injection
*   -----
*
0010000 air-tank  tmdpvol
0010101 1.0+6 1.0+6 0.0 0.0 0.0 0.0 0.0 0.0 00000
0010200 104
0010201 0.0 2.26+5 397.0 0.0 * the state is forced to dry air condition
*
0020000 air-in  tmdpjun
0020101 001000000 222000000 0.0

```

```

0020200 1
0020201 -1.0 0.0 0.0 0.0
0020202 0.0 0.0 0.0 0.0
0020203 1.0+6 0.0 0.0 0.0
*
*   STEAM Inlet
*   -----
*
0030000 vap-tank   tmdpvol
0030101 1.0+6 1.0+6 0.0 0.0 0.0 0.0 0.0 0.0 00000
0030200 102   401
0030201 0.0 2.25+5 1.0
0030202 0.0 2.25+5 1.0
0030203 0.0 2.25+5 1.0
0030204 20.0 2.26+5 1.0
0030205 40.0 2.27+5 1.0
0030206 60.0 2.28+5 1.0
0030207 80.0 2.29+5 1.0
0030208 100.0 2.30+5 1.0
0030209 120.0 2.31+5 1.0
0030210 140.0 2.31+5 1.0
0030211 160.0 2.32+5 1.0
0030212 180.0 2.33+5 1.0
0030213 200.0 2.34+5 1.0
0030214 220.0 2.35+5 1.0
0030215 240.0 2.36+5 1.0
0030216 260.0 2.37+5 1.0
0030217 280.0 2.38+5 1.0
0030218 300.0 2.39+5 1.0
0030219 320.0 2.40+5 1.0
0030220 340.0 2.41+5 1.0
0030221 360.0 2.42+5 1.0
0030222 380.0 2.43+5 1.0
0030223 400.0 2.44+5 1.0
0030224 420.0 2.46+5 1.0
0030225 440.0 2.47+5 1.0
0030226 460.0 2.47+5 1.0
0030227 480.0 2.49+5 1.0
0030228 500.0 2.50+5 1.0
0030229 520.0 2.51+5 1.0
0030230 540.0 2.52+5 1.0
0030231 560.0 2.53+5 1.0
0030232 580.0 2.55+5 1.0
0030233 600.0 2.56+5 1.0
0030234 620.0 2.57+5 1.0
0030235 640.0 2.58+5 1.0
0030236 660.0 2.59+5 1.0
0030237 680.0 2.61+5 1.0
0030238 700.0 2.62+5 1.0
0030239 720.0 2.63+5 1.0
0030240 740.0 2.64+5 1.0
0030241 760.0 2.65+5 1.0
0030242 780.0 2.66+5 1.0
0030243 800.0 2.68+5 1.0

```

```

0030244 820.0 2.69+5 1.0
0030245 840.0 2.70+5 1.0
0030246 860.0 2.71+5 1.0
0030247 880.0 2.73+5 1.0
0030248 900.0 2.74+5 1.0
0030249 920.0 2.75+5 1.0
0030250 940.0 2.76+5 1.0
0030251 960.0 2.77+5 1.0
0030252 980.0 2.79+5 1.0
0030253 1000.0 2.80+5 1.0
*
*
0040000 vap-in  sngljun
0040101 003000000 222000000 0.0 0.0 0.0 001000
0040201 1 0.0 0.0 0.0
*
*0040000 vap-in      tmdpjun
*0040101 003000000 222000000 0.0
*0040200 1
*0040201 -1.0 0.0 0.0 0.0
*0040202 0.0 0.0 4.5-3 0.0
*0040203 1.0+6 0.0 4.5-3 0.0
*
*
****   Pipe Between Boiler and Condenser
*   -----
*   Di = 38.1 mm
*   Ai = 0.00114 m2
*   L = 0.5 m (L of horizontal piping: 1.8 m)
*
2220000 pipe  snglvol
2220101 0.00114 0.5 0.0 0.0 0.0 0.0 6.0-5 0.0 00000
2220200 104 2.25+5 397.1 1.0
*
2230000 cond-in1  sngljun
2230101 222010000 224000000 0.0 0.0 0.0 001000
2230201 1 0.0 0.0 0.0
*
****   Test Section Entrance
*   -----
*
*   Di = 38.1 mm
*   Ai = 0.00114 m2
*   L = 0.110 m (from horizontal pipe to flange)
*
2240000 pipe  snglvol
2240101 0.00114 0.110 0.0 0.0 -90.0 -0.110 6.0-5 0.0 00000
2240200 104 2.25+5 397.1 1.0
*
2250000 cond-in2  sngljun
2250101 224010000 226000000 0.0 0.0 0.0 001100
2250201 1 0.0 0.0 0.0
* Di = 33.5 mm

```

```

*      Ai = 0.000881 m2
*      L = 0.220 m (from flange to test section)
*
2260000 pipe    snglvol
2260101 0.000881 0.220 0.0 0.0 -90.0 -0.220 6.0-5 0.0 00000
2260200 104 2.25+5 397.1 1.0
*
2270000 cond-in2 sngljun
2270101 226010000 402000000 0.0 0.0 0.0 001000
2270201 1 0.0 0.0 0.0
*****
*
*      HEAT EXCHANGER
*
*      (TEST SECTION)
*
*****
*
*      HX Primary Side
*      -----
*
*      total number of tubes = 1
*      Di = 33.0 mm
*      Do = 39.0 mm
*      Ai = 0.0008553 m2
*      Ao = 0.0011946 m2
*      L = 2.158 m (active), 0.22 m (entrance), 0.07 m (to the exit pipe)
*      Vi = 0.0018457 m3 (L = 2.158 m)
*
4020000 hx-prm    pipe * Heights of volumes are adjusted
4020001 17        * with respect to TC locations
4020101 0.0008553 17
4020201 0.0       16
4020301 0.116    1 * TC:1
4020302 0.017    2
4020303 0.050    3 * TC:2
4020304 0.025    4
4020305 0.100    5 * TC:3
4020306 0.100    6 * TC:4
4020307 0.100    7 * TC:5
4020308 0.100    8 * TC:6
4020309 0.050    9
4020310 0.200    10 * TC:7
4020311 0.200    11 * TC:8
4020312 0.200    12 * TC:9
4020313 0.200    13 * TC:10
4020314 0.200    14 * TC:11
4020315 0.200    15 * TC:12
4020316 0.200    16 * TC:13
4020317 0.100    17 *
4020401 0.0       17
4020601 -90.0     17

```

4020801 6.0-5 0.033 17
 4020901 0.0 0.0 16
 4021001 0000000 17
 4021101 001000 16
 4021201 105 397.1 0.12 0.00000001 0.0 0.0 1 *** state taken from den3.out !
 4021202 105 397.1 0.121 0.00000001 0.0 0.0 2
 4021203 105 397.1 0.097 0.00000001 0.0 0.0 3
 4021204 105 397.1 0.105 0.00000001 0.0 0.0 4
 4021205 105 397.1 0.082 0.00000001 0.0 0.0 5
 4021206 105 397.1 0.079 0.00000001 0.0 0.0 6
 4021207 105 397.1 0.061 0.00000001 0.0 0.0 7
 4021208 105 397.1 0.083 0.00000001 0.0 0.0 8
 4021209 105 397.1 0.022 0.00000001 0.0 0.0 9
 4021210 105 397.1 0.167 0.00000001 0.0 0.0 10
 4021211 105 379.92 0.001 0.532 0.0 0.0 11
 4021212 105 348.05 0.00000001 0.887 0.0 0.0 12
 4021213 105 340.60 0.00000001 0.920 0.0 0.0 13
 4021214 105 336.50 0.00000001 0.935 0.0 0.0 14
 4021215 105 333.80 0.00000001 0.943 0.0 0.0 15
 4021216 105 331.97 0.00000001 0.948 0.0 0.0 16
 4021217 105 331.40 0.00000001 0.950 0.0 0.0 17
 4021300 1
 4021301 0.0 0.0 0.0 16
 *

4030000 cond-out sngljun
 4030101 402010000 404000000 0.0 0.0 0.0 001100
 4030201 1 0.0 0.0 0.0
 *

**** dead volume at the bottom of the test section
 * A-eq=0.00227 m2

4040000 pipe snglvol
 4040101 0.0 0.240 0.000545 0.0 -90.0 -0.240 6.0-5 0.0 00000
 4040200 105 338.0 0.00000001 0.507
 *

4120000 cond-out tmdpjun * No Flow !
 4120101 404010000 405000000 0.0
 4120200 1
 4120201 -1.0 0.0 0.0 0.0
 4120202 0.0 0.0 0.0 0.0
 4120203 1.0+6 0.0 0.0 0.0
 *

4050000 atm tmdpvvol
 4050101 1.0+6 1.0+6 0.0 0.0 0.0 0.0 0.0 0.0 00000
 4050200 102
 4050201 0.0 1.0135+5 1.0
 *

*
 * HX Secondary Side
 * -----
 *
 * Feedwater Inlet
 * -----

5010000 hxfw-in tmdpvvol
 5010101 1.0+6 1.0+6 0.0 0.0 0.0 0.0 0.0 0.0 00000

5010200 103
5010201 0.0 1.0135+5 288.05
5110000 hxfw-in tmdpjun
5110101 501000000 502000000 2.85-4 * 1 x 3/4 in. tube
5110200 1 401
5110201 -1.0 0.181 0.0 0.0
5110202 0.0 0.181 0.0 0.0
5110203 0.0 0.0 0.0 0.0
5110204 1.0+6 0.0 0.0 0.0
*
* HX Shell-Side
* -----
* Di = 81.2 mm
* Ai = 0.0051785 m2
* Aflow = 0.0039839 m2
* L = 2.158 m (active)
* V = 0.008597 m3
*
5020000 hx-sec pipe
5020001 17
5020101 0.0039839 17
5020201 0.0 16
5020301 0.100 1
5020302 0.200 2 * TC:13
5020303 0.200 3 * TC:12
5020304 0.200 4 * TC:11
5020305 0.200 5 * TC:10
5020306 0.200 6 * TC:9
5020307 0.200 7 * TC:8
5020308 0.200 8 * TC:7
5020309 0.050 9
5020310 0.100 10 * TC:6
5020311 0.100 11 * TC:5
5020312 0.100 12 * TC:4
5020313 0.100 13 * TC:3
5020314 0.025 14
5020315 0.050 15 * TC:2
5020316 0.017 16
5020317 0.116 17 * TC:1
5020401 0.0 17
5020601 90.0 17
5020801 6.0-5 0.0422 17 * Dh = 0.0422 m (annulus) -> 0.0211 m (gap)
5020901 0.0 0.0 16
5021001 00000 17
5021101 001000 16
5021201 103 1.0135+5 288.05 0.0 0.0 0.0 17
5021300 1
5021301 0.181 0.0 0.0 16
* Feedwater Outlet
* -----
5120000 hxfw-out sngljun * 1 x 3/4 in. tube
5120101 502010000 503000000 2.85-4 0.0 0.0 001000
5120201 1 0.181 0.0 0.0

5030000 dump tmdpvol
 5030101 1.0+6 1.0+6 0.0 0.0 0.0 0.0 0.0 0.0 00000
 5030200 102
 5030201 0.0 1.0135+5 1.0

* *
 * HEAT STRUCTURES *
 * *

* CONDENSER TUBE SECTION
 * -----

* HX tube
 * number of tubes:1
 * Di = 33 mm, Do = 39 mm
 * meat thickness: 3 mm
 * tube length: 2.158 m (active)
 *

14021000 17 13 2 1 0.0165
 14021100 0 1
 14021101 12 0.0195 * num. of ints., right coordinate
 14021201 001 12 * st. steel
 14021301 0.0 12
 14021400 0
 14021401 400.0 13
 14021501 402010000 0 1 1 0.116 1 * TC:1
 14021502 402020000 0 1 1 0.017 2
 14021503 402030000 0 1 1 0.050 3 * TC:2
 14021504 402040000 0 1 1 0.025 4
 14021505 402050000 0 1 1 0.100 5 * TC:3
 14021506 402060000 0 1 1 0.100 6 * TC:4
 14021507 402070000 0 1 1 0.100 7 * TC:5
 14021508 402080000 0 1 1 0.100 8 * TC:6
 14021509 402090000 0 1 1 0.050 9
 14021510 402100000 0 1 1 0.200 10 * TC:7
 14021511 402110000 0 1 1 0.200 11 * TC:8
 14021512 402120000 0 1 1 0.200 12 * TC:9
 14021513 402130000 0 1 1 0.200 13 * TC:10
 14021514 402140000 0 1 1 0.200 14 * TC:11
 14021515 402150000 0 1 1 0.200 15 * TC:12
 14021516 402160000 0 1 1 0.200 16 * TC:13
 14021517 402170000 0 1 1 0.100 17 *
 14021601 502170000 0 1 1 0.116 1 * TC:1
 14021602 502160000 0 1 1 0.017 2
 14021603 502150000 0 1 1 0.050 3 * TC:2
 14021604 502140000 0 1 1 0.025 4
 14021605 502130000 0 1 1 0.100 5 * TC:3
 14021606 502120000 0 1 1 0.100 6 * TC:4
 14021607 502110000 0 1 1 0.100 7 * TC:5
 14021608 502100000 0 1 1 0.100 8 * TC:6
 14021609 502090000 0 1 1 0.050 9
 14021610 502080000 0 1 1 0.200 10 * TC:7
 14021611 502070000 0 1 1 0.200 11 * TC:8
 14021612 502060000 0 1 1 0.200 12 * TC:9

14021613 502050000 0 1 1 0.200 13 * TC:10
 14021614 502040000 0 1 1 0.200 14 * TC:11
 14021615 502030000 0 1 1 0.200 15 * TC:12
 14021616 502020000 0 1 1 0.200 16 * TC:13
 14021617 502010000 0 1 1 0.100 17 *
 14021701 0 0.0 0.0 0.0 17
 14021801 0.033 100. 100. 5. 5. 0. 0. 1. 17
 14021901 0.130 100. 100. 5. 5. 0. 0. 1. 17

*
*

*
* MATERIAL DATA *
*

*
*

20100100 tbl/fctn 1 1 * stainless-steel
(AISI 304L)

*

* temp. cond. (W/m-K)

20100101 273.15 13.0
 20100102 293.0 15.0
 20100103 373.0 15.5
 20100104 473.0 17.5
 20100105 673.0 20.0
 20100106 873.0 22.5
 20100107 1073.0 25.5
 20100108 1500.0 26.0

* temp. heat cap. (J/m3-K)

20100151 273.15 3.900+06
 20100152 373.0 3.900+06
 20100153 473.0 4.070+06
 20100154 573.0 4.230+06
 20100155 673.0 4.330+06
 20100156 1000.0 4.500+06
 20100157 1500.0 5.380+06

*

* GENERAL TABLES *

*

* Temperature of Environment

20200100 temp
 20200101 -1.0 297.0
 20200102 0.0 297.0
 20200103 1.0+6 297.0

* Heat Transfer Coeff. of Environment

20200200 htc-t
20200201 -1.0 7.0
20200202 0.0 7.0
20200203 1.0+6 7.0

* CONTROL VARIABLES *

*

***** COLLAPSED LEVEL CALCULATIONS *****

*

*

* HX Primary Side

*

20501100 hx-tube1 sum 1.0 0.0 1
20501101 0.0 0.116 voidf 402010000
20501102 0.017 voidf 402020000
20501103 0.050 voidf 402030000
20501104 0.025 voidf 402040000
20501105 0.100 voidf 402050000
20501106 0.100 voidf 402060000
20501107 0.100 voidf 402070000
20501108 0.100 voidf 402080000
20501109 0.050 voidf 402090000
20501110 0.200 voidf 402100000
20501111 0.200 voidf 402110000
20501112 0.200 voidf 402120000
20501113 0.200 voidf 402130000
20501114 0.200 voidf 402140000
20501115 0.200 voidf 402150000
20501116 0.200 voidf 402160000
20501117 0.100 voidf 402170000
20500100 hx-tube sum 1.0 0.0 1
20500101 0.0 1.0 cntrlvar 11

*

* HX Secondary Side

*

20502200 hx-shel1 sum 1.0 0.0 1
20502201 0.0 0.100 voidf 502010000
20502202 0.200 voidf 502020000
20502203 0.200 voidf 502030000
20502204 0.200 voidf 502040000
20502205 0.200 voidf 502050000
20502206 0.200 voidf 502060000
20502207 0.200 voidf 502070000
20502208 0.200 voidf 502080000
20502209 0.050 voidf 502090000
20502210 0.100 voidf 502100000
20502211 0.100 voidf 502110000
20502212 0.100 voidf 502120000
20502213 0.100 voidf 502130000
20502214 0.025 voidf 502140000
20502215 0.050 voidf 502150000
20502216 0.017 voidf 502160000
20502217 0.116 voidf 502170000

20500200 hx-shell sum 1.0 0.0 1
20500201 0.0 1.0 cntrlvar 22

*

* % Level Ratios ((Collapsed Level / Total Height) * 100)

*

* HX Primary Side Tot. Height: 2.158 m

20510100 hxpr-rat mult 46.339 0.0 1

20510101 cntrlvar 1

*

* HX Secondary Side Tot. Height: 2.158 m

20510200 hxsc-rat mult 46.339 0.0 1

20510201 cntrlvar 2

*

*

* Calculation for Condensate Accumulated

*

* Total Mass Flow Rate of Condensate (kg/s)

*

20521100 cond-rt1 sum -0.0008553 0.0 1

20521101 0.0 0.116 vapgen 402010000

20521102 0.017 vapgen 402020000

20521103 0.050 vapgen 402030000

20521104 0.025 vapgen 402040000

20521105 0.100 vapgen 402050000

20521106 0.100 vapgen 402060000

20521107 0.100 vapgen 402070000

20521108 0.100 vapgen 402080000

20521109 0.050 vapgen 402090000

20521110 0.200 vapgen 402100000

20521111 0.200 vapgen 402110000

20521112 0.200 vapgen 402120000

20521113 0.200 vapgen 402130000

20521114 0.200 vapgen 402140000

20521115 0.200 vapgen 402150000

20521116 0.200 vapgen 402160000

20521117 0.100 vapgen 402170000

*

20520000 cond-rat sum 1.0 0.0 1

20520001 0.0 1.0 cntrlvar 211

*

*

* Total Mass of Condensate (kg)

20530000 condmass integral 1.0 0.0 1

20530001 cntrlvar 200

*

***** POWER CALCULATIONS *****

* Steam Generator:

20561000 pow-hx1 sum 1.0 0.0 1
20561001 0.0 1.0 q 402010000
20561002 1.0 q 402020000
20561003 1.0 q 402030000
20561004 1.0 q 402040000
20561005 1.0 q 402050000
20561006 1.0 q 402060000
20561007 1.0 q 402070000
20561008 1.0 q 402080000
20561009 1.0 q 402090000
20561010 1.0 q 402100000
20561011 1.0 q 402110000
20561012 1.0 q 402120000
20561013 1.0 q 402130000
20561014 1.0 q 402140000
20561015 1.0 q 402150000
20561016 1.0 q 402160000
20561017 1.0 q 402170000
*

20560000 pow-hx sum 1.0 0.0 1
20560001 0.0 1.0 cntrlvar 610
*

*

* Mass Calculations:

* -----

* Mass of Vapor-in

20570000 mass-vap integral 1.0 0.0 1

20570001 mflowj 004000000
*

* Mass of Air-in

20570100 mass-air integral 1.0 0.0 1

20570101 mflowj 002000000
*

* Mass of Mixture-in

20570200 mass-mix integral 1.0 0.0 1

20570201 mflowj 227000000
*

* Mass of Mixture-out

20570300 mass-mix integral 1.0 0.0 1

20570301 mflowj 412000000
*

*

*

* END OF INPUT FILE *

.

APPENDIX B

RELAP5 INPUT OF THE UMCP 2X4 TEST FACILITY

```

*****
*
* A RELAP5/MOD3 model for the UMCP 2x4 loop
*
* Set up for natural circulation test initial conditions
*
*
* Two-Loop modified UMCP-facility model (Combined CLs)
*
* Steady-state cold condition:
*   - core power: 0.0 kW
*   - primary and secondary pressure: 1.013+5 Pa
*   - temperature of volumes: 303 K
*   - SG-I primary 53 % filled
*   - SG-II primary 42 % filled
*   - SG secondary 100 % filled
*   - feed-water flow rate: 0.115 kg/s
*   - volumes not filled are occupied by air
* Steady-state hot condition:
*   - core power 34.9 kW
*   - SG 75% filled
*   (modeled by constant pressure boundary
*   condition at feedwater inlet)
*   - primary pressure 4.4+5 kPa
*
*           2 - L O O P   M O D E L
*
* volumes filled with air is in saturated condition (flag 104: Xs=1.0)
*****
= UMCP 2 x 4 Model: Loss of RHRS and FWS
*
100 new transnt
*
110 air * noncondensable
*
* Hydrodynamic System Control Cards
* -----
120 101010000 0.0 h2o primary
121 405010000 0.0 h2o secondary
*
* time step cards
* -----
*
201 200.0 1.-6 .01 3 2000 20000 20000
202 1200.0 1.-6 .01 3 2000 100000 100000
203 5000.0 1.-6 .005 3 4000 380000 380000
204 6000.0 1.-6 .01 3 2000 100000 100000
205 9000.0 1.-6 .01 3 2000 300000 300000
*
***** TRIP CONTROL LOGIC *****

```

```

* trip for problem termination:
*401 p 123010000 ge null 0 4.4+5 n
*600 401
*
* RVVV opening pressure:
401 p 122010000 ge p 142010000 510.0 n * for Mass = 133.5 gr
*
* del-p = 0.074 psi
*****
*
* HYDRODYNAMIC COMPONENTS *
*
* Energy Loss Coefficients for Flow Direction *
* Changes are taken from Popp *
*
*****
*
*****
*
* PRESSURE VESSEL *
*
* V = 0.22203 m3 (with DC) *
* V = 0.17029 m3 (w/o DC) *
*
*****
* LOWER PLENUM
* -----
* A = 0.18497 m2
1010000 low-plen snglvol
1010101 0.0 .13462 .02490 0.0 90.0 0.13462 1.-5 0.0 00000
1010200 103 1.013+5 303.0
*
1610000 lp-core sngljun * core support plate = 1.9 cm
1610101 101010000 111000000 0.03325 2.0 2.0 000000 * K values are assumed!
1610201 1 0.0 0.0 0.0
* CORE
* ----
* A = 0.12264 m2
1110000 core pipe
1110001 3
1110101 0.0 3
1110201 0.0 2
1110301 0.2032 3
1110401 0.02492 3
1110601 90.0 3
1110701 0.2032 3
1110801 1.-5 0.184 3 * Dh = 0.184 m (circular pattern + vessel)
1110901 0.0 0.0 2
1111001 00100 3
1111101 000000 2
1111201 103 1.013+5 303.0 0.0 0.0 0.0 1
1111202 103 1.013+5 303.0 0.0 0.0 0.0 2
1111203 103 1.013+5 303.0 0.0 0.0 0.0 3

```

```

1111300 1
1111301 0.0 0.0 0.0 2
1710000 core-up sngljun * core support plate = 1.9 cm
1710101 111010000 121000000 0.03325 2.0 2.0 000000 * K values are assumed !
1710201 1 0.0 0.0 0.0
*
      UPPER PLENUM
*
      -----
*
      A = 0.08153 m2
1210000 up-plen1 snglvol
1210101 0.0 0.16764 0.013667 0.0 90.0 0.16764 1.-5 0.0 00000
1210200 103 1.013+5 303.0
*
1810000 up-1 sngljun
1810101 121010000 122000000 0.0 0.0 0.0 000000
1810201 1 0.0 0.0 0.0
1220000 up-plen2 branch
1220001 2 1
1220101 0.0 0.1397 0.011389 0.0 90.0 0.1397 1.-5 0.0 00000
1220200 103 1.013+5 303.0
1221101 122000000 201000000 0.00638 0.0 0.0 000100 * hot leg-I connection
1222101 122000000 701000000 0.00638 0.0 0.0 000100 * hot leg-II connection
1221201 0.0 0.0 0.0
1222201 0.0 0.0 0.0
*
1820000 up-2 sngljun
1820101 122010000 123000000 0.0 0.0 0.0 000000
1820201 1 0.0 0.0 0.0
*
1230000 up-plen3 snglvol * A = 0.0815 m2 (V/L)
1230101 0.0 0.09906 0.008076 0.0 90.0 0.09906 1.-5 0.0 00000
1230200 103 1.013+5 303.0
*
1830000 up-uh sngljun
1830101 123010000 131000000 0.0 0.0 0.0 000100
1830201 1 0.0 0.0 0.0
*
      UPPER HEAD
*
      -----
*
      A = 0.1737 m2
1310000 up-head pipe
1310001 2
1310101 0.0 2
1310301 0.14758924 1
1310302 0.06831076 2
1310401 0.025635 1
1310402 0.011865 2
1310601 90.0 2
1310801 1.-5 0.0 2
1310901 0.0 0.0 1
1311001 00000 2
1311101 000000 1
1311201 003 1.013+5 303.0 0.0 0.0 0.0 1
1311202 004 1.013+5 303.0 1.0 0.0 0.0 2 * noncond.
1311300 1

```

```

1311301 0.0 0.0 0.0 1
*
*   DOWNCOMER
*   -----
*
1410000 uppr-dc2 snglvol
1410101 0.04497 0.23876 0.0 0.0 -90.0 -0.23876 1.-5 0.0635 00000
1410200 103 1.013+5 303.0
*
1520000 dc-1 sngljun
1520101 141010000 142000000 0.0 0.0 0.0 000000
1520201 1 0.0 0.0 0.0
*
1420000 dc-cl branch
1420001 2 1
1420101 0.04497 0.16764 0.0 0.0 -90.0 -0.16764 1.-5 0.0635 00000
1420200 103 1.013+5 303.0
1421101 607010000 142000000 0.00954 0.0 0.0 000100 * connection to cold leg-I
1422101 907010000 142000000 0.00954 0.0 0.0 000100 * connection to cold leg-II
1421201 0.0 0.0 0.0
1422201 0.0 0.0 0.0
*
1530000 dc-2 sngljun
1530101 142010000 143000000 0.0 0.0 0.0 000000
1530201 1 0.0 0.0 0.0
*
1430000 dc-ann annulus
1430001 1
1430101 0.04497 1
1430301 0.74422 1
1430401 0.0 1
1430601 -90.0 1
1430701 -0.74422 1
1430801 1.-5 0.0635 1
1431001 00000 1
1431201 103 1.013+5 303.0 0.0 0.0 0.0 1
*
1510000 dc-lp sngljun
1510101 143010000 101000000 0.01115 0.7 0.7 000100 * 180 deg. change in flow
dir. (given)
1510201 1 0.0 0.0 0.0 * Aj is from UMCP input
*
*****
*
*   RVVV Model:
*   -----
*1990000 rvvv valve
*1990101 123000000 141000000 7.35-4 0.0 0.0 000000
*1990201 1 0.0 0.0 0.0
*1990300 srvvlv * servo valve
*1990301 199
*1990401 0.0 0.0 0.0
*1990402 0.09 5.17 5.17

```

```

*1990403 0.2 9.68 9.68
*1990404 0.4 16.36 16.36
*1990405 1.0 30.60 30.60
*      0.7 x A -> Aflow = 7.35-4 m2 (D = 3.65 cm; A = 1.047-3 m2)
*      Number of vent valves: 8
*
1990000 rvvv-l valve * Ajun = 8 x 7.35-4 m2 !
1990101 122000000 142000000 0.00586 2.0 2.0 000000 * Kf, Kr taken from Popp
1990201 1 0.0 0.0 0.0 * K values are for fully open valve
1990300 trpvlv * trip valve * (angle = 20 degrees)
1990301 401
*      control variable for normalized area calculation:
*20519900 rvv-area function 1.0 0.0 1
*20519901 cntrlvar 700 200
*
*      control variable for dP calculation between vols 123-141:
20570000 rvv-delp sum 1.0 0.0 1
20570001 0.0 1.0 p 122010000
20570002 -1.0 p 142010000
*
*      general table for del-p versus normalized area:
*20220000 reac-t
*20220001 -1.0+9 0.0
*20220002 0.0 0.0
*20220003 172.0 0.0
*20220004 482.0 1.0
*20220005 1.0+9 1.0
*
*****
*
*      HOT LEG - I *
*
*      (RPV - SG) *
*
*      Di = 0.0901 m *
*      A = 0.00638 m2 *
*      L = 5.00845 m *
*      V = 0.03195 m3 *
*
*****
2010000 hl-1 snglvol
2010101 0.00638 0.684 0.0 0.0 0.0 0.0 4.5-5 0.0 01000
2010200 103 1.013+5 303.0
*
2110000 hl-1 sngljun
2110101 201010000 202000000 0.0 0.27 0.27 000000 * 90 deg. bend (given)
2110201 1 0.0 0.0 0.0
2020000 hl-2 branch * the height is adjusted to the PRZ surge line inlet
2020001 2 1
2020101 0.00638 0.381 0.0 0.0 90.0 0.381 4.5-5 0.0 00000
2020200 103 1.013+5 303.0
2021101 202010000 203000000 0.0 0.0 0.0 000000 * hot leg connection
2022101 202010000 310000000 3.44-4 0.0 0.0 000100 * PRZ connection

```

2021201 0.0 0.0 0.0
 2022201 0.0 0.0 0.0
 2030000 hl-3 pipe
 2030001 3
 2030101 0.00638 3
 2030301 0.46355 1
 2030302 0.84455 3
 2030401 0.0 3
 2030601 90.0 3
 2030801 4.5-5 0.0 3
 2031001 00000 3
 2031101 000000 2
 2031201 104 1.013+5 303.0 1.0 0.0 0.0 3 * noncond.
 2031300 1
 2031301 0.0 0.0 0.0 2
 *
 2130000 hl-3 sngljun
 2130101 203010000 204000000 0.0 0.14 0.14 000000 * 45 deg. bend (given)
 2130201 1 0.0 0.0 0.0
 *
 2040000 hl-4 snglvol
 2040101 0.00638 0.6504 0.0 0.0 41.6 0.4318 4.5-5 0.0 00000
 2040200 104 1.013+5 303.0 1.0 * noncond.
 *
 2140000 hl-4 sngljun
 2140101 204010000 205000000 0.0 0.14 0.14 000000 * 45 deg. bend (given)
 2140201 1 0.0 0.0 0.0
 *
 2050000 hl-5 snglvol
 2050101 0.00638 0.490 0.0 0.0 0.0 0.0 4.5-5 0.0 01000
 2050200 104 1.013+5 303.0 1.0 * noncond.
 *
 2150000 hl-5 sngljun
 2150101 205010000 206000000 0.0 0.14 0.14 000000 * 45 deg. bend (given)
 2150201 1 0.0 0.0 0.0
 *
 2060000 hl-6 snglvol
 2060101 0.00638 0.6504 0.0 0.0 -41.6 -0.4318 4.5-5 0.0 00000
 2060200 104 1.013+5 303.0 1.0 * noncond.
 *
 2160000 hl-sg-in sngljun
 2160101 206010000 401000000 0.00638 0.14 0.14 000100 * 45 deg. bend (given)
 2160201 1 0.0 0.0 0.0

* *
 * PRESSURIZER AND SURGE LINE *
 * *

* SURGE LINE
 * -----
 * Di = 20.93 mm
 * A = 0.000344 m2
 * L = 4.8769 m
 * V = 0.001678 m3

3100000 surge pipe
3100001 8
3100101 3.44-4 8
3100201 0.0 7
3100301 0.2667 1
3100302 0.7811 2
3100303 0.6731 4
3100304 0.95885 6
3100305 0.2794 7
3100306 0.2858 8
3100401 0.0 8
3100601 0.0 1
3100602 -90.0 2
3100603 0.0 4
3100604 90.0 6
3100605 0.0 7
3100606 90.0 8
3100701 0.0 1
3100702 -0.7811 2
3100703 0.0 4
3100704 0.95885 6
3100705 0.0 7
3100706 0.2858 8
3100801 3.33-5 0.0 8
3100901 0.0 0.0 7
3101001 01000 1
3101002 00000 2
3101003 01000 4
3101004 00000 6
3101005 01000 7
3101006 00000 8
3101101 000000 4
3101102 000000 5
3101103 000000 7
3101201 104 1.013+5 303.0 1.0 0.0 0.0 8 * noncond.
3101300 1
3101301 0.0 0.0 0.0 7
3150000 surge sngljun
3150101 310010000 320000000 0.0 0.0 0.0 000100
3150201 1 0.0 0.0 0.0
* PRESSURIZER TANK
* -----
* Di = 0.31115 m
* A = 0.07604 m2
* L = 1.3208 m
* V = 0.1 m3
*
3200000 prz-tank pipe
3200001 5
3200101 0.07604 5 * modified by using standard Di value !
3200201 0.0793 4
3200301 0.26416 5
3200401 0.0 5
3200601 90.0 5

```

3200701 0.26416 5
3200801 5.0-5 0.0 5
3200901 0.0 0.0 4
3201001 00000 5
3201101 000000 4
3201201 104 1.013+5 303.0 1.0 0.0 0.0 5 * noncond.
3201300 1
3201301 0.0 0.0 0.0 4
*
*****
*
*          STEAM GENERATOR - I          *
*
*          V = 0.11675 m3 (incl. plenums) *
*          L = 4.48045 m (incl. plenums)  *
*
*****
*
*          SG-I PRIMARY SIDE
*          -----
*
*          SG UPPER PLENUM
*          -----
*          A = 0.06929 m2
*
4010000 upperpl  snglvol
4010101 0.0 0.28575 .0198 0.0 -90.0 -0.28575 5.0-5 0.0 00000
4010200 104 1.013+5 303.0 1.0 * noncond.
*
4150000 stg-in  sngljun
4150101 401010000 402000000 0.0 0.23 1.0 000000 * Kf, Kr given for
4150201 1 0.0 0.0 0.0 * slightly rounded entrance
*          * S/Di = 1.66 -> Kf=0.25
*
*          SG TUBES
*          -----
*          total number of tubes lumped: 28
*          Di = 29.972 mm
*          Do = 31.75 mm
*          t(meat) = 0.89 mm
*          A = 0.0007055 m2
*          Atot = 0.0197551 m2 (28 tubes)
*          L = 3.90525 m
*          V = 0.0771486 m3
*
4020000 sg-1-prm  pipe
4020001 11
4020101 0.0197551 11
4020201 0.0 10
4020301 0.3550227 4
4020302 0.4000454 5
4020303 0.31 6
4020304 0.3550227 11

```

4020401 0.0 11
4020601 -90.0 11
4020801 6.0-5 0.029972 11
4020901 0.0 0.0 10
4021001 00000 11
4021101 000000 10
4021201 104 1.013+5 303.0 1.0 0.0 0.0 5 * noncond.
4021202 103 1.013+5 303.0 0.0 0.0 0.0 11
4021300 1
4021301 0.0 0.0 0.0 10
*
* LOWER PLENUM
* -----
* A = 0.06841 m2
*
4030000 lowpl branch
4030001 2 1
4030101 0.0 0.28945 0.0198 0.0 -90.0 -0.28945 5.0-5 0.0 00000
4030200 103 1.013+5 297.0
4031101 402010000 403000000 0.0 1.0 0.23 000000 * Kf, Kr (slightly rounded
exit)
4032101 403010000 601000000 0.0 0.0 0.0 000100 * cold leg connection
4031201 0.0 0.0 0.0
4032201 0.0 0.0 0.0
*
*
* SG-I SECONDARY SIDE
* -----
* FEEDWATER INLET
* -----
4050000 sgfw-in tmdpvoll
4050101 1.0+6 1.0+6 0.0 0.0 0.0 0.0 0.0 0.0 00000
4050200 103
4050201 0.0 1.013+5 297.0
*
4060000 sgfw-in tmdpjun
4060101 405000000 451000000 0.0
4060200 1
4060201 -1.0 0.115 0.0 0.0
4060202 0.0 0.115 0.0 0.0
4060203 1.0+6 0.115 0.0 0.0
*
* SG SHELL SIDE
* -----
* Di = 31.115 cm
* A = 0.07604 m2 (total)
* Aflow = 0.0515 m2 (A - 31 tubes)
* Dh = 0.0543 m (triangular lattice)
* Dh = 0.0573 m (considering 28 tubes and shell side)
* L = 3.90525 m
* V = 0.2011 m3
* S = 4.9784 cm -> S/Di = 1.66
*

4510000 sg-1-sec pipe
 4510001 11
 4510101 0.0515 11
 4510201 0.0 10
 4510301 0.3550227 5
 4510302 0.31 6
 4510303 0.4000454 7
 4510304 0.3550227 11
 4510401 0.0 11
 4510601 90.0 11
 4510801 5.0-5 0.0543 11 * Dh = 0.0543 m (triangular lattice)
 4510901 0.0 0.0 10
 4511001 00000 11
 4511101 000000 10
 4511201 103 1.013+5 297.0 0.0 0.0 0.0 11
 4511300 1
 4511301 0.115 0.0 0.0 10

*
 * FEEDWATER OUTLET
 * -----

4070000 sg-out sngljun
 4070101 451010000 408000000 0.0 0.0 0.0 000000
 4070201 1 0.115 0.0 0.0

4080000 dump tmdpvol
 4080101 1.0+6 1.0+6 0.0 0.0 0.0 0.0 0.0 0.0 00000
 4080200 102
 4080201 0.0 1.013+5 1.0

*
 * COMBINED COLD LEG - I (2 x 1) *
 * (SG - RPV) *
 * Di = 0.07793 m *
 * A = 0.00477 m2 (1 x A) *
 * A = 0.00954 m2 (2 x A) *
 * L = 4.56445 m *
 * V = 0.04354 m3 (2 x V) *
 *

*
 6010000 cl-1 snglvol
 6010101 .00954 .16435 0.0 0.0 -75. -.15505 4.676-5 0.0 00000
 6010200 103 1.013+5 297.0

6110000 cl-1 sngljun
 6110101 601010000 602000000 0.0 0.27 0.27 000000 * 75 deg. bend (given)
 6110201 1 0.0 0.0 0.0
 6020000 cl-2 pipe
 6020001 2
 6020101 .00954 2
 6020301 .217 2

6020401 0.0 2
6020601 0.0 2
6020801 4.676-5 0.0 2
6021001 01000 2
6021101 000000 1
6021201 103 1.013+5 297.0 0.0 0.0 0.0 2
6021300 1
6021301 0.0 0.0 0.0 1
*
6120000 cl-2 sngljun
6120101 602010000 603000000 0.0 0.32 0.32 000000 * 90 deg. bend (given)
6120201 1 0.0 0.0 0.0
*
6030000 cl-3 pipe
6030001 3
6030101 .00954 3
6030301 .686 3
6030401 0.0 3
6030601 90. 3
6030801 4.676-5 0.0 3
6031001 00000 3
6031101 000000 2
6031201 103 1.013+5 297.0 0.0 0.0 0.0 1
6031202 103 1.013+5 300.0 0.0 0.0 0.0 2
6031203 103 1.013+5 303.0 0.0 0.0 0.0 3
6031300 1
6031301 0.0 0.0 0.0 2
*
6130000 cl-3 sngljun
6130101 603010000 604000000 0.0 1.7 1.7 000000 * orifice plate (given)
6130201 1 0.0 0.0 0.0
*
6040000 cl-4 snglvol
6040101 .00954 .2407 0.0 0.0 90.0 .2407 4.676-5 0.0 00000
6040200 103 1.013+5 303.0
*
6140000 cl-4 sngljun
6140101 604010000 605000000 0.0 0.32 0.32 000000 * 90 deg. bend (given)
6140201 1 0.0 0.0 0.0
*
6050000 cl-5 pipe
6050001 2
6050101 .00954 2
6050301 .2025 2
6050401 0.0 2
6050601 0.0 2
6050801 4.676-5 0.0 2
6051001 01000 2
6051101 000000 1
6051201 103 1.013+5 303.0 0.0 0.0 0.0 2
6051300 1
6051301 0.0 0.0 0.0 1
*

```

6150000 cl-5 sngljun
6150101 605010000 606000000 0.0 0.16 0.16 000000 * 45 deg. bend (given)
6150201 1 0.0 0.0 0.0
*
6060000 cl-6 snglvol
6060101 .00954 .2784 0.0 0.0 -45. -.19685 4.676-5 0.0 00000
6060200 103 1.013+5 303.0
*
6160000 cl-6 sngljun
6160101 606010000 607000000 0.0 0.16 0.16 000000 * 45 deg. bend (given)
6160201 1 0.0 0.0 0.0
*
6070000 cl-7 pipe
6070001 2
6070101 .00954 2
6070301 .492 2
6070401 0.0 2
6070601 0.0 2
6070801 4.676-5 0.0 2
6070901 0.27 0.27 1 * 75 deg. bend (given)
6071001 01000 2
6071101 000000 1
6071201 103 1.013+5 303.0 0.0 0.0 0.0 2
6071300 1
6071301 0.0 0.0 0.0 1
*
*****
*
* HOT LEG - II *
*
* (RPV - SG) *
*
* Di = 0.0901 m *
* A = 0.00638 m2 *
* L = 5.00845 m *
* V = 0.03195 m3 *
*
*****
*
7010000 hl-1 snglvol
7010101 0.00638 0.684 0.0 0.0 0.0 0.0 4.5-5 0.0 01000
7010200 103 1.013+5 303.0
*
7110000 hl-1 sngljun
7110101 701010000 702000000 0.0 0.27 0.27 000000 * 90 deg. bend
7110201 1 0.0 0.0 0.0
*
7020000 hl-2 branch * the height is adjusted to the PRZ surge line inlet
7020001 1 1
7020101 0.00638 0.381 0.0 0.0 90.0 0.381 4.5-5 0.0 00000
7020200 103 1.013+5 303.0
7021101 702010000 703000000 0.0 0.0 0.0 000000 * hot leg connection
7021201 0.0 0.0 0.0
*

```

```

7030000 hl-3 pipe
7030001 3
7030101 0.00638 3
7030301 0.46355 1
7030302 0.84455 3
7030401 0.0 3
7030601 90.0 3
7030801 4.5-5 0.0 3
7031001 00000 3
7031101 000000 2
7031201 104 1.013+5 303.0 1.0 0.0 0.0 3 * noncond.
7031300 1
7031301 0.0 0.0 0.0 2
*
7130000 hl-3 sngljun
7130101 703010000 704000000 0.0 0.14 0.14 000000 * 45 deg. bend
7130201 1 0.0 0.0 0.0
*
7040000 hl-4 snglvol
7040101 0.00638 0.6504 0.0 0.0 41.6 0.4318 4.5-5 0.0 00000
7040200 104 1.013+5 303.0 1.0 * noncond.
*
7140000 hl-4 sngljun
7140101 704010000 705000000 0.0 0.14 0.14 000000 * 45 deg. bend
7140201 1 0.0 0.0 0.0
*
7050000 hl-5 snglvol
7050101 0.00638 0.490 0.0 0.0 0.0 0.0 4.5-5 0.0 01000
7050200 104 1.013+5 303.0 1.0 * noncond.
*
7150000 hl-5 sngljun
7150101 705010000 706000000 0.0 0.14 0.14 000000 * 45 deg. bend
7150201 1 0.0 0.0 0.0
*
7060000 hl-6 snglvol
7060101 0.00638 0.6504 0.0 0.0 -41.6 -0.4318 4.5-5 0.0 00000
7060200 104 1.013+5 303.0 1.0 * noncond.
*
7160000 hl-sg-in sngljun
7160101 706010000 801000000 0.00638 0.14 0.14 000100 * 45 deg. bend
7160201 1 0.0 0.0 0.0

```

```

*
*
*          STEAM GENERATOR - II          *
*
*          *
*          V = 0.11675 m3 (incl. plenums)  *
*          L = 4.48045 m (incl. plenums)   *
*
*

```

```

*
*
*          SG-II PRIMARY SIDE
*          -----
*

```

* SG UPPER PLENUM

* -----
 * A = 0.06929 m2
 *

8010000 upperpl snglvol
 8010101 0.0 0.28575 .0198 0.0 -90.0 -0.28575 5.0-5 0.0 00000
 8010200 104 1.013+5 303.0 1.0 * noncond.

*
 8150000 stg-in sngljun
 8150101 801010000 802000000 0.0 0.23 1.0 000000 * Kf, Kr given for slightly
 8150201 1 0.0 0.0 0.0 * rounded entrance
 * S/Di = 1.66 -> Kf=0.25
 *

* SG TUBES

* -----
 * total number of tubes lumped: 28
 * Di = 29.972 mm
 * A = 0.0007055 m2
 * Atot = 0.0197551 m2 (28 tubes)
 * L = 3.90525 m
 * V = 0.0771486 m3
 *

8020000 sg-2-prm pipe
 8020001 11
 8020101 0.0197551 11
 8020201 0.0 10
 8020301 0.3550227 6
 8020302 0.1827227 7
 8020303 0.5273227 8
 8020304 0.3550227 11
 8020401 0.0 11
 8020601 -90.0 11
 8020801 6.0-5 0.029972 11
 8020901 0.0 0.0 10
 8021001 00000 11
 8021101 000000 10
 8021201 104 1.013+5 303.0 1.0 0.0 0.0 7 * noncond.
 8021202 103 1.013+5 303.0 0.0 0.0 0.0 11
 8021300 1
 8021301 0.0 0.0 0.0 10
 *

* SG LOWER PLENUM

* -----
 * A = 0.06841 m2
 *

8030000 lowpl branch
 8030001 2 1
 8030101 0.0 0.28945 0.0198 0.0 -90.0 -0.28945 5.0-5 0.0 00000
 8030200 103 1.013+5 297.0
 8031101 802010000 803000000 0.0 1.0 0.23 000000 * Kf, Kr (slightly rounded
 exit)
 8032101 803010000 901000000 0.0 0.0 0.0 000100 * cold leg connection
 8031201 0.0 0.0 0.0
 8032201 0.0 0.0 0.0

* SG - II SECONDARY SIDE

* -----

* NOT MODELED !!

* *
* COMBINED COLD LEG - II (2 x 1) *
* *
* (SG - RPV) *
* *
* Di = 0.07793 m *
* A = 0.00477 m2 (1 x A) *
* A = 0.00954 m2 (2 x A) *
* L = 4.56445 m *
* V = 0.04354 m3 (2 x V) *
* *

9010000 cl-1 snglvol
9010101 .00954 .16435 0.0 0.0 -75. -.15505 4.676-5 0.0 00000
9010200 103 1.013+5 297.0
*
9110000 cl-1 sngljun
9110101 901010000 902000000 0.0 0.27 0.27 000000 * 75 deg. bend
9110201 1 0.0 0.0 0.0
*
9020000 cl-2 pipe
9020001 2
9020101 .00954 2
9020301 .217 2
9020401 0.0 2
9020601 0.0 2
9020801 4.676-5 0.0 2
9021001 01000 2
9021101 000000 1
9021201 103 1.013+5 297.0 0.0 0.0 0.0 2
9021300 1
9021301 0.0 0.0 0.0 1
*
9120000 cl-2 sngljun
9120101 902010000 903000000 0.0 0.32 0.32 000000 * 90 deg. bend
9120201 1 0.0 0.0 0.0
*
9030000 cl-3 pipe
9030001 3
9030101 .00954 3
9030301 .686 3
9030401 0.0 3
9030601 90. 3
9030801 4.676-5 0.0 3
9031001 00000 3
9031101 000000 2
9031201 103 1.013+5 297.0 0.0 0.0 0.0 1

```

9031202 103 1.013+5 297.0 0.0 0.0 0.0 2
9031203 103 1.013+5 297.0 0.0 0.0 0.0 3
9031300 1
9031301 0.0 0.0 0.0 2
*
9220000 cl-2 tmdpjun
9220101 903010000 933000000 0.0
9220200 1
9220201 -1.0 0.0 0.0 0.0
9220202 0.0 0.0 0.0 0.0
9220203 1.0+6 0.0 0.0 0.0
*
9330000 block tmdpvovl
9330101 1.0+6 1.0+6 0.0 0.0 0.0 0.0 0.0 0.0 00000
9330200 103
9330201 0.0 1.013+5 297.0
*
***** B L O C K E D *****
***** B L O C K E D *****
*
9440000 block tmdpvovl
9440101 1.0+6 1.0+6 0.0 0.0 0.0 0.0 0.0 0.0 00000
9440200 103
9440201 0.0 1.013+5 303.0
*
9130000 cl-2 tmdpjun
9130101 944000000 904000000 0.0
9130200 1
9130201 -1.0 0.0 0.0 0.0
9130202 0.0 0.0 0.0 0.0
9130203 1.0+6 0.0 0.0 0.0
*
9040000 cl-4 snglvovl
9040101 .00954 .2407 0.0 0.0 90.0 .2407 4.676-5 0.0 00000
9040200 103 1.013+5 303.0
*
9140000 cl-4 sngljun
9140101 904010000 905000000 0.0 0.32 0.32 000000 * 90 deg. bend
9140201 1 0.0 0.0 0.0
*
9050000 cl-5 pipe
9050001 2
9050101 .00954 2
9050301 .2025 2
9050401 0.0 2
9050601 0.0 2
9050801 4.676-5 0.0 2
9051001 01000 2
9051101 000000 1
9051201 103 1.013+5 303.0 0.0 0.0 0.0 2
9051300 1
9051301 0.0 0.0 0.0 1
*

```

```

9150000 cl-5 sngljun
9150101 905010000 906000000 0.0 0.16 0.16 000000 * 45 deg. bend
9150201 1 0.0 0.0 0.0
9060000 cl-6 snglvol
9060101 .00954 .2784 0.0 0.0 -45. -.19685 4.676-5 0.0 00000
9060200 103 1.013+5 303.0
*
9160000 cl-6 sngljun
9160101 906010000 907000000 0.0 0.16 0.16 000000 * 45 deg. bend
9160201 1 0.0 0.0 0.0
*
9070000 cl-7 pipe
9070001 2
9070101 .00954 2
9070301 .492 2
9070401 0.0 2
9070601 0.0 2
9070801 4.676-5 0.0 2
9070901 0.27 0.27 1 * 75 deg. bend
9071001 01000 2
9071101 000000 1
9071201 103 1.013+5 303.0 0.0 0.0 0.0 2
9071300 1
9071301 0.0 0.0 0.0 1
*

```

```

*****
*                               HEAT STRUCTURES                               *
*****

```

```

*
*   Heater Rods
*   -----
*   number of heaters: 15
*   rod diameter (Do): 2.54 cm (25.4 mm)
*   active length: 0.6096 m
*   total heat transfer area: 0.7297 m2
*
11111000 3 5 2 1 0.0
11111100 0 2 * mesh flag
11111101 0.0034 3 * mesh interval data
11111102 0.0025 4 * mesh interval data (clad thickness assumed to be 2.5 mm)
11111201 001 3 * composition data (MgO powder)
11111202 002 4 * composition data (st. steel)
11111301 1.0 3 * source distribution (radial)
11111302 0.0 4 * source distribution (radial)
11111400 0 * initial temp. flg
11111401 303.0 5 * initial temp.
11111501 0 0 0 1 3.0480371 3 * left bound. cond.
11111601 111010000 10000 1 1 3.0480371 3 * right bound. cond.
11111701 001 0.333333 0.0 0.0 3 * source data
11111901 .184 100.0 100.0 0.0 0.0 0.0 0.0 1.0 3 * right boundary
*

```

```

*   SG-I Tubes
*   -----

```

* number of tubes: 28
 * Di = 2.9972 cm (29.972 mm), Do = 3.175 cm (31.75 mm)
 * meat thickness: 0.0889 cm
 * tube length: 3.90525 m
 *

14021000 11 5 2 1 0.014986
 14021100 0 2
 14021101 0.00022225 4
 14021201 002 4 * st. steel
 14021301 1.0 4
 14021400 0
 14021401 303.0 5
 14021501 402010000 10000 1 1 9.94064 4
 14021502 402050000 0 1 1 11.201271 5
 14021503 402060000 0 1 1 8.68 6
 14021504 402070000 10000 1 1 9.94064 11
 14021601 451110000 -10000 1 1 9.94064 4
 14021602 451070000 0 1 1 11.201271 5
 14021603 451060000 0 1 1 8.68 6
 14021604 451050000 -10000 1 1 9.94064 11
 14021701 0 0 0.0 0.0 11
 14021801 0.029972 100.0 100.0 0.0 0.0 0.0 0.0 1.0 11
 14021901 0.0543 100.0 100.0 0.0 0.0 0.0 0.0 1.0 11

* SG Shell Side

* -----
 * Di = 0.31115 m
 * Do = 0.32385 m
 * t-ins = 0.0508 m
 *

14511000 11 3 2 1 0.155575
 14511100 0 2
 14511101 0.00635 1
 14511102 0.0508 2
 14511201 002 1
 14511202 003 2
 14511301 0.0 2
 14511400 0
 14511401 303.0 3
 14511501 451010000 010000 1 1 0.3550227 5
 14511502 451060000 0 1 1 0.31 6
 14511503 451070000 0 1 1 0.4000454 7
 14511504 451080000 010000 1 1 0.3550227 11
 14511601 -002 0 3003 1 0.3550227 5
 14511602 -002 0 3003 1 0.31 6
 14511603 -002 0 3003 1 0.4000454 7
 14511604 -002 0 3003 1 0.3550227 11
 14511701 0 0.0 0.0 0.0 11
 14511801 0.0543 100.0 100.0 0.0 0.0 0.0 0.0 1.0 11

* Pressurizer Tank

* -----
 * Di = 0.31115 m
 * Do = 0.32385 m
 * t-ins = 0.0762 m

13201000 5 3 2 1 0.155575
 13201100 0 2
 13201101 0.00635 1
 13201102 0.0762 2
 13201201 002 1
 13201202 003 2
 13201301 0.0 2
 13201400 0
 13201401 303.0 3
 13201501 320010000 010000 1 1 0.26416 5
 13201601 -002 0 3003 1 0.26416 5
 13201701 0 0.0 0.0 0.0 5
 13201801 0.0 100.0 100.0 0.0 0.0 0.0 0.0 1.0 5

*
 * Pressurizer Surge Line
 * -----
 * Di = 0.02093 m
 * Do = 0.02674 m
 * t-ins = 0.0762 m
 *

13101000 8 3 2 1 0.0105
 13101100 0 2
 13101101 0.00287 1
 13101102 0.0762 2
 13101201 002 1
 13101202 003 2
 13101301 0.0 2
 13101400 0
 13101401 303.0 3
 13101501 310010000 0 1 1 0.2667 1
 13101502 310020000 0 1 1 0.7811 2
 13101503 310030000 010000 1 1 0.6731 4
 13101504 310050000 010000 1 1 0.95885 6
 13101505 310070000 0 1 1 0.2794 7
 13101506 310080000 0 1 1 0.2858 8
 13101601 -002 0 3003 1 0.2667 1
 13101602 -002 0 3003 1 0.7811 2
 13101603 -002 0 3003 1 0.6731 3
 13101604 -002 0 3003 1 0.6731 4
 13101605 -002 0 3003 1 0.95885 5
 13101606 -002 0 3003 1 0.95885 6
 13101607 -002 0 3003 1 0.2794 7
 13101608 -002 0 3003 1 0.2858 8
 13101701 0 0.0 0.0 0.0 8
 13101801 0.0 100.0 100.0 0.0 0.0 0.0 0.0 1.0 8

*
 * Hot-leg-I (RPV - SG)
 * -----
 * Di = 0.0901 m
 * Do = 0.10158 m
 * t-ins = 0.0762 m
 *

12001000 8 3 2 1 0.04505
 12001100 0 2

12001101 0.00574 1
12001102 0.0762 2
12001201 002 1
12001202 003 2
12001301 0.0 2
12001400 0
12001401 303.0 3
12001501 201010000 0 1 1 0.684 1
12001502 202010000 0 1 1 0.381 2
12001503 203010000 0 1 1 0.46355 3
12001504 203020000 010000 1 1 0.84455 5
12001505 204010000 0 1 1 0.6504 6
12001506 205010000 0 1 1 0.490 7
12001507 206010000 0 1 1 0.6504 8
12001601 -002 0 3003 1 0.684 1
12001602 -002 0 3003 1 0.381 2
12001603 -002 0 3003 1 0.46355 3
12001604 -002 0 3003 1 0.84455 4
12001605 -002 0 3003 1 0.84455 5
12001606 -002 0 3003 1 0.6504 6
12001607 -002 0 3003 1 0.490 7
12001608 -002 0 3003 1 0.6504 8
12001701 0 0.0 0.0 0.0 8
12001801 0.0 100.0 100.0 0.0 0.0 0.0 0.0 1.0 8
* Hot-leg-II (RPV - SG)
* -----
* Di = 0.0901 m
* Do = 0.10158 m
* t-ins = 0.0762 m
17001000 8 3 2 1 0.045
17001100 0 2
17001101 0.00574 1
17001102 0.0762 2
17001201 002 1
17001202 003 2
17001301 0.0 2
17001400 0
17001401 303.0 3
17001501 701010000 0 1 1 0.684 1
17001502 702010000 0 1 1 0.381 2
17001503 703010000 0 1 1 0.46355 3
17001504 703020000 010000 1 1 0.84455 5
17001505 704010000 0 1 1 0.6504 6
17001506 705010000 0 1 1 0.490 7
17001507 706010000 0 1 1 0.6504 8
17001601 -002 0 3003 1 0.684 1
17001602 -002 0 3003 1 0.381 2
17001603 -002 0 3003 1 0.46355 3
17001604 -002 0 3003 1 0.84455 4
17001605 -002 0 3003 1 0.84455 5
17001606 -002 0 3003 1 0.6504 6
17001607 -002 0 3003 1 0.490 7
17001608 -002 0 3003 1 0.6504 8
17001701 0 0.0 0.0 0.0 8

17001801 0.0 100.0 100.0 0.0 0.0 0.0 0.0 1.0 8

*

* Cold-leg-I (SG - RPV)

*

* Di = 0.07793 m

* Do = 0.08892 m

* t-ins = 0.0762 m

*

16001000 12 3 2 1 0.03897

16001100 0 2

16001101 0.00549 1

16001102 0.0762 2

16001201 002 1

16001202 003 2

16001301 0.0 2

16001400 0

16001401 303.0 3

16001501 601010000 0 1 1 0.16435 1

16001502 602010000 010000 1 1 0.217 3

16001503 603010000 010000 1 1 0.686 6

16001504 604010000 0 1 1 0.2407 7

16001505 605010000 010000 1 1 0.2025 9

16001506 606010000 0 1 1 0.2784 10

16001507 607010000 010000 1 1 0.492 12

16001601 -002 0 3003 1 0.16435 1

16001602 -002 0 3003 1 0.217 3

16001603 -002 0 3003 1 0.686 6

16001604 -002 0 3003 1 0.2407 7

16001605 -002 0 3003 1 0.2025 9

16001606 -002 0 3003 1 0.2784 10

16001607 -002 0 3003 1 0.492 12

16001701 0 0.0 0.0 0.0 12

16001801 0.0 100.0 100.0 0.0 0.0 0.0 0.0 1.0 12

*

* Cold-leg-II (SG - BLOCKAGE - RPV)

*

* Di = 0.07793 m

* Do = 0.08892 m

* t-ins = 0.0762 m

19001000 12 3 2 1 0.039

19001100 0 2

19001101 0.00549 1

19001102 0.0762 2

19001201 002 1

19001202 003 2

19001301 0.0 2

19001400 0

19001401 303.0 3

19001501 901010000 0 1 1 0.16435 1

19001502 902010000 010000 1 1 0.217 3

19001503 903010000 010000 1 1 0.686 6

19001504 904010000 0 1 1 0.2407 7

19001505 905010000 010000 1 1 0.2025 9

19001506 906010000 0 1 1 0.2784 10
 19001507 907010000 010000 1 1 0.492 12
 19001601 -002 0 3003 1 0.16435 1
 19001602 -002 0 3003 1 0.217 3
 19001603 -002 0 3003 1 0.686 6
 19001604 -002 0 3003 1 0.2407 7
 19001605 -002 0 3003 1 0.2025 9
 19001606 -002 0 3003 1 0.2784 10
 19001607 -002 0 3003 1 0.492 12
 19001701 0 0.0 0.0 0.0 12
 19001801 0.0 100.0 100.0 0.0 0.0 0.0 0.0 1.0 12

*

* MATERIAL DATA *

*
 20100100 tbl/fctn 1 1 * MgO powder
 *

* temp. cond. (W/m-K)
 20100101 273.15 30.0
 20100102 373.0 9.0
 20100103 473.0 3.0
 20100104 573.0 2.2
 20100105 673.0 2.0
 20100106 1500.0 2.0
 *

* temp. heat cap. (J/m3-K)
 20100151 273.15 2.68+6
 20100152 1500.0 2.68+6
 *

*
 20100200 tbl/fctn 1 1 * stainless-steel
 *

* temp. cond. (W/m-K)
 20100201 273.15 13.0
 20100202 293.0 15.0
 20100203 373.0 15.5
 20100204 473.0 17.5
 20100205 673.0 20.0
 20100206 873.0 22.5
 20100207 1073.0 25.5
 20100208 1500.0 26.0
 *

* temp. heat cap. (J/m3-K)
 20100251 273.15 3.900+06
 20100252 373.0 3.900+06
 20100253 473.0 4.070+06
 20100254 573.0 4.230+06
 20100255 673.0 4.330+06
 20100256 1000.0 4.500+06
 20100257 1500.0 5.380+06
 *

*

20100300 tbl/fctn 1 1 * PV-E insulator
 * * approx. same as fiberglass !
 * temp. con. (W/m-K)
 20100301 273.15 0.033
 20100302 283.0 0.033
 20100303 373.0 0.04
 20100304 573.0 0.071
 20100305 1500.0 0.1

* temp. heat cap. (J/m3-K)
 20100351 273.15 9.6+4
 20100352 1500.0 9.6+4

 * GENERAL TABLES *

* power input

*
 20200100 power
 20200101 0.0 0.0+3 * time(sec) vs. power(watt)
 20200102 200.0 0.0+3
 20200103 200.0 5.0+3
 20200104 220.0 5.0+3
 20200105 220.0 10.0+3
 20200106 240.0 10.0+3
 20200107 240.0 20.0+3
 20200108 260.0 20.0+3
 20200109 260.0 25.0+3
 20200110 280.0 25.0+3
 20200111 280.0 34.9+3
 20200112 1.0+6 34.9+3

* Temperature of Environment

*
 20200200 temp
 20200201 -1.0 297.0
 20200202 0.0 297.0
 20200203 1.0+6 297.0

* Heat Transfer Coeff. of Environment

*
 20200300 htc-t
 20200301 -1.0 7.0
 20200302 0.0 7.0
 20200303 1.0+6 7.0

 * CONTROL VARIABLES *

***** COLLAPSED LEVEL CALCULATIONS *****

* -----

```

* Vessel:
* -----
* Lower plenum - upper dome
20500100 vessel sum 1.0 0.0 1
20500101 0.0 0.13462 voidf 101010000
20500102 0.20320 voidf 111010000
20500103 0.20320 voidf 111020000
20500104 0.20320 voidf 111030000
20500105 0.16764 voidf 121010000
20500106 0.13970 voidf 122010000
20500107 0.09906 voidf 123010000
20500108 0.14758924 voidf 131010000
20500109 0.06831076 voidf 131020000
*
* Downcomer
20500200 downcomr sum 1.0 0.0 1
20500201 0.0 0.23876 voidf 141010000
20500202 0.16764 voidf 142010000
20500203 0.74422 voidf 143010000
*
* Pressurizer
* -----
20500400 prz sum 1.0 0.0 1
20500401 0.0 0.26416 voidf 320010000
20500402 0.26416 voidf 320020000
20500403 0.26416 voidf 320030000
20500404 0.26416 voidf 320040000
20500405 0.26416 voidf 320050000
*
***** LOOP - I *****
*
* Hot Leg-I
* -----
20501000 hl-1-1 sum 1.0 0.0 1
20501001 0.0 0.381 voidf 202010000
20501002 0.46355 voidf 203010000
20501003 0.84455 voidf 203020000
20501004 0.84455 voidf 203030000
20501005 0.4318 voidf 204010000
*
*****
* Same Elevation Relative to SG-PR
* -----
* vol.205 - vol.403(bottom)
20591000 hlsg1-hl sum 20.357 0.0 1
20591001 1.9468 1.0 cntrlvar 10
*
*****
*
20501100 hl-1-2 sum 1.0 0.0 1
20501101 0.0 0.4318 voidf 206010000
*
* Steam Generator-I
* -----

```

```

20501200 sg-tb-1 sum 1.0 0.0 1
20501201 0.0 0.3550227 voidf 402010000
20501202 0.3550227 voidf 402020000
20501203 0.3550227 voidf 402030000
20501204 0.3550227 voidf 402040000
20501205 0.4000454 voidf 402050000
20501206 0.31 voidf 402060000
20501207 0.3550227 voidf 402070000
20501208 0.3550227 voidf 402080000
20501209 0.3550227 voidf 402090000
20501210 0.3550227 voidf 402100000
20501211 0.3550227 voidf 402110000
*
20501300 sg-1-pl sum 1.0 0.0 1
20501301 0.0 1.0 cntrlvar 12
20501302 0.28575 voidf 401010000
20501303 0.28945 voidf 403010000
*
* SG-1 + Plenums + vol.205 + vol.206
20591100 sg-1-tot sum 1.0 0.0 1
20591101 0.0 1.0 cntrlvar 13
20591102 1.0 cntrlvar 11
*
*****
*
* vol.205 - vol.403(bottom)
20591200 hlsg1-sg sum 20.357 0.0 1
20591201 0.0 1.0 cntrlvar 911
*
*****
* Total Height of SG Side (vols.206+401+402+403+601)
* Total H = 5.0673 m
* -----
20591300 sg-hl-cl sum 19.734 0.0 1
20591301 0.0 1.0 cntrlvar 911
20591302 0.15505 voidf 601010000
*
* Cold Leg-I
* -----
20501400 cl-1 sum 1.0 0.0 1
20501401 0.0 0.686 voidf 603010000
20501402 0.686 voidf 603020000
20501403 0.686 voidf 603030000
20501404 0.2407 voidf 604010000
*
* SG-I Secondary Side
* -----
20501500 sg-sh-1 sum 1.0 0.0 1
20501501 0.0 0.3550227 voidf 451010000
20501502 0.3550227 voidf 451020000
20501503 0.3550227 voidf 451030000
20501504 0.3550227 voidf 451040000
20501505 0.3550227 voidf 451050000

```

20501506 0.31 voidf 451060000
 20501507 0.4000454 voidf 451070000
 20501508 0.3550227 voidf 451080000
 20501509 0.3550227 voidf 451090000
 20501510 0.3550227 voidf 451100000
 20501511 0.3550227 voidf 451110000

*
 ***** LOOP - II *****

*
 * Hot Leg-II
 * -----

20502000 hl-2-1 sum 1.0 0.0 1
 20502001 0.0 0.381 voidf 702010000
 20502002 0.46355 voidf 703010000
 20502003 0.84455 voidf 703020000
 20502004 0.84455 voidf 703030000
 20502005 0.4318 voidf 704010000

*

 * Same Elevation Relative to SG-PR
 * -----

* vol.705 - vol.803(bottom)
 20592000 hlsg2-hl sum 20.357 0.0 1
 20592001 1.9468 1.0 cntrlvar 20

*

20502100 hl-2-2 sum 1.0 0.0 1
 20502101 0.0 0.4318 voidf 706010000

*
 * Steam Generator-II
 * -----

20502200 sg-tb-2 sum 1.0 0.0 1
 20502201 0.0 0.3550227 voidf 802010000
 20502202 0.3550227 voidf 802020000
 20502203 0.3550227 voidf 802030000
 20502204 0.3550227 voidf 802040000
 20502205 0.3550227 voidf 802050000
 20502206 0.3550227 voidf 802060000
 20502207 0.1827227 voidf 802070000
 20502208 0.5273227 voidf 802080000
 20502209 0.3550227 voidf 802090000
 20502210 0.3550227 voidf 802100000
 20502211 0.3550227 voidf 802110000

*
 20502300 sg-2-pl sum 1.0 0.0 1
 20502301 0.0 1.0 cntrlvar 22
 20502302 0.28575 voidf 801010000
 20502303 0.28945 voidf 803010000

*
 * SG-2 + Plenums + vol.705 + vol.706
 20592100 sg-2-tot sum 1.0 0.0 1
 20592101 0.0 1.0 cntrlvar 23
 20592102 1.0 cntrlvar 21

```

*****
*
*       vol.705 - vol.803(bottom)
20592200 hlsg2-sg sum 20.357 0.0 1
20592201 0.0 1.0 cntrlvar 921
*
*****
*
*       Cold Leg-II
*       -----
20502400 cl-2 sum 1.0 0.0 1
20502401 0.0 0.686 voidf 903010000
20502402 0.686 voidf 903020000
20502403 0.686 voidf 903030000
20502404 0.2407 voidf 904010000
*
*
*
*       % Level Ratios ((Collapsed Level / Total Height) * 100)
*       -----
*
*       Vessel Tot. Height: 1.36652 m
20510100 ves-rat mult 73.179 0.0 1
20510101 cntrlvar 1
*
*       Pressurizer Tot. Height: 1.3208 m
20510400 prz-rat mult 75.712 0.0 1
20510401 cntrlvar 4
*
*       Hot Leg-I Tot. Height: 2.96545 m
20511000 hl-1-rat mult 33.722 0.0 1
20511001 cntrlvar 10
*
*       Hot Leg-II Tot. Height: 2.96545 m
20512000 hl-2-rat mult 33.722 0.0 1
20512001 cntrlvar 20
*
*       SG-I Primary Side Tot. Height: 4.4804 m (incl. plns.)
20511300 sgp1-rat mult 22.319 0.0 1
20511301 cntrlvar 13
*
*       SG-II Primary Side Tot. Height: 4.4804 m (incl. plns.)
20512300 sgp2-rat mult 22.319 0.0 1
20512301 cntrlvar 23
*
*       SG-I Secondary Side Tot. Height: 3.90525 m (only tubes)
20511500 sgs1-rat mult 25.607 0.0 1
20511501 cntrlvar 15
*
*       SG-I Primary Side Tot. Height: 3.90525 m (only tubes)
20511700 sgp1-rat mult 25.607 0.0 1
20511701 cntrlvar 12
*
*

```

```

*****          POWER CALCULATIONS          *****
*          -----
*          Core:
*          ----
20550000 pow-core sum 1.0 0.0 1
20550001 0.0      1.0 q 111010000
20550002          1.0 q 111020000
20550003          1.0 q 111030000
*
*          Steam Generator:
*          -----
20560000 pow-sg   sum 1.0 0.0 1
20560001 0.0     1.0 q 402010000
20560002          1.0 q 402020000
20560003          1.0 q 402030000
20560004          1.0 q 402040000
20560005          1.0 q 402050000
20560006          1.0 q 402060000
20560007          1.0 q 402070000
20560008          1.0 q 402080000
20560009          1.0 q 402090000
20560010          1.0 q 402100000
20560011          1.0 q 402110000
*
*
*----- END OF INPUT FILE -----*
.

```

APPENDIX C

SPECIFICATIONS OF INSTRUMENTATION AND DATA ACQUISITION SYSTEMS OF METU-CTF

1) Thermocouples:

Manufacturer: ELIMKO Co., Turkey
Type: L (Fe-Const type designed according to German DIN standard)
J (Fe-Const type designed according to USA standard)

Class: 2
Temperature Range: $-40\text{ }^{\circ}\text{C}$ to $333\text{ }^{\circ}\text{C}$
Tolerance Value: $\pm 2.5\text{ }^{\circ}\text{C}$ according to the standard IEC 584-2

2) Pressure Transducer:

Manufacturer: Transinstruments Inc., England
Type: Strain gauge
Working Medium: Water, steam, gas
Pressure Range: 0–6 bar (g)
Output Signal: 4–20 mA (linear)

3) Flowmeter:

Manufacturer: ABB Kent-Taylor, Italy
Type: Differential pressure transmitter
Working Medium: Water, steam, gas
dP Range: 11.7–70 kPa
Output Signal: 4–20 mA (linear)

4) Data Acquisition System:

Manufacturer: Advantech Co., Ltd.
Data Acquisition Card: PCL-812PG
Analog Input: 16 single-ended channels
12 bits resolution
 $\pm 5\text{V}$, $\pm 2.5\text{V}$, $\pm 1.25\text{V}$, $\pm 0.625\text{V}$, and $\pm 0.3125\text{V}$ input range
0.015% of reading ± 1 bit accuracy
Analog Output: 2 channels
12 bits resolution
Amplifier/Multiplexer Board: PCLD-889
Input Channel: 16
Input Range: $\pm 10\text{V}$ maximum
Cold Junction Compensation: $+24.4\text{V}/^{\circ}\text{C}$
 0.0V at $0.0\text{ }^{\circ}\text{C}$

APPENDIX D ERROR ANALYSIS FOR METU-CTF MEASUREMENTS

The total error of a function F with independent measured variables $x_1, x_2, x_3, \dots, x_n$, was obtained as [12]:

$$\sigma_F = \left[\left(\frac{\partial F}{\partial x_1} \sigma_{x_1} \right)^2 + \left(\frac{\partial F}{\partial x_2} \sigma_{x_2} \right)^2 + \dots + \left(\frac{\partial F}{\partial x_n} \sigma_{x_n} \right)^2 \right]^{1/2} \quad (D.1)$$

The relative error can be found by dividing the expression given above by F:

$$\frac{\sigma_F}{F} = \left[\left(\frac{\sigma_{x_1}}{x_1} \right)^2 + \left(\frac{\sigma_{x_2}}{x_2} \right)^2 + \dots + \left(\frac{\sigma_{x_n}}{x_n} \right)^2 \right]^{1/2} \quad (D.2)$$

The experimental heat flux is defined as:

$$q''(x) = - \frac{\dot{m}_{cw} c_p}{\pi d_i} \frac{dT_{cw}(x)}{dx} \quad (D.3)$$

Therefore:

$$\frac{\partial q''}{\partial \dot{m}_{cw}} = - \frac{c_p}{\pi d_i} \frac{dT_{cw}(x)}{dx} \quad (D.4)$$

$$\frac{\partial q''}{\partial (dT_{cw}/dx)} = - \frac{\dot{m}_{cw} c_p}{\pi d} \quad (D.5)$$

Substituting Equations (D.4) and (D.5) into Equation (D.1) and dividing both sides of by $(q'')^2$ we find the relative error for q'' :

$$\frac{\sigma_{q''}}{q''} = \left[\left(\frac{\sigma_{\dot{m}_{cw}}}{\dot{m}_{cw}} \right)^2 + \left(\frac{\sigma_{(dT_{cw}/dx)}}{dT_{cw}(x)/dx} \right)^2 \right]^{1/2} \quad (D.6)$$

The variables c_p , and d are assumed to be error free.

Similarly, the relative error for the condensation heat transfer coefficient is found from the following equation:

$$h_{exp}(x) = \frac{q''(x)}{(T_s(x) - T_w(x))} \quad (D.7)$$

The relative error for h_{exp} is:

$$\frac{\sigma_{h_{\text{exp}}}}{h_{\text{exp}}} = \left[\left(\frac{\sigma_{q'}}{q''} \right)^2 + \left(\frac{\sigma_{(T_s - T_w)}}{(T_s - T_w)} \right)^2 \right]^{1/2} \quad (\text{D.8})$$

Since we did not use a flow meter for cooling water flow measurement, the relative error for measured flow rate is taken from the maximum weight deviation calculated from the measurement performed in the beginning and end of each run. It is found that the maximum relative error associated with the cooling water measurement is 0.05, on the average, which corresponds to a deviation of 200 gr at the 4300 gr total weight of cooling water collected for a period of 15 s.

The slope of the coolant water axial temperature profile, i.e. dT_{cw}/dx , was determined from an exponential fit of the measured coolant temperatures as the function of the measurement distance, and for almost all the runs the R^2 value for the fit of the data to the exponential relation was greater than 0.98. This means that error associated to the curve fitting is very small. However, it is difficult to predict the error associated with the temperature gradient directly. Only an estimation was made by considering the effect of measured temperature data with higher deviation than the general trend of the temperature distribution. It was found that the effect of measured temperature data with high deviation yields an error of ± 10 .

For the prediction of the uncertainty associated with the heat transfer coefficient, the standard deviation of the thermocouples must be known. The experimental data of isothermal check of thermocouples were used for determining the standard deviation of thermocouples. The experimental data, as given in Table 2.3.1, yields a maximum standard deviation of 0.762. Since this is an experimental result, the calculated standard deviation includes the tolerances given by the factory.

The aforementioned values of standard deviations and data needed for Equations (D.6) and (D.8) are summarized as follows:

$$\sigma_m = 0.05 m_{\text{cw}} \quad (\text{D.9})$$

$$\sigma_{T_s} = \sigma_{T_w} = 0.762 \quad (\text{D.10})$$

$$\sigma_{(dT/dx)} = 0.10 (dT_{\text{cw}}/dx) \quad (\text{D.11})$$

$$(T_s - T_w) = 5 \text{ }^\circ\text{C} \quad (\text{D.12})$$

$$\sigma_{(T_s - T_w)} = (\sigma_{T_s}^2 + \sigma_{T_w}^2)^{1/2} \quad (\text{D.13})$$

Substituting values from Equations (D.9) to (D.13) in Equations (D.6) and (D.8) we get:

$$\left[\frac{\sigma_{q'}}{q''} \right]_{\text{max}} = 0.11$$

and

$$\left[\frac{\sigma_h}{h} \right]_{\text{max}} = 0.24$$

Therefore the maximum uncertainties associated with the heat flux and the heat transfer coefficient are $\pm 11\%$ and $\pm 24\%$, respectively. The temperature difference ($T_s - T_w$) was equal to or greater than $5\text{ }^\circ\text{C}$ in the major part of the condenser tube length in all experiments. However, this temperature difference is less than $5\text{ }^\circ\text{C}$ in entrance region ($\sim 0.25\text{ m}$) and the uncertainty associated with the heat transfer coefficient escalates to $\pm 38\%$ when a temperature difference of $3\text{ }^\circ\text{C}$ is assumed. It is also observed that the error associated with the heat flux and the heat transfer coefficient increases when the coolant temperature change per unit length decreases which happens towards the end of the condenser tube. If we assume a conservative value for the deviation of the coolant temperature gradient such as 15% (instead of 10%), the uncertainties become 16% and 27% for heat flux and heat transfer coefficient, respectively. This reveals that the uncertainty band increases at the entrance region much more than the end of the test section.